PGCOMP - Programa de Pós-Graduação em Ciência da Computação
Universidade Federal da Bahia (UFBA)
Av. Milton Santos, s/n - Ondina
Salvador, BA, Brasil, 40170-110

https://pgcomp.ufba.br
pgcomp@ufba.br

The global health systems are currently unable to adequately meet the high demand for care for people with neurological disorders. This impacts the quality of treatment offered, leading to issues such as the prescription of improper medications, difficulty accessing treatment, late detection of diseases, and more. Neurological disorders include conditions such as dementia, epilepsy, Alzheimer's, Parkinson's, multiple sclerosis, and others. To improve the treatment of these diseases, devices for the acquisition of electrical biosignals have been developed to provide greater accuracy, patient comfort, and, in some cases, lower costs. Recognizing this scenario, we aimed to investigate the possibility of using transfer learning among artificial neural networks to address these problems. Additionally, we attempted to reduce the mathematical complexity of electrical biosignal data by transforming it from time domain to frequency domain, representing it as algebraic functions rather than sine functions. Based on these ideas, we explored the potential of transfer learning to enhance the predictive accuracy of a neural network model processing diverse electrical biosignals with non-identical features and label spaces in a frequency domain. We integrated similarity analysis between biosignals into our methodology to prevent negative transfer learning using the dynamic time warping (DTW) technique. We selected the long short-term memory (LSTM) neural network to develop the proposed architecture, and the public datasets used for the experiment were the TUEG EEG Corpora (electroencephalogram), ECG Heartbeat Categorization (electrocardiogram), and EMG Classify Gestures (electroneuromyography). Using the baseline outcomes as a reference, we selected the ECG as the source domain. Then, we calculated the similarity between the biosignals, trained the model with the features identified as having the lowest distance, and transferred the weights and bias to the EEG and EMG models to process their own dataset, named the target domain. In summary, we present two scenarios to experiment and explore the potential of an effective transfer learning application with heterogeneous electrical biosignals in the frequency domain, from ECG to EMG and ECG to EEG, respectively. We discovered a promising outcome in the first scenario when the source and target datasets were balanced, even with a small target dataset. In the second context, we observed a discreet decrease in performance, also referred to as negative transfer learning, when utilizing a balanced source domain with an imbalanced and robust target dataset. Although we encountered some limitations, such as the high computational cost of calculating the similarity between the biosignals and the preprocessing strategy applied, among others detailed in this work, our experiment demonstrated the potential for transferring learning between neural networks processing heterogeneous electric biosignal datasets.

Keywords: Transfer learning, Electrical Biosignals, Recurrent Neural Network (RNN).

MSC | 185 | 2024

Transfer learning between deep neural networks using heterogeneous electrical biosignals

Andréa Leão Jesus Menezes dos Santos

UFBA

Transfer learning between deep neural networks using heterogeneous electrical biosignals

Andréa Leão Jesus Menezes dos Santos

Dissertação de Mestrado

Universidade Federal da Bahia

Programa de Pós-Graduação em
Ciência da Computação

September | 2024

Universidade Federal da Bahia
Instituto de Computação

Programa de Pós-Graduação em Ciência da Computação

TRANSFER LEARNING BETWEEN DEEP NEURAL NETWORKS USING HETEROGENEOUS ELECTRICAL BIOSIGNALS

Andréa Leão Jesus Menezes dos Santos

DISSERTAÇÃO DE MESTRADO

Salvador
2024-09-20

ANDRÉA LEÃO JESUS MENEZES DOS SANTOS

TRANSFER LEARNING BETWEEN DEEP NEURAL NETWORKS USING HETEROGENEOUS ELECTRICAL BIOSIGNALS

Esta Dissertação de Mestrado foi apresentada ao Programa de Pós-Graduação em Ciência da Computação da Universidade Federal da Bahia, como requisito parcial para obtenção do grau de Mestre em Ciência da Computação.

Orientadora: Prof. Dr. Luciano Rebouças de Oliveira
Co-orientador: Prof. Dr. Marcos Ennes Barreto

Salvador
2024-09-20

Ficha catalográfica elaborada pela Biblioteca Universitária de Ciências e Tecnologias Prof. Omar Catunda, SIBI – UFBA.

S237 Santos, Andréa Leão Jesus Menezes dos

Transfer learning between deep neural networks using heterogeneous electrical biosignals – Salvador, 2024.

74 f.

Orientador: Prof. Dr. Luciano Rebouças de Oliveira

Coorientador: Prof. Dr. Marcos Ennes Barreto

Dissertação (Mestrado) – Universidade Federal da Bahia. Instituto de Computação, 2024.

1.Transfer learning. 2.Electrical Biosignals. 3.Recurrent Neural Network. I. Oliveira, Luciano Rebouças de. II. Barreto, Marcos Ennes. III. Universidade Federal da Bahia. IV. Título.

CDU: 004

MINISTÉRIO DA EDUCAÇÃO
UNIVERSIDADE FEDERAL DA BAHIA
INSTITUTO DE COMPUTAÇÃO
PGCOMP - Programa de Pós-Graduação em Ciência da Computação
http://pgcomp.ufba.br

"*Transferência de aprendizado entre redes neurais profundas usando biossinais elétricos heterogêneos*"

Andrea Leão Jesus Menezes dos Santos

Dissertação apresentada ao Colegiado do Programa de Pós-Graduação em Ciência da Computação na Universidade Federal da Bahia, como requisito parcial para obtenção do Título de Mestre em Ciência da Computação.

Banca Examinadora

gov.br Documento assinado digitalmente
LUCIANO REBOUCAS DE OLIVEIRA
Data: 20/09/2024 16:08:42-0300
Verifique em https://validar.iti.gov.br

Prof. Dr. Luciano Rebouças de Oliveira (Orientador - PGCOMP)

gov.br Documento assinado digitalmente
MICHELE FULVIA ANGELO
Data: 23/09/2024 09:22:57-0300
Verifique em https://validar.iti.gov.br

Profa. Dra. Michele Fúlvia Angelo (UEFS)

gov.br Documento assinado digitalmente
VINICIUS GADIS RIBEIRO
Data: 22/09/2024 17:31:11-0300
Verifique em https://validar.iti.gov.br

Prof. Dr. Vinicius Gadis Ribeiro (UFRGS)

I dedicate this work to God and to my mother, Eliene Leo de Jesus.
Dedico este trabalho Deus e a minha me, Eliene Leo de Jesus.

ACKNOWLEDGEMENTS

The master's degree is significant for the revolutionary process of knowledge it provides. I am very grateful to God for allowing me to experience this moment. I also recognize the unfailing support given to my academic journey by my mother, Eliene Leão. To my siblings Daiana Santos and Leandro Leão, and my friends Adelair Santos, Ana Paula Gomes, Taís Santangelo, and Érica Georgia, thank you for encouraging me to explore the limits of knowledge even further. I thank my friends Emília and Christian Schmit for their excellent revision of the text. To my friends Mirlei Moura, Ph.D. student, and Daniela Almeida, Master's student, I thank you for your support and shared learning throughout the course of my master's degree. I also thank my supervisors Marcos Ennes Barreto and Luciano Rebouças de Oliveira for guiding me through this process and keeping my mind engaged with the questions of academic knowledge. Thank you very much to all of you.

Dessa vez eu me achei no caminho
Mas no me apeguei, pois sei que ele mudar.
Forte correnteza do rio
Que tanta certeza me d
Tira-me o cho
Leva-me consigo at no mais me suportar
Lana-me em novos afluentes
Para que eu possa, novamente, me desbravar
E nessa ciranda eu vou
At o mar me encontrar.

—ANDRA LEO (Descobrimentos Meus, 2021)

RESUMO

Os sistemas de saúde globais atualmente não conseguem atender adequadamente à alta demanda por cuidados de pessoas com distúrbios neurológicos. E essa lacuna impacta na qualidade do tratamento oferecido, ocasionando problemas como a prescrição de medicamentos inadequados, dificuldade de acesso ao tratamento, detecção tardia de doenças, entre outros. Os distúrbios neurológicos incluem condições como demência, epilepsia, Alzheimer, Parkinson, esclerose múltipla, entre outros. Para melhorar o tratamento dessas doenças, dispositivos têm sido desenvolvidos para a aquisição de biossinais elétricos visando obter biosinais com maior precisão, conforto ao paciente e, em alguns casos, custos mais baixos. Reconhecendo esse cenário, nosso objetivo foi investigar a possibilidade de usar a transferência de conhecimento entre redes neurais artificiais para abordar os problemas mencionados. Além disso, tentamos reduzir a complexidade matemática dos dados de biossinais elétricos, transformando-os do domínio do tempo para o domínio da frequência podendo assim representá-los através de funções algébricas em vez de funções senoidais. Com base nessas ideias, exploramos o potencial da transferência de conhecimento para melhorar a precisão preditiva de um modelo de rede neural que processa biossinais elétricos com características e rótulos não idênticos. Para evitar a transferência negativa, integramos a análise de similaridade entre biossinais em nossa metodologia usando a técnica de dynamic time warping (DTW). Selecionamos a rede neural long short-term memory (LSTM) para desenvolver a arquitetura proposta, e os conjuntos de dados públicos usados no experimento foram o TUEG EEG Corpora (eletroencefalograma), ECG Heartbeat Categorization (eletrocardiograma) e EMG Classify Gestures (eletromiografia para classificação de gestos). Usando os resultados dos modelos base como referência, selecionamos o ECG como domínio de origem. Em seguida, calculamos a similaridade entre os biossinais, treinamos o modelo com as características identificadas com a menor distância e transferimos os pesos e bias para os modelos EEG e EMG processarem seus próprios conjuntos de dados, chamados de domínio alvo. Em resumo, apresentamos dois cenários diferentes para experimentar e explorar o potencial de uma aplicação eficaz de aprendizado de transferência com biossinais elétricos heterogêneos no domínio de frequência, do ECG para o EMG e do ECG para o EEG, respectivamente. No primeiro cenário, descobrimos um resultado promissor quando os conjuntos de dados de origem e destino estavam equilibrados, mesmo com um conjunto de dados de destino pequeno. No segundo contexto, observamos uma diminuição discreta no desempenho, também referida como transferência de aprendizado negativa, ao utilizar um domínio de origem equilibrado com um conjunto de dados de destino desequilibrado e robusto. Embora tenhámos encontrado algumas limitações, como o alto custo computacional para calcular a similaridade entre os biossinais e a estratégia de pré-processamento aplicada, entre outras detalhadas neste trabalho, nosso experimento demonstrou o potencial para realização da transferência de

aprendizado entre redes neurais que processam dados bioelétricos heregeneous.

Palavras-chave: Transferência de Aprendizado, Biosinais Elétricos, Rede Neural Recorrente (RNN).

ABSTRACT

The global health systems are currently unable to adequately meet the high demand for care for people with neurological disorders. This impacts the quality of treatment offered, leading to issues such as the prescription of improper medications, difficulty accessing treatment, late detection of diseases, and more. Neurological disorders include conditions such as dementia, epilepsy, Alzheimer's, Parkinson's, multiple sclerosis, and others. To improve the treatment of these diseases, devices for the acquisition of electrical biosignals have been developed to provide greater accuracy, patient comfort, and, in some cases, lower costs. Recognizing this scenario, we aimed to investigate the possibility of using transfer learning among artificial neural networks to address these problems. Additionally, we attempted to reduce the mathematical complexity of electrical biosignal data by transforming it from time domain to frequency domain, representing it as algebraic functions rather than sine functions. Based on these ideas, we explored the potential of transfer learning to enhance the predictive accuracy of a neural network model processing diverse electrical biosignals with non-identical features and label spaces in a frequency domain. We integrated similarity analysis between biosignals into our methodology to prevent negative transfer learning using the dynamic time warping (DTW) technique. We selected the long short-term memory (LSTM) neural network to develop the proposed architecture, and the public datasets used for the experiment were the TUEG EEG Corpora (electroencephalogram), ECG Heartbeat Categorization (electrocardiogram), and EMG Classify Gestures (electroneuromyography). Using the baseline outcomes as a reference, we selected the ECG as the source domain. Then, we calculated the similarity between the biosignals, trained the model with the features identified as having the lowest distance, and transferred the weights and bias to the EEG and EMG models to process their own dataset, named the target domain. In summary, we present two scenarios to experiment and explore the potential of an effective transfer learning application with heterogeneous electrical biosignals in the frequency domain, from ECG to EMG and ECG to EEG, respectively. We discovered a promising outcome in the first scenario when the source and target datasets were balanced, even with a small target dataset. In the second context, we observed a discreet decrease in performance, also referred to as negative transfer learning, when utilizing a balanced source domain with an imbalanced and robust target dataset. Although we encountered some limitations, such as the high computational cost of calculating the similarity between the biosignals and the preprocessing strategy applied, among others detailed in this work, our experiment demonstrated the potential for transferring learning between neural networks processing heterogeneous electric biosignal datasets.

Keywords: Transfer learning, Electrical Biosignals, Recurrent Neural Network (RNN).

CONTENTS

LIST OF FIGURES

LIST OF TABLES

ABBREVIATIONS

EEG	Electroencephalogram
ECG	Electrocardiogram
EMG	Electroneuromyography
EOG	Electrooculography
LSTM	Long short-term memory
DTW	Dynamic time warping
PDF	Probability density function
FT	Fourier transform
IFT	Inverse fourier transform
PSD	Power spectral density function
C-PSD	Cross-power spectral density function
iEEG	Intracerebral electroencephalogram
CMAP	Compound muscle action potential
mV	Millivolts
ms	Milliseconds
CNN	Convolutional Neural Networks
SVM	Support Vector Machine
ADHD	Attention-deficit/hyperactivity disorder
VGG-16	Visual geometry group 16
MLP	Multilayer Perceptron Network
LR	Logistic Regression
TCA	Transfer Component Analysis
AAR	Automatic Artifact Removal
TSK-FS	Takagi-Sugeno-Kang fuzzy system
STFT	Short-Time Fourier Transform
EESC	EEG signal classification model
GHMM	Generalized fidden mapping model
VGG-19	Visual geometry group 19

RPS Reconstructed phase space
NFLE Nocturnal frontal lobe epilepsy
3DCNN 3D convolution neural network
BTRN BCI-Transfer learning method based on Relation Network
ILA Improved Label Space Alignment
CWT Continuous wavelet transform
LDA Linear discriminant analysis
QDA Quadratic discriminant analysis
MFTL Multi-source fusion transfer learning
CPS Common spatial pattern
ELM Extreme learning machine
HDNN-TL Hybrid deep neural network with transfer learning
MsCNN Multiscale convolutional neural network
ESVMs Ensemble of support vector machines
RA Rule adaptation
ARNN Attentional RNN network
RNN Recurrent neural network
HVG Horizontal visibility graph
TLCNN-DF Transfer learning convolutional neural network for data fusion
TUH Temple university hospital
EDF+ European data format
MIT Massachusetts institute of technology
CSV Comma-separated values
RMSE Root mean squared error

Chapter 1

"We all are in pursuit of one collective destiny. We all need just one. One dream. One day. One hour. One minute. One second. One moment." Sage Hasson

INTRODUCTION

1.1 CONTEXT AND MOTIVATION

Neurological and mental disorders, along with those caused by substance use, account for 13% of the global disease burden. These disorders include dementia, epilepsy, Alzheimer's disease, Parkinson's disease, and multiple sclerosis, to cite a few (WHO, 2021). Given the widespread prevalence of these diseases and the critical importance of proper treatment, it is essential to develop robust global health systems capable of adequately treating these conditions. In response to this scenario, numerous research projects have investigated brain functions to understand how neurological, mental, and substance use disorders manifest in the body (PISANO et al., 2020; ABDOLLAHPOUR et al., 2020; SHALBAF; BAGHERZADEH; MAGHSOUDI, 2020). These studies also explore the correlations between brain functions and various psychological and physiological factors, including musical stimulation (ER; ÇIĞ; AYDILEK, 2021) and emotional responses (LI et al., 2020), as well as genetic and behavioral predispositions for alcoholism (ZHANG et al., 2020b). Additionally, some studies address the problem of biomedical signal processing, focusing on the connections and interactions among various types of biosignals to better understand and interpret them (PHAN et al., 2020). Despite the interest in this research area, access to data such as electroencephalogram (EEG), electrocardiogram (ECG), electroneuromyography (EMG), electrooculography (EOG) and others is highly restricted due to its classification as sensitive data (KARI; SCHURIG; GERSCH, 2024).

The restrictions on data access are usually regulated by each country's official medical board, which sets rules for accessing patient profiles. Recently, some countries and states, including Brazil[1], California[2], and the European Union[3], have enacted specific laws to

[1]Brazil's Law <http://www.planalto.gov.br/ccivil_03/_ato2015-2018/2018/lei/L13709compilado.htm>

[2]California's Law <https://www.caprivacy.org/annotated-cpra-text-with-ccpa-changes/>

[3]EU's Law <https://eur-lex.europa.eu/legal-content/EN/TXT/HTML/?uri=CELEX:32016R0679&

protect personal data, including health data. There are also additional limitations associated with the global health system for neurological, mental, and substance use disorders. These include the low number of specialized and general health professionals to meet the demand, the poor quality of treatments, the lack of human and equipment resources, and their inequitable distribution worldwide. These issues result in the late detection of diseases and their stages of development, delayed onset of treatment, and the prescription of inappropriate medications for patients' needs (WHO, 2021). The legal restrictions on collecting, processing, and sharing sensitive data, coupled with the high cost of hiring qualified and specialized health professionals to evaluate and annotate the results, are factors that directly impact the costs of the biosignal data (CAO et al., 2019; TAN et al., 2019).

Given the aforementioned context, many researchers are exploring various approaches to mitigate the data restrictions and achieve more precise results in artificial intelligence methods for automatically classifying biosignals. One of the solutions is transfer learning (ZHANG et al., 2021; XU et al., 2019), which is recommended in contexts with insufficient data available to train a neural network and high costs associated with collecting and annotating datasets. This approach consists of techniques based on reusing pre-trained parameters from neural networks to improve performance in classification, regression, segmentation, and clustering tasks (TAN et al., 2018). The pre-trained parameters are a set of values that the neural network learns during its training phase. These include weights and biases, representations of the layers within the network, the overall structure of the network, and hyperparameters. These pre-trained parameters can be used, individually or together, to improve another neural network's performance by transferring this learned knowledge. This set of parameters is used to fine-tune the function $f(.)$, which predicts the likelihood (or probability) of a specific event happening. For instance, given a piece of data, x_i, from a dataset, the function $f(.)$ can estimate the chance that a certain label y (which represents the event) will occur (PAN, 2014). It can be expressed as the conditional probability $P(X|Y)$, which shows the probability of the data X given the event Y (WAN et al., 2021). One dataset, referred to as the source domain, is used to train a neural network to recognize and generalize features, thereby providing the parameters for transfer. The other dataset is the target domain, which the neural network will process using the pre-trained parameters. When the source and target domains consist of the same data with identical features and labels, this is termed homogeneous transfer learning. Conversely, when the datasets involve diverse collection processes, different features, distinct labels, or represent different data, it is known as heterogeneous transfer learning (WAN et al., 2021). In heterogeneous transfer learning, the focus lies in understanding the characteristics of different datasets, establishing connections among them, transferring pre-trained parameters to the target neural network, and improving its outcomes.

In the context of biosignals, data can be classified according to their physical char-

from=EN>

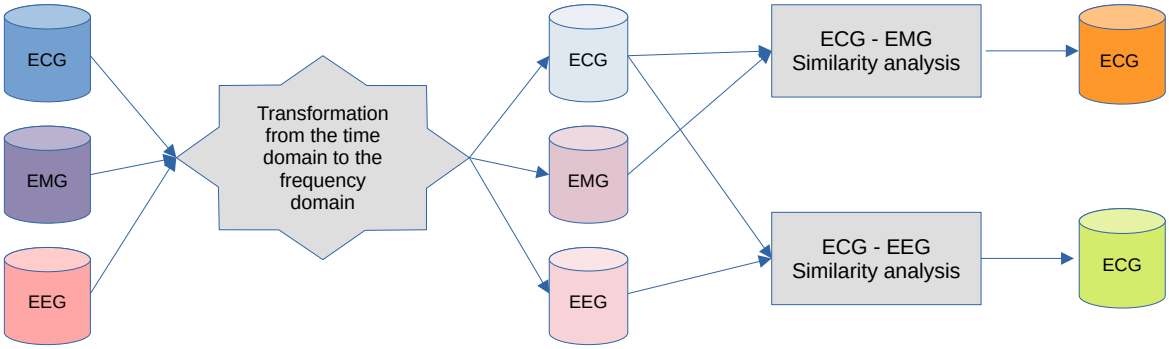

Figure 1.1: This sequential process describes the transformation of ECG, EMG, and EEG electrical biosignals from the time domain to the frequency domain, followed by the calculation of similarities between ECG and EMG and between ECG and EEG. This process results in two datasets comprising the most similar ECG waves from ECG-EMG and ECG-EEG.

acteristics, such as chemical, electrical, mechanical, and others (COHEN, 2006). We focused our attention on electrical biosignals. Once the electrical biosignals are available for research and the type of transfer learning – whether homogeneous or heterogeneous – is defined, it is important to determine the domain in which the data will be analyzed. There are three possible domains to analyze electrical biosignals: time, frequency, and time-frequency. To better understand time domain behavior, sinusoidal functions can be employed, whereas frequency domain analysis can utilize algebraic functions, which often involve simpler equations compared to those in the time domain. Time-frequency analysis employs both sinusoidal and algebraic functions. All studies referenced in this dissertation that involve transfer learning are either in the time or time-frequency domain in their investigations. In these studies, we have also observed limited experiments with non-identical datasets. Presumably, this occurs based on the state-of-the-art assumption in transfer learning that source and target datasets must lie within the same subject area and have the same event distribution to enable effective transfer (WAN et al., 2021; CHUANQI et al., 2018; WEISS; KHOSHGOFTAAR; WANG, 2016; PAN; YANG, 2010). Additionally, we did not find, in the literature, a robust analysis regarding the negative effects of transfer learning on their experiments, which usually occur when it leads to the degradation of the target neural network performance (CAO et al., 2019; WAN et al., 2021). This discussion is relevant for identifying situations where transfer learning should not be conducted and/or indicating good practices to avoid negative transfer.

The perception of the previously mentioned shortcomings guided us to explore the potential of heterogeneous transfer learning with different electrical biosignals. Our ini-

tial step was to select three types of electrical biosignals: ECG Heartbeat Categorization (MOODY; MARK, 2001), EMG Gesture Classification (ZHAI et al., 2017), and TUEG EEG Corpora (OBEID; PICONE, 2016). We then decided that the analysis of these biosignals would be conducted in the frequency domain to achieve a mathematical simplification of wave representations, thereby facilitating their evaluation by a long short-term memory (LSTM) model. We employed the discrete Fourier transform technique to convert the biosignals from the time domain to the frequency domain. The next step was to determine which dataset could be used to train an LSTM model that would provide parameters to the other LSTM model processing the target domain.

In this process of selecting source and target datasets, our strategy was guided by baseline outcomes. The dataset that was better mapped by the LSTM baseline, which produced superior outcomes, was designated as the source domain, while others were assigned as the target domain. Consequently, due to the superior outcomes observed with the ECG LSTM baseline, we selected the ECG dataset as the source domain, with EMG and EEG designated as the target domains. After this selection, we applied the similarity analysis method between the source and target domains to select the most similar ECG waves to train the ECG LSTM model. That approach, named similarity analysis, was conducted using the dynamic time warping (DTW) method due to its superior distance measurement capabilities, which result from its consideration of variations in the waves' time and amplitude. DTW resolves distortions and shifts in time series data by non-linearly aligning the sequences, ensuring similar patterns are matched even if they occur at different times (GIORGINO, 2009). We conducted two similarity comparisons: one between ECG and EMG biosignals and another between ECG and EEG biosignals. Following this process, we created two new ECG datasets, each comprising the most similar waves identified from the ECG-EMG and ECG-EEG comparisons (see Figure 1.1). This process enabled us to observe how lower distances, indicating high similarity between the biosignal waves, contributed to an improved understanding and generalization of biosignals by the LSTM model and mitigated the negative transfer effects in our two transfer learning scenarios. Finally, we trained two LSTM models, each using one of these ECG datasets generated through the similarity comparison process, and implemented heterogeneous transfer learning.

We chose to use a model reuse strategy to implement the transfer learning. It involves the reuse of all weights, biases, and parameters from all layers of the pre-trained LSTM model, as illustrated in Figure 1.2. Reusing model parameters allowed us to capitalize on previously acquired knowledge, reducing the need for extensive labeled data in the target domain. This strategy facilitated the efficient configuration of neural network architectures for novel tasks, thereby enhancing their ability to generalize and improve overall performance. The transfer learning from ECG to EMG demonstrated positive results, indicating a successful process. In contrast, transfer learning from ECG to EEG exhibited a slight decline in performance, indicative of negative transfer. This outcome suggests that state-of-the-art concepts in transfer learning may be extended by identifying common characteristics across heterogeneous data. Further validation of this extension

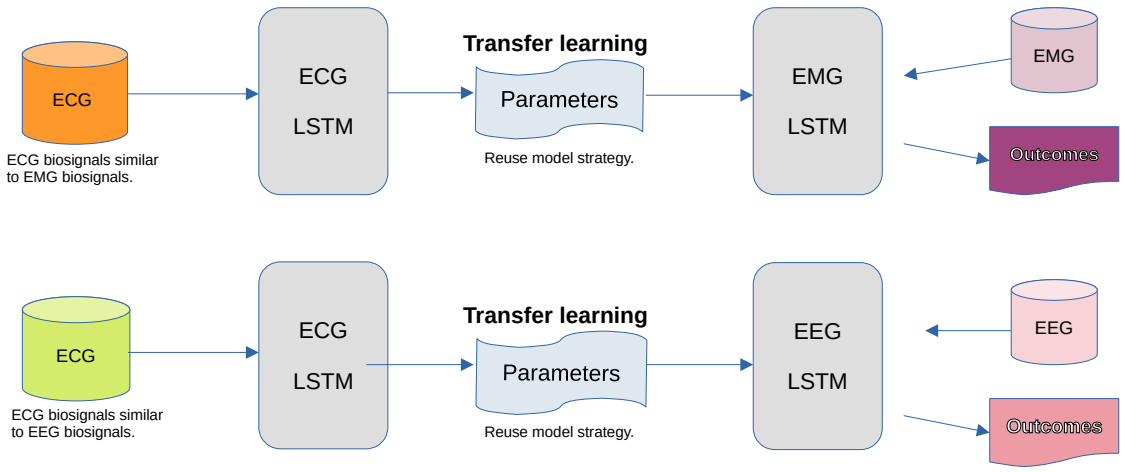

Figure 1.2: Two LSTM neural networks were trained using the most similar ECG datasets identified during the similarity analysis, followed by the application of a transfer learning approach using the reuse model strategy. This process involved transferring the trained LSTM architecture, including its layers, weights, and biases, to process the EMG and EEG biosignals in the frequency domain.

can be achieved through future complementary studies.

1.2 RESEARCH QUESTIONS

We formulated the following research question:

Does transfer learning between neural network models processing heterogeneous electrical biosignals in frequency domain have the potential to increase the predictive accuracy of the target model?

Additionally, we also addressed the following secondary questions:

Question 01: In which scenarios did negative transfer occur?

Question 02: Can processing data in the frequency domain mitigate the effect of unbalanced data?

Question 03: Can the evaluation of similarity between the signals lead to gains in the accuracy of the target model?

1.3 CONTRIBUTIONS

The main contributions of our research are as follows: We present an exploratory study on heterogeneous transfer learning using three distinct electrical biosignal datasets (ECG, EMG, and EEG) in the frequency domain. In this context, our findings suggest

that it is feasible to apply transfer learning between neural networks processing different types of electrical biosignals, particularly between ECG and EMG. Additionally, our work indicates that processing data in the frequency domain can mitigate the effects of unbalanced data; however, it was not sufficiently effective to avoid slight negative transfer learning in the ECG-EEG scenario. Finally, our study highlights that the similarity analysis did not significantly enhance the accuracy of the target models.

1.4 CHAPTER MAP

The next chapters are organized as follows:

Chapter 2 explains how the concepts of transfer learning were developed, defines different transfer learning models, describes the characteristics of electrical biosignals, details electroencephalogram, electrocardiogram, and electromyography biosignals, and presents a literature review of transfer learning with electrical biosignals.

Chapter 3 describes our research process, detailing the methodology, baselines, and measures used.

Chapter 4 describes the execution of the experiment phases, its outcomes, and the analysis of the process and results.

Chapter 5 presents the concluding remarks, summarizing the significant learnings achieved through this research and suggesting future work.

Chapter 2

"Education is our passport to the future, for tomorrow belongs to the people who prepare for it today."
Malcolm X

BACKGROUND

2.1 TRANSFER LEARNING

Transfer learning encompasses a set of techniques that enable neural networks to achieve enhanced performance by utilizing previously acquired knowledge, represented through weights, biases, layers, the overall structure of the network, and hyperparameters (WANG; YANG, 2019). Within this process, a source model is trained to recognize information from one or more source domain datasets. The parameters acquired by the source neural network model will subsequently be transferred, individually or collectively, to a target neural network, aiming to facilitate the extraction of information from the target domain (WEISS; KHOSHGOFTAAR; WANG, 2016). By leveraging this approach, transfer learning enhances the reuse of pre-trained parameters across disparate domains. This paradigm challenges the conventional assumption that data must reside within the same feature space and possess an identical distribution to facilitate transfer. In contrast, traditional concept maintain these assumptions as true, thereby limiting the applicability of transfer learning techniques in real-world scenarios (HE; WU, 2020). In practice to this view, it is not feasible to ensure a high level of equality between different application domains due to the variability in projects, their objectives, and their data collection methods.

2.1.1 Notations and definitions

We will explain the notations and definitions presented by Pan e Yang (2010), which will help us understand the purpose of each element, as illustrated in Figure 2.1, and how transfer learning processes them. The elements are as follows:

- *Domain*($\mathcal{D}$) - two elements express it: the feature space $\mathcal{S}$ and the marginal probability distribution $\mathcal{P}(\mathcal{X})$, where $\mathcal{S} = \{x_1, x_2, \ldots, x_n\} \in X$. The x_i represents the items that compose the feature space. In other words, x_i is the i-th feature vector

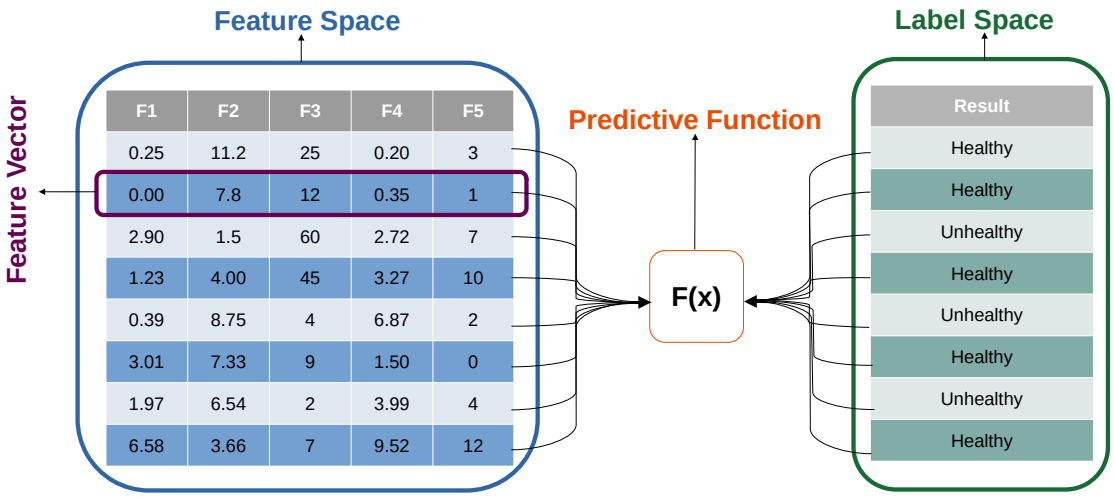

Figure 2.1: The components of transfer learning include the feature space, feature vector, label space, and predictive function. The feature space corresponds to specific features of the data. Feature vectors are represented as points in a multi-dimensional space, where each point corresponds to a data instance with particular features. The label space is the set of possible output labels for classification. The predictive function is the function that maps feature vectors to their corresponding labels.

(instance) in the feature space. The marginal probability distribution is the probability distribution of the feature vector contained in the subset. It demonstrates how the feature space's data is distributed and allows us to explore the interrelationship between each feature in a domain (ASSUNCAO, 2021). To illustrate, assume that our learning task is to classify epilepsy seizure phases using electroencephalogram (EEG) scans. In the EEG dataset, each measured signal parameter is a feature, so $\mathcal{X}$ is the space for all parameters in the set, where x_i is the i-th feature that correlates with the seizure phases. As a result, the domain representation is $\mathcal{D} = \{X, P(X)\}$.

- *Task*($\mathcal{T}$) - two elements define the task: the label space $\mathcal{Y}$ and the predictive function $f(.)$. Therefore, the representation of the task is $\mathcal{T} = \{Y, f(.)\}$. The training process of a model aims to learn how to determine the elements of the task, consisting of pairs $\{x_i, y_i\}$ where $x_i \in \mathcal{X}$ and $y_i \in \mathcal{Y}$. The function $f(.)$ can predict the corresponding label of a new instance x with $f(x)$. In summary, the function $f(.)$ receives a new instance x to infer the corresponding label with $f(x)$. In a probabilistic view, $\mathcal{P}(\mathcal{Y}|\mathcal{X})$ represents the function $f(.)$, denoting the probability that $\mathcal{Y}$ occurs under the condition $\mathcal{X}$ (conditional probability) (WAN et al., 2021). For example, $\mathcal{Y}$ represents the states of an epileptic attack (GAO et al., 2020). Then, a new instance x is provided to the function $f(x)$ to predict the epileptic seizure phase.

In possession of these notations, we can define the source domain ($\mathcal{D}_S$) and target

domain ($\mathcal{D}_\mathcal{T}$) as:

$$D_S = \{(x_{S1}, y_{S1}), ..., (x_{Sn}, y_{Sn})\} \tag{2.1}$$

$$D_T = \{(x_{T1}, y_{T1}), ..., (x_{Tn}, y_{Tn})\} \tag{2.2}$$

in Equation 2.1, $x_{S_i} \in \mathcal{X}_\mathcal{S}$ and is the i-th data instance of $\mathcal{D}_\mathcal{S}$. Just as $y_{S_i} \in \mathcal{Y}_\mathcal{S}$ and represents the class label for x_{S_i}. We have a similar correspondence in Equation 2.2, where $x_{T_i} \in \mathcal{X}_\mathcal{T}$ and is the i-th data instance of $\mathcal{D}_\mathcal{T}$ as well as $y_{T_i} \in \mathcal{Y}_\mathcal{T}$ and describes the class label for x_{T_i}. Furthermore, $\mathcal{T}_\mathcal{S}$ represents the source task, $\mathcal{T}_\mathcal{T}$, the target task, $f_S(.)$, the source prediction function, and $f_T(.)$, the target prediction function (WEISS; KHOSHGOFTAAR; WANG, 2016). Given this information, we can formally present the main definition of transfer learning:

> **Transfer Learning**: Given a source domain $\mathcal{D}_\mathcal{S}$ and learning task $\mathcal{T}_\mathcal{S}$, a target domain $\mathcal{D}_\mathcal{T}$ and learning task $\mathcal{T}_\mathcal{T}$, transfer learning intends to help enhance the learning of the target predictive function $f_T(.)$ in $\mathcal{D}_\mathcal{T}$, using knowledge in $\mathcal{D}_\mathcal{S}$ and $\mathcal{T}_\mathcal{S}$, where $\mathcal{D}_\mathcal{S} \neq \mathcal{D}_\mathcal{T}$, or $\mathcal{T}_\mathcal{S} \neq \mathcal{T}_\mathcal{T}$ (PAN; YANG, 2010).

Formally, given a domain $\mathcal{D} = \{X, P(X)\}$, this definition specifies the condition where $\mathcal{D}_\mathcal{S} \neq \mathcal{D}_\mathcal{T}$ assumes either $\mathcal{X}_\mathcal{S} \neq \mathcal{X}_\mathcal{T}$ or $\mathcal{P}(\mathcal{X}_\mathcal{S}) \neq \mathcal{P}(\mathcal{X}_\mathcal{T})$. Similarly, given a task $\mathcal{T} = \{Y, P(Y|X)\}$ the condition that $\mathcal{T}_\mathcal{S} \neq \mathcal{T}_\mathcal{T}$ implies either $\mathcal{Y}_\mathcal{S} \neq \mathcal{Y}_\mathcal{T}$ or $\mathcal{P}(\mathcal{Y}_\mathcal{S}|\mathcal{X}_\mathcal{S}) \neq \mathcal{P}(\mathcal{Y}_\mathcal{T}|\mathcal{X}_\mathcal{T})$ (WEISS; KHOSHGOFTAAR; WANG, 2016).

Transfer learning can be applied to various real-world scenarios. The simplest scenario involves a source domain D_S and a target domain D_T, as illustrated in Figure 2.2. More complex structures can be modeled by incorporating additional source domains. Consequently, transfer learning proposal have facilitated the use of data with different spatial distributions or resources, enhancing the potential for parameters reuse among models. This approach reduces the distance between the source and target domains and ensures the sharing of similarities based on their feature spaces and/or labels (WAN et al., 2021).

2.1.2 Heterogeneous transfer learning

Based on the previous concepts, Pan e Yang (2010) proposed three questions to analyze the feasibility of the transfer: What knowledge should be transferred? How can the transfer be achieved? When is it appropriate to perform the transfer? The first question guides us in analyzing the domains and tasks to identify the type of knowledge and what can be transferred. The second question pertains to the selected transfer technique. Finally, the third question involves evaluating whether the learned parameters should be shared across domains or tasks in the proposed scenario. If, after this analysis, we decide to share incompatible knowledge between the source and target domains, the process

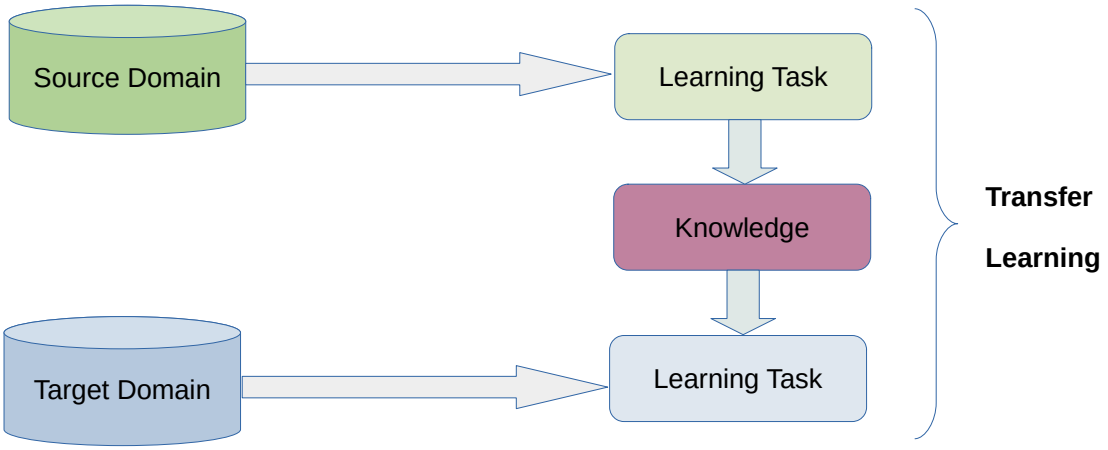

Figure 2.2: The transfer learning process representation: training a model with the source domain, transferring the acquired knowledge (weights and biases) to another learning task, and subsequently processing the target domain, taken from (CHUANQI et al., 2018).

may result in decreased learning performance in the target domain. This phenomenon is known as negative transfer.

After analyzing the three questions mentioned, our research focused in the feature types concept which examines the semantics in the source and target domains, $\mathcal{D}_\mathcal{S} = \{X_S, P(X_S)\}$ and $\mathcal{D}_\mathcal{T} = \{X_T, P(X_T)\}$ to realize heterogeneous transfer learning. This approach involves understanding the characteristics of different datasets, establishing connections among them, transferring pre-trained parameters to the target neural network, and ultimately improving its outcomes. The source and target datasets are considered heterogeneous if they are created using diverse collection processes, have non-identical features or labels, or represent different data. Essentially, the semantics and dimensions of the domains are different (WAN et al., 2021), as detailed mathematically below:

> **Definition**: Given a source domain $\mathcal{D}_\mathcal{S}$ and learning task $\mathcal{T}_\mathcal{S}$, a target domain $\mathcal{D}_\mathcal{T}$ and learning task $\mathcal{T}_\mathcal{T}$, heterogeneous transfer learning aims to improve the learning of the target predictive function $f_T(.)$ in $\mathcal{D}_\mathcal{T}$ using the knowledge in $\mathcal{D}_\mathcal{S}$ and $\mathcal{T}_\mathcal{S}$, where $\mathcal{X}_\mathcal{S} \cap \mathcal{X}_\mathcal{T} = \emptyset$ and\or $\mathcal{Y}_\mathcal{S} \neq \mathcal{Y}_\mathcal{T}$ (PAN, 2014).

There are two strategies for developing heterogeneous transfer learning. The first is called heterogeneous feature spaces, which offer two implementation possibilities: symmetric transformation, which attempts to learn a pair of feature mappings related to the

source and target domains. The mapped features are then grouped into a common latent space to compose a new feature space (WEISS; KHOSHGOFTAAR; WANG, 2016). The other possibility is asymmetric transformation, which learns about the source domain features and transfers them to the target domain (PAN, 2014). The second strategy involves different label spaces. It observes the relationship between the label spaces of the source and target domains. Based on this observation, the technique propagates knowledge across the domains (PAN, 2014).

2.1.3 Advantages and disadvantages

The appropriate selection of source subjects and the ability to choose data with high similarity to the target subject are crucial for establishing an effective environment for transfer learning (LIANG; MA, 2020). This principle offers several advantages, including knowledge reuse, cost reduction, and improved outcomes. Knowledge reuse entails transferring previously established parameters to other neural network models to enhance the predictive function ($f_T(.)$) of the target model (WANG et al., 2020). Cost reduction aims to minimize the reliance of neural networks on extensive datasets for training and achieving broad generalization capabilities. Transfer learning can reduce expenses associated with data collection, annotation, and the training process, making it more feasible, especially in scenarios with limited training data or high project costs (WANG et al., 2020).

However, the disadvantage of using transfer learning is known as negative transfer. This occurs when the transferred parameters degrade the performance of the target prediction function ($f_T(.)$) (CAO et al., 2019). This phenomenon can arise when the characteristics of the source and target domains are inadequately related. Incorrect data selection may lead to the transfer of unrelated parameters, thereby reducing the likelihood of successful transfer. Additionally, choosing an inappropriate transfer technique can also contribute to negative transfer. Selecting an incorrect method for the data scenario may compromise the entire transfer process, potentially exerting a more detrimental effect on the target model's performance than if no transfer had been attempted (WAN et al., 2021; PAN; YANG, 2010; LIN, 2019).

2.2 ELECTRICAL BIOSIGNALS

Electrical biosignals are fluctuations of energy, produced by muscles and nerve cells, that provide valuable information for understanding some parts of the complex pathophysiological mechanisms of living systems (SEMMLOW; GRIFFEL, 2014; LIANG; BRONZINO; PETERSON, 2012). These systems generate signals that encode various aspects of the system's health and human physiology (RUTH; NEILS, 2020) and allow for the analysis of many internal structures of the body (KANT et al., 2020).

Table 2.1: Biomedical signal characteristics are described as follows: Bioelectric classification categorizes signals based on their segmentation according to frequency range groups. Acquisition specifies the equipment used for biosignal collection. Frequency range defines the spectrum of frequencies over which the signal exhibits significant activity or variation. Dynamic range measures the amplitude or intensity range of a signal by calculating the ratio between its largest and smallest detectable values. Comments provide additional complementary information about the biosignals. (COHEN, 2006).

Bioelectric Classification	Acquisition	Frequency range	Dynamic range	Comments
Electroencephalogram (EEG)				
Surface	Surface electrodes	0.5–100 Hz	2–100 µV	Multichannel (6 – 32) scalp potential
Delta range		0.5–4 Hz		Young children, deep sleep and pathologies
Theta range		4–8 Hz		Temporal and central areas during alert states
Alpha range		8–13 Hz		Awake, relaxed, closed eyes
Beta range		13–22 Hz		
Sleep spindles		6–15 Hz	50–100 µV	Bursts of about 0.2–0.6 sec
K-complexes		12–14 Hz	100–200 µV	Bursts during moderate and deep sleep
Surface EMG (SEMG)	Surface electrodes			
Skeletal muscle		2–500 Hz	50 µV–5 mV	
Smooth muscle		0.01–1 Hz		
Electrocardiogram (ECG)	Surface electrodes	0.05–100 Hz	1–10 mV	
High-frequency ECG	Surface electrodes	100 Hz–1 kHz	100 µV–2 mV	Notchs and slus waveforms superimposed on the ECG

2.2.1 Characteristics

There is a diversity of electrical biosignals, primarily categorized into permanent and induced groups. The permanent group includes all electrical biosignals that manifest without external stimulus, while the induced group requires artificial provocation for manifestation (KANIUSAS, 2019; WANG et al., 2019a). Both groups share common characteristics such as recording mode, representation, dynamic and frequency range, embedded noise, and time-series data storage, and etc (COHEN, 2006), as presented in Table 2.1.

2.2.1.1 Record mode typically categorizes a signal as either continuous or discrete. A continuous signal, represented by the function $s(t)$, spans a time interval and can assume any real value and amplitude during this period (BROCKWELL; DAVIS, 2002; **??**). In contrast, a discrete signal, represented by the function $s(m)$, provides information at specific points on the time axis with distinct levels of amplitude at each point (SEMMLOW, 2017). The discrete function $s(m)$ is derived from the continuous signal $s(t)$ through a process known as sampling

$$s(m) = s(t)|_{t=mT_s} \quad \text{m = ..., -1, 0, 1, ...} \tag{2.3}$$

where m represents a point in the time axis and the sampling interval is given by T_s in Equation 2.3 (COHEN, 2006).

2.2.1.2 Representation categorizes signals into deterministic or stochastic types. Deterministic signals, accurately represented mathematically or graphically, do not typically correspond to real-world signals that often contain noise (COHEN, 2006). Their predictable behavior allows forecasting based on previous records, represented as $s(t)$ (SEMMLOW, 2017), as expressed below

$$s(t) = s(t + nT) \tag{2.4}$$

where t is the given time, T is the period, and $n \in \mathbb{Z}$. Stochastic signals represent real-world scenarios where inherent uncertainty and randomness are present from their inception (COHEN, 2006). As a result of this inherent randomness, stochastic signals cannot be precisely represented by mathematical or graphical expressions. However, they can be effectively described in terms of ensemble probabilities $S(t)$, where the ensemble maintains the same probability distribution despite individual signal variations (SEMMLOW, 2017). In this context, random variables are denoted by corresponding lowercase letters $s(t)$. The Nth order statistical behavior and interdependence of the process can be described using the joint probability function

$$P[s(t_1) \leq s_1, [s(t_2) \leq s_2, ..., s(t_N) \leq s_N] = P(s_1, s_2, ..., s_N) \tag{2.5}$$

where s_N represent the signal in its maximum duration in seconds.

2.2.1.3 Time and frequency domain analysis methods examine electrical signals to extract characteristics useful for diagnosing, monitoring, or intervening in bodily events such as diseases, organ behavior, and fitness (YANG et al., 2015; COHEN, 2006; BIZOPOULOS; KOUTSOURIS, 2019; KHAN et al., 2020). The time domain facilitates the extraction of features based on how signal changes occur along the time axis (BALAFAS; RAJAGOPAL; KIREMIDJIAN, 2015; YANG et al., 2015; BROCKWELL; DAVIS, 2002). These features reveal attributes of the waveform, such as kurtosis, amplitude, and period (YANG et al., 2015). By deriving the joint probability function (Equation 2.5), the joint probability density function (PDF) is obtained, which is often used to estimate the probability distribution of the set (MOESLUND et al., 2020). The PDF is defined as

$$p(s_1, s_2, ..., s_n) = \frac{\partial^n}{\partial_{S_1} \partial_{S_2} L \partial_{S_n}} [P(s_1, s_2, ..., s_n)] \tag{2.6}$$

where ∂^n is the unit impulse function calculated for a given signal time n, also known as the Dirac delta function (FENG et al., 2023). If we replace $S(t_i)$ for S_i, we have an abbreviation of the Equation 2.6

$$p(s, t) = p_{s_1, s_2, ..., s_n}(s_1, s_2, ..., s_n) \tag{2.7}$$

The first and second order PDFs are the two relevant cases in PDF: considering m a discrete point on the time axis, the expectation of the process $S(t)$ is a mean statistical function expressed as:

$$\mu_S(t) = E[S(t)] = \int_{-\infty}^{+\infty} s(t) * p(s,t)\, d_s \tag{2.8}$$

The Nth order moment (nth-order) is called expectation of the process $S^n(t)$(BALAFAS; RAJAGOPAL; KIREMIDJIAN, 2015; COHEN, 2006) which is defined as

$$E[S^n(t)] = \int_{-\infty}^{+\infty} s^n(t) * p(s,t)\, d_s \tag{2.9}$$

There are some other statistical operations to extract information from the signal ensemble, such as the Nth central moment (BALAFAS; RAJAGOPAL; KIREMIDJIAN, 2015; COHEN, 2006)

$$\mu_n = E\{(S(t) - m_s)^n\} = \int_{-\infty}^{+\infty} (s(t) - m_s)^n\, p(s,t)\, d_s \tag{2.10}$$

The variance σ^2, also denominated second central moment, is the square root of which standard deviation

$$\sigma^2 = \mu_2 = E\{(S(t) - m_s)^2\} = \int_{-\infty}^{+\infty} (s(t) - m_s)^2\, p(s,t)\, d_s \tag{2.11}$$

The auto-correlation function r_{ss} is the second-order joint moment which is defined by the joint PDF

$$r_{ss}(t_1,t_2) = E\{(S(t_1) - S(t_2)\} = \int_{-\infty}^{+\infty}\int_{-\infty}^{+\infty} s(t_1)s(t_2)\, p(s_1,s_2)\, d_{s1}d_{s2} \tag{2.12}$$

The cross-correlation function also defined as the second joint moment of the signal s at time t_1, $s(t_1)$ and the signal y at time t_2, $y(t_2)$

$$r_{sy}(t_1,t_2) = E\{(s(t_1) - y(t_2)\} = \int_{-\infty}^{+\infty}\int_{-\infty}^{+\infty} s(t_1)y(t_2)\, p(s_1,y_2)\, d_{s1}d_{y2} \tag{2.13}$$

All the aforementioned functions can help to explore the stochastic signal and to understand its behavior in time domain. The analysis in the frequency domain describes the electric biosignal as a continuous set of sine waves characterized by their magnitude and phase (COHEN, 2006). This is represented by the complex function $S(\omega)$, which is given by:

$$S(\omega) = |S(\omega)|\, e^{j\theta(\omega)} \tag{2.14}$$

where $|S(\omega)|$ represents the amount of content the original signal has at the frequency ω, and the complex exponential $e^{j\theta(\omega)}$ describes the magnitude and phase spectrum at

frequency. To convert the perspective of an electric biosignal from the time domain to the frequency domain, the *fourier transform* (FT) is used, as

$$S(\omega) = \int_{-\infty}^{+\infty} s(t)\, e^{-j\omega t}\, d_t = F[s(t)] \tag{2.15}$$

where the angular frequency is $\omega = 2\pi f$ and the fourier operator is represented by F(*). The *inverse fourier transform* (IFT) transforms the signal perspective from the frequency domain to the time domain

$$s(t) = \frac{1}{2\pi} \int_{-\infty}^{+\infty} S(\omega)\, e^{j\omega t}\, dw = F^{-1}\left[S(\omega)\right] \tag{2.16}$$

The correlation function of the process is a deterministic function that is another option of frequency representation. The correlation function produces a deterministic frequency function when it is applied to the FT. As a result of the FT of the correlation function, we have the power spectral density function (PSD) (BALAFAS; RAJAGOPAL; KIREMIDJIAN, 2015; COHEN, 2006)

$$PSD[s(t)] = S_{ss}(\omega) = F[r_{ss}\,(\tau)] = \int_{-\infty}^{+\infty} r_{ss}(\tau) e^{-j\omega t}\, d\tau \tag{2.17}$$

where $S_{ss}(\omega)$ symbolize the power spectral density function which is always real and non-negative, and the spectrum of a real valued process. And $r_{ss}(\tau)$ is the auto correlation function. When we want to explore the relationship between two signals, we use the cross-correlation function, as presented by Equation 2.13 in the time domain view. In the frequency representation, the FT of the cross-correlation function generates the cross-power spectral density function (C-PSD), also called cross-spectrum

$$S_{sy}(\omega) = F[r_{sy}\,(\tau)] = |S_{sy}(\omega)| e^{j\theta_{sy}(\omega)} \tag{2.18}$$

where $s(t)$ and $y(t)$ are understood as stationary signals. Hence, the cross-correlation function is not on the time perspective but that of the time difference t. Similarly, the auto-correlation function $r_{sy}\,(\tau)$ is also not on the time perspective. This scenario makes the FT of auto-correlation not real because is not possible transform it from frequency domain to time domain. Another characteristic is that C-PSD require the absolute value and phase. The absolute value of the C-PSD bound is:

$$|S_{sy}(\omega)|^2 \leq S_{ss}(\omega) S_{yy}(\omega) \tag{2.19}$$

The coherence function is the normalized absolute value of the C-PSD:

$$Y_{sy}^2\, \frac{|S_{sy}(\omega)|^2}{S_{ss}(\omega) S_{yy}(\omega)} \leq 1 \tag{2.20}$$

2.2.2 Types of Biosignals

In the previous section, we mentioned that muscles and cells emit electrical signals that propagate through the body (KANT et al., 2020). In this section, we detail the

functioning of organs and muscles, the collection of the electrical signals, and the main characteristics of the signals used in this research. The goal is to understand the generated electrical signal and its characteristics.

2.2.2.1 Eletroencephalogram biosignal (EEG) The brain emits electrical waves through nerve impulses, which propagate until they reach the scalp (WAN et al., 2021; XU et al., 2019). The electroencephalogram is an instrument used to measure and record the voltage oscillations of these electrical waves, employing electrodes strategically positioned as sensors (ABDELHAMEED; BAYOUMI, 2018). There are two methods to register these biosignals: intracerebral electroencephalogram (iEEG), which is an invasive procedure involving electrode implantation inside the cranial cavity directly onto the brain surface (NEJEDLY et al., 2019), and standard EEG examination, which non-invasively measures brain wave types using electrodes placed on the scalp (ROMAY et al., 2020), see all scalp points map at the Figure 2.4. Both EEG and iEEG record brain waves originating from specialized regions, each responsible for distinct functions: the motor area controls voluntary muscle movements; the sensory area processes sensations like temperature, pressure, and pain; the frontal lobe regulates movement, problem-solving, concentration, thinking, behavior, personality, and mood; Broca's area governs speech production; the temporal lobe coordinates hearing, language, and memory; the brainstem oversees consciousness, breathing, and heart rate; the parietal lobe manages sensations, language, perception, body awareness, and attention; the occipital lobe handles vision and visual perception; Wernicke's area controls language comprehension; and the cerebellum coordinates posture, balance, and movement (MANSOOR et al., 2020) (see Figure 2.3).

2.2.2.2 Eletrocardiogram biosignal (ECG) The muscular contractions of the heart generate an electrical biosignal (KACHUEE; FAZELI; SARRAFZADEH, 2018). This biosignal is primarily produced by two types of specialized heart muscle cells: the myocardium of the atria and the myocardium of the ventricles (RANGAYYAN, 2015). These signals propagate through the body, and are recorded using electrodes during an electrocardiogram (ECG) examination. Some electrodes capture signals directly from the heart muscle using intracardiac electrodes for precise cardiac signal recording (KANIUSAS, 2019), while others register the biosignal through contact with the skin of the upper limbs, lower limbs, and chest (NAÏT-ALI, 2009). The heart operates by receiving deoxygenated blood from the upper and lower parts of the body is brought by the superior and inferior vena cavae respectively, both leading into the right atrium. Here, the sinoatrial node serves as the heart's natural pacemaker, initiating the electrical impulse that begins each heartbeat. From the right atrium, blood flows through the tricuspid valve into the right ventricle, which then pumps it through the pulmonary valve into the pulmonary artery. This artery carries the blood to the lungs for oxygenation. Oxygenated blood returns to the heart via the pulmonary veins, entering the left atrium. The left atrium contracts, pushing blood through the mitral valve into the left ventricle, which then pumps oxygen-rich blood through the aortic valve into the aorta. The aorta distributes this oxygenated blood throughout the body. Throughout these processes, the atrioventricular node, bundle branches (including the right and left bundle branches and

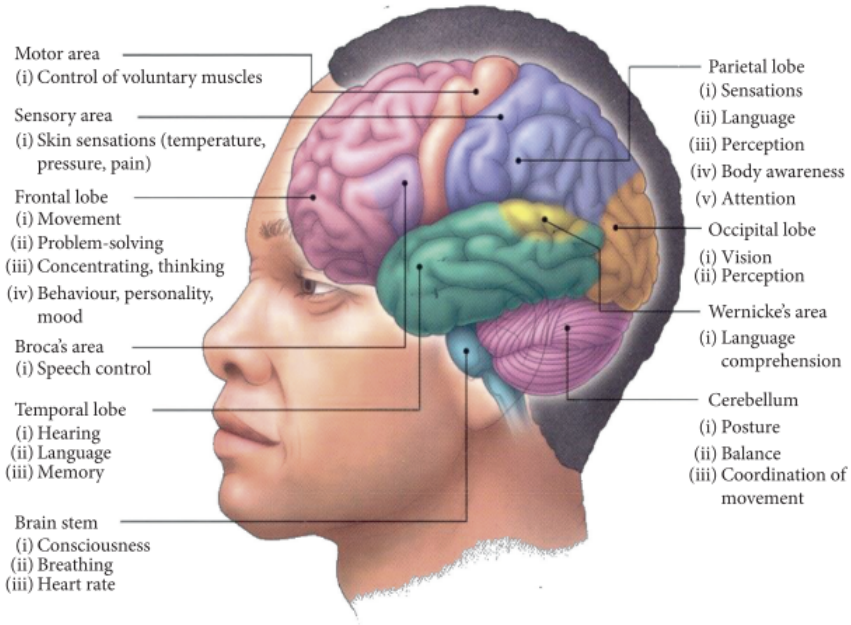

Figure 2.3: The brain is anatomically and functionally segmented into specialized regions, each tasked with specific cognitive and physiological functions, including sensory perception, motor control, language processing, and emotional regulation, taken from (MANSOOR et al., 2020).

the His-Purkinje system), and various valves (such as the pulmonary and aortic valves, as well as the tricuspid and mitral valves) ensure coordinated contractions of the heart muscle (RANGAYYAN, 2015), see Figure 2.5.

The heart signal can have different waveforms and morphologies. Five types of waves compose a typical ECG beat, as named cardiac cycle: the P wave represents atrial depolarization, characterized by a frequency range between 10 and 15 Hz, an amplitude of less than 300 µV, and a duration of less than 0.120s. Following this, the QRS complex denotes ventricular depolarization, with an amplitude around 3 µV and a duration between 0.070s and 0.110s, marking the contraction of the right and left ventricles. The T wave signifies ventricular repolarization, notable for its lower frequency characteristics. The ST segment represents the period when the ventricles are in a depolarized state. The RR interval provides insight into the heart rate and helps detect any arrhythmias during its duration. Additionally, the PQ and QT intervals serve as crucial indicators in diagnosing various cardiac conditions and abnormalities (KACHUEE; FAZELI; SARRAFZADEH, 2018). , see Figure 2.6. Each wave maps a heart moment which is useful to monitor the heart functioning, to detect arrhythmias, and to prevent myocardial ischemia and infarctions, and other intercurrences, taken from (RANGAYYAN, 2015; NAÏT-ALI, 2009).

2.2.2.3 Electromyography biosignal (EMG) The muscular activity, voluntary or involuntary, generates electrical biosignal recorded by electromyography (EMG). The

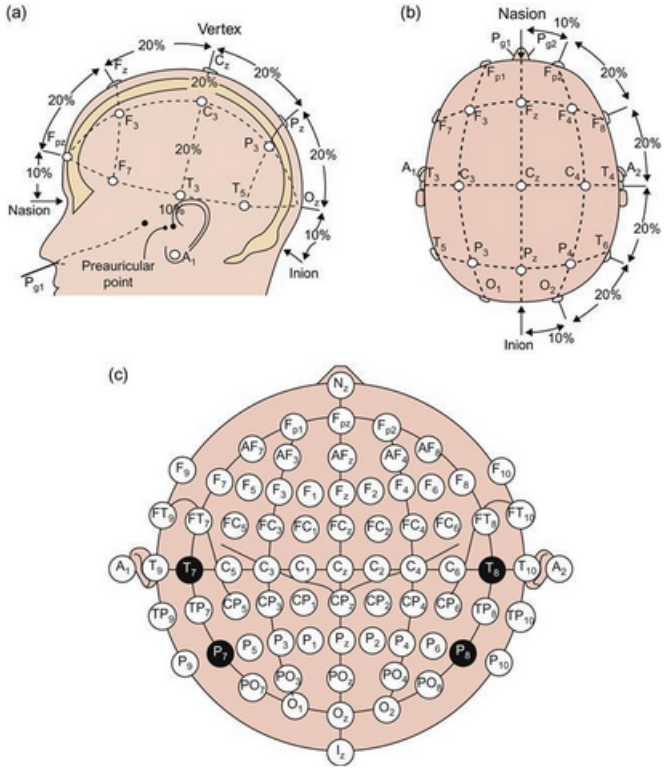

Figure 2.4: The EEG scalp map provides a topographical representation of electrical activity across different regions of the scalp, following the international standard known as the 10-20 system. Key landmarks include the nasion, which serves as a reference point for frontal electrode placement; the vertex, positioned at the skull's highest point; the inion, located at the external occipital protuberance on the back of the skull; and the preauricular points, situated in front of each ear. (a) It illustrates the side view of the skull, highlighting these landmarks and points on the EEG scalp map. (b) It presents a top view of the scalp map, defining the systematic placement of electrodes based on these landmarks. (c) Electroencephalogram map points, taken from (GANDHI, 2014).

EMG registers the potential variation of the signal to investigate some specific diseases related to the electrical activity of the muscle (NAÏT-ALI, 2009). Different from nerve cells, muscles cells are large, their electrical signals are more intense, and give rise to large potential gradients (KANIUSAS, 2019). There are two approaches to acquire these signals from the muscle: electromyography with implanted electrode near the muscle cell fiber and electromyography with external electrodes laced on the skin surface (BIRD et al., 2020; KATIRJI, 2018).

In EMG analysis, several key concepts are essential for interpreting the biosignal. Action potentials represent the electrical signals generated by muscles (PRESTON; SHAPIRO, 2012). The compound muscle action potential (CMAP) is the summary record of synchronously activated muscle action potentials (KATIRJI, 2018). Amplitude denotes the

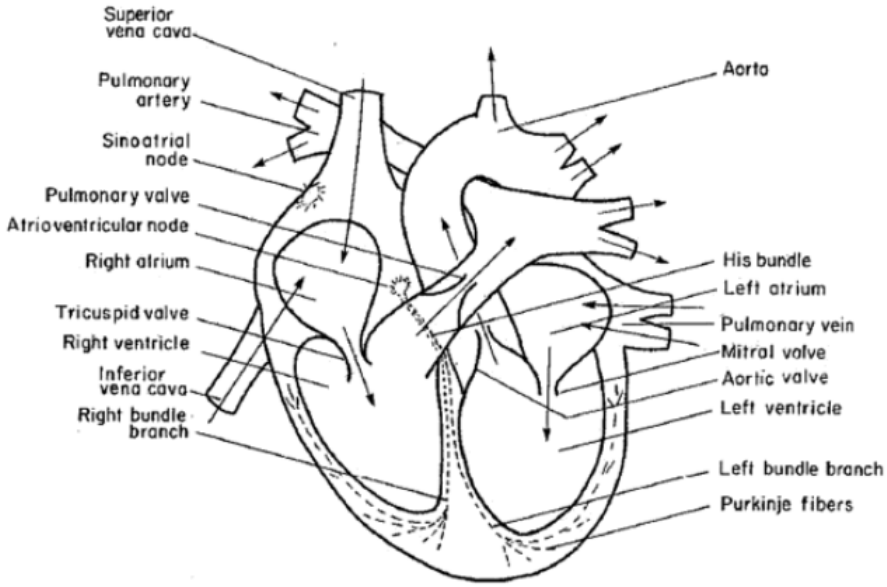

Figure 2.5: Heart structures and main vessels, taken from (RANGAYYAN, 2015).

peak height of an action potential, measured in millivolts (mV) (WEISS; WEISS; SILVER, 2015) Typically, the baseline of amplitude is marked by a negative peak in the recorded signal. Duration measures the time from the initial positive deflection to the first negative phase of the evoked potential, expressed in milliseconds (ms) (KATIRJI, 2018). Antidromic conduction describes an action potential moving against the usual physiological direction, while orthodromic conduction follows the expected path (WEISS; WEISS; SILVER, 2015). Motor conduction velocity evaluates the speed of the fastest signal segment, calculated by dividing the distance traveled by nerve conduction time (PRESTON; SHAPIRO, 2012). Lastly, latency refers to the time between signal emission and response onset, encompassing nerve conduction, neuromuscular junction delay, and muscle depolarization times (PRESTON; SHAPIRO, 2012), see Figure 2.8. These parameters provide critical insights into muscle function and nerve conduction.

2.3 RELATED WORK

The transfer learning approach is widely applied to achieve accurate results in various areas of healthcare. Some reasons for the current increasing use of the approach are the scarcity of labeled data available for training the models, the need to learn more detailed data patterns, the need to predict random events such as seizure timing or early fatigue stage to improve the individual's quality of life, among many other situations.

In this section, we present how different transfer learning techniques have been explored between 2016 and 2024 to improve the accuracy of classification and prediction models. This research is from the health field and uses electrical biosignals to diagnose

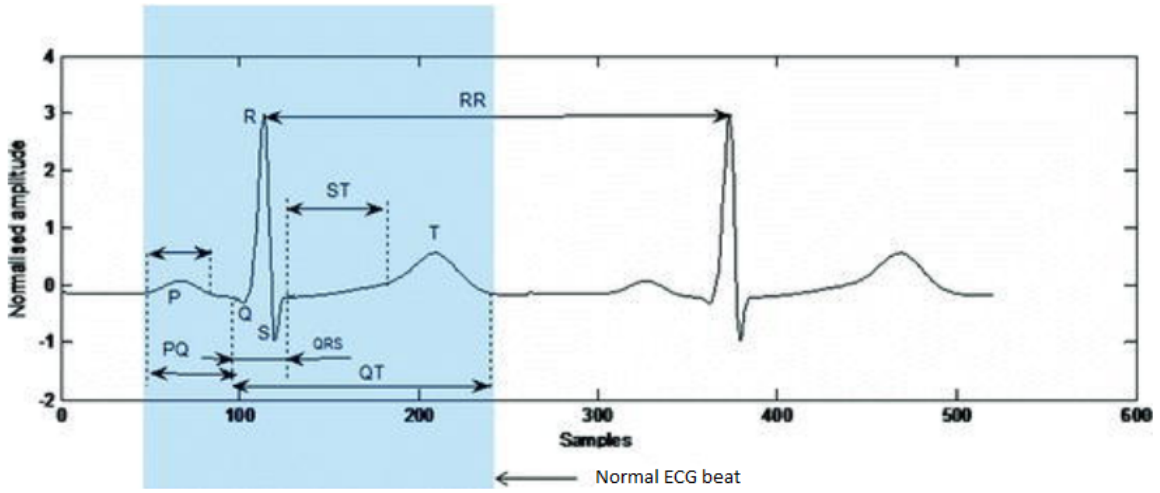

Figure 2.6: The regular pattern of electrical impulses coordinates the contraction and relaxation of the heart muscle. Each interval of the signal represents a specific aspect of the cardiac cycle, taken from (NAÏT-ALI, 2009).

and monitor human health. Through these studies, we can visualize how the transfer learning approach provides accurate answers. Thus, physicians have more robust support to help them mitigate problems caused by disease or bodily dysfunction. Another advantage of these researches is allowing us to see the knowledge gaps that we can study to elucidate them in our investigation.

2.3.1 Selection criteria

We searched papers from four repositories (IEEE [1], ACM [2], PubMed [3] and Scopus [4]) using the following key words: transfer learning, biosignal or signal, and electroencephalogram or EEG. The repositories returned 146 papers. We applied seven exclusion criteria listed below to filter out the documents useful to our investigation, if the paper: has no results OR experimentation, is theoretical only (some exception for comprehensive systematic reviews), is not about the transfer learning or EEG, does not use computational models, duplicated paper, is not in English or Portuguese, is outside of the health domain. After filtering the retrieved articles, 50 articles were selected. We categorized them by disease and focused our deep analysis on three points: the learning transfer technique, the machine learning architecture developed and the result presented by the model. We opted to study about electroencephalogram biosignals (EEG) characteristics and then transfer its knowledge to another neural network model which work with others kind of

[1] http://ieeexplore.ieee.org
[2] http://portal.acm.org
[3] https://www-ncbi-nlm-nih.ez10.periodicos.capes.gov.br/pmc/
[4] https://www.scopus.com

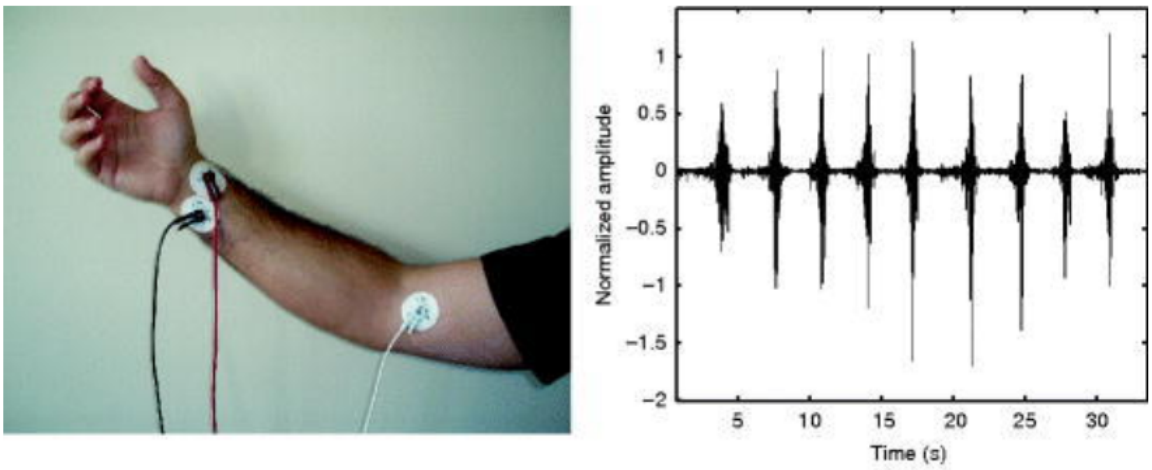

Figure 2.7: EMG of open/close hand movement. (a) Electrodes positioned on the arm to capture biosignals during the movement. (b) Graph of the electromyography biosignal recorded during open/close hand movements, showing normalized amplitude versus time, taken from (NAÏT-ALI, 2009).

electrical signals as ECG and EMG.

2.3.2 Tranfer learning with electrical biosignals

After selecting the papers, we analyzed each one and provided a summary of the themes discussed, organized by the disease studied as follows.

2.3.2.1 Alcoholism - Silva et al. (2020) suggested that alcohol addiction alters brain behavior and consequently, its brain signal pattern. Based on this assumption, the authors investigate the predisposition to alcoholism by image- transformed EEG signals. They applied the transfer learning approach to diagnosing with more reliable results and lower time costs. The architecture concept had a neural network layer, a feature extraction strategy, and a classical classified layer. Then they combined different Convolutional Neural Networks (CNN) and classical classifiers and compared the results. The architecture with the best outcome was MobileNet combined with the Support Vector Machine (SVM) classifier.

2.3.2.2 Brain disorders - Zhang e Li (2019) proposed a model to detect attention-deficit/hyperactivity disorder (ADHD). They transformed EEG signals into images and created two models based on the visual geometry group (VGG-16) network. They trained the first model (rVGG) from scratch. On the second model (tVGG), they applied parameters transfer learning techniques. The first layer of tVGG received the weights from rVGG and was unchanged during the performance. The other layers used the gaussian

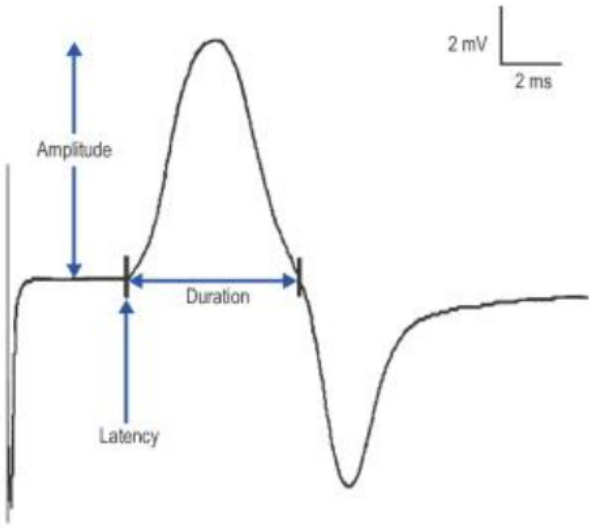

Figure 2.8: EMG biosignal graph explaining the amplitude, which represents the magnitude of the electrical activity within the muscle, typically measured in microvolts (µV), and indicates the strength of the muscle contraction. The duration refers to the length of time a muscle activity event occurs, while the latency is the time interval between the onset of a stimulus and the beginning of the muscle response, taken from (PRESTON; SHAPIRO, 2012)

distribution to initialize their weights. The measured accuracy was 94.39% for the tVGG model, but the sparse data sample limitation may indicate bias in this result.

Alhussein, Muhammad e Hossain (2019) investigated how to recognize brain pathologies using EEG. The first step was to pre-process the EEG signal, by removing noise. Then, they used the AlexNet model, a Convolutional Neural Network, pre-trained by replacing its last layer with three fully connected Multilayer Perceptron Network (MLP) layers to perform signal classification. In this model, the authors used AlexNet to extract the signal feature and transfer it to the classifier model, resulting in 78.12% model accuracy.

Shalbaf, Bagherzadeh e Maghsoudi (2020) designed a Convolutional Neural Network (CNN) model for detecting schizophrenia in patients for early diagnosis and treatment. They converted EEG signals into images and submitted them to four different and pre-trained CNNs (AlexNet, Resnet-18, VGG-19, and Inception-V3). A Support Vector Machine (SVM) classifier with tuned parameters replaced the classifier layer of all CNN. This model implemented two transfer learning techniques: feature extraction and parameters transfer learning. The Resnet-18/SVM showed the best results with 98.60% accuracy, 99.65% sensitivity, and 96.92% specificity.

2.3.2.3 Driver and mental fatigue - Shalash (2019) proposed an AlexNet model applying transfer learning to identify driver fatigue through drowsiness signals on spe-

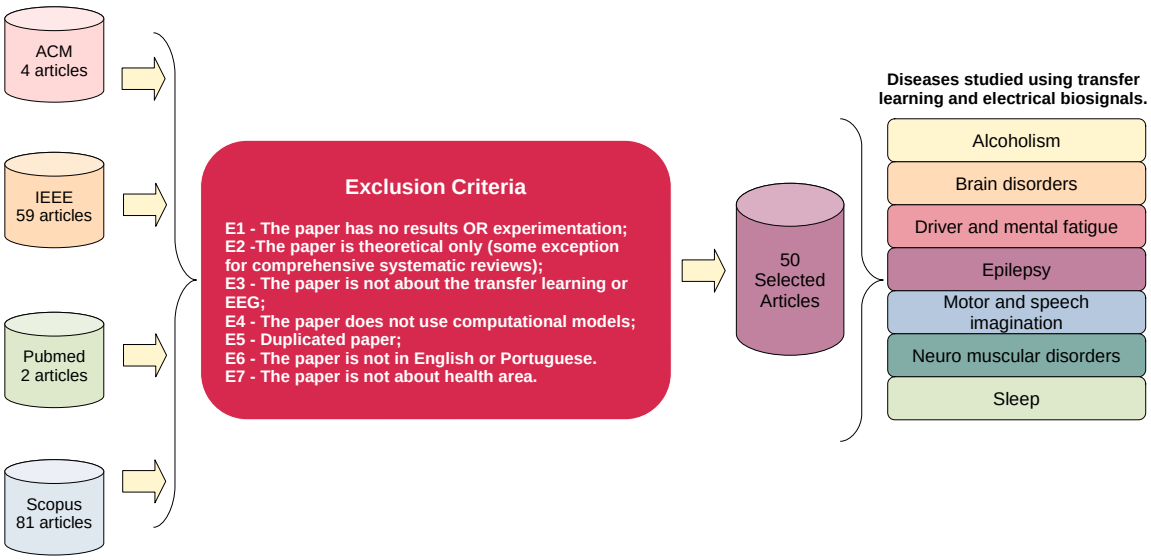

Figure 2.9: The systematic review were conducted as follows: collecting papers from repositories, establishing exclusion criteria, selecting papers based on these criteria, and classifying the papers according to the diseases studied.

cific EEG signal channels. The transfer learning occurred at two points for the AlexNet model: the first layer received the features extracted from the EEG signals by the CNN model, and the fine-tuning technique updated the classification layer with a pre-trained layer. First, the noise was removed from the biosignals, and the bandwidth was limited between 0.5Hz and 45Hz. Then, the CNN model received them and acted as a feature extraction layer. AlexNet model received the features learned by the CNN model and a new, pre-trained classification layer replaced the untrained Alextnet classification layer. The best result was obtained with FP1 and T3 channels. They presented an accuracy of 90% and 91%.

Different from Shalash (2019), Liu et al. (2019) presented a study on the performance of cross-subject fatigue recognition focused on improving the calibration step. They built and compared the result of three models: a Logistic Regression (LR), a Transfer Component Analysis (TCA) with LR, and a deep learning-based classifier (EEGNet). The EEG data pre-processing removed ocular and muscular noise, also called artifacts, by Automatic Artifact Removal (AAR). They chose the TCA model because it mitigates the imbalance of the distributions between source and target data, addressed by the homogeneous transfer learning approach. TCA + LR showed the best result (72.70% accuracy).

2.3.2.4 Epilepsy - many studies try to precisely identify if the EEG signal represents a normal or epileptic signal. Jiang et al. (2020) researched a robust classifier model to detect

when the EEG signal has a normal or epileptic frequency. They associated two transfer learning strategies to the Takagi-Sugeno-Kang fuzzy system (TSK-FS) framework to maximize model learning: Multi-Source Transfer Learning (MST) and Multi-Source Regularization (MR). Using Short-Time Fourier Transform (STFT) as the feature extraction method, the accuracy was 0.971. The authors highlighted the time consumed by the grid search and cross-validation and the use of a single fuzzy system as a weakness. Zhang et al. (2020a) also investigated how to detect seizures in EEG signals using three CNN models (VGG16, VGG19, and ResNet50). They duplicated each model structure and trained one of each model. Then, they transferred the knowledge from the pre-trained model to the upper layers (updating the weights) and kept the fully connected and the softmax output layers with their trainable features. VGG16 performed the best classification with 97.75% accuracy.

Continuing the search for the best model to classify brain signals, Xie et al. (2018) designed a model focused on implementing transductive transfer learning for many traditional intelligent models to recognize epileptic EEG signals. The proposed Generalized Hidden Mapping Model (GHMM) allows the unification of several classical intelligent model representations. The GHMM identifies which traditional model has little EEG data and allows an improved training model by transductive learning. The GHMM-TTL (RBF-Ker) was the model with the highest level of accuracy (0.9805). Agrawal, Jana e Gupta (2019) demonstrated an approach to classify EEG signals into seizure and non-seizure based on deep transfer learning. They compared the performance of three CNN networks (GoogleNet, Resnet101, and VGG-19) pre-trained with the ImageNet database to present an extraction task and an SVM classifier. The model configuration with GoogleNet and SVM showed the best accuracy (above 99%).

An epileptic seizure has different phases, and their knowledge can help physicians and patients to propose measures to mitigate seizure effects. In accord with this viewpoint, Gao et al. (2020) aimed to distinguish epileptic seizure states (interictal, preictal I, preictal II, and seizure). They built an EEG signal classification model (EESC) and initially set its parameters with the pre-trained weights from the ImageNet dataset, and during PSDED images processing, the model weights were updated. This transfer learning approach allows the EESC network to start its validation using already learned knowledge. The preictal phase of the epileptic seizure was the phase best classified by the model. Ilakiyaselvan, Khan e Shahina (2020) used another seizure phase classification. Furthermore, they proposed to model the nonlinear dynamics of the EEG signal using the reconstructed phase space (RPS) technique. Based on this, they could classify the signal into two groups: (1) seizure and non-seizure or (2) normal, interictal, and ictal precisely. They adopted a pre-trained AlexNet (CNN) network as a transfer learning technique. They then re-trained the AlexNet with RPS images. The accuracy of the models for seizure and non-seizure was 98.5% and for normal, interictal, and ictal was 95%.

Other studies try to detect the early preictal stage of seizure. On this basis, patients would have the necessary time to take important measures to avoid accidents. Daoud e

Bayoumi (2019) designed a model to automatically extract the relevant features from the raw EEG signals and then accurately detects in real-time the state of the preictal brain accurately. A pre-trained Autoencoder (AE) generalized the knowledge of the preictal seizure model and avoided the overlap effect. This transfer learning technique aimed to mitigate optimization problems. The model predicted the preictal stage with 99.6% accuracy. Wang et al. (2019b) proposed a classification model with a lower granular time scale of the preictal phase of the epileptic seizure. They selected the mean amplitude spectrum (MAS) of the subband signal with 0.3-70 Hz from the EEG and transformed it into an image. Afterwards, they applied the feature extraction technique using three CNN models (Inception-v3, Resnet152, and Inception-Resnetv2) to learn about this subband pattern. The best performing model composition was MAS and Inception-Resnet-v2 network with 94.21% accuracy. Abdelhameed e Bayoumi (2018) developed a semi-supervised system to predict the onset of seizures in an epileptic patient based on EEG signals. They trained an autoenconder model with unlabeled data to extract feature data. Then they transferred these features to a bidirectional short-term recurrent neural network to classify the EEG signal. The sensitivity rate of the model was 87.8%.

Researches are also focusing on epileptic signals according to the brain region where they occur. It can help diagnose or monitor where and how epileptic activity happens. Qu e Yuan (2019) presented a method based on deep CNN with transfer learning to detect the epileptogenic region in the brain. The signals from the brain area that emit the epileptic signals are called focal signals. Based on them, the model detected automatically whether the EEG signal referred to a focal signal or a non-focal signal. The authors used a pre-trained AlexNet model to perform feature extraction of the EEG signals. Then they transferred to another AlexNet network the parameters of the last three layers to classify the data. The accuracy of the model was 95%. Narin (2020) researched a method to accurately predict the location of the epileptic seizure in the brain and whether the stage was focal or non-focal epileptic. She pre-trained the AlexNet, InceptionV3, Inception-ResNetV2, ResNet50, and VGG16 models with images from the Keras and MATLAB websites. Afterwards, she used the models to classify 2D-scalogram images from EEG signals. After comparing their results, the InceptionV3 model showed the best accuracy (92.27%). Bajaj et al. (2019) also researched a model to identify the affected portion of the brain with an unexpected electrical disturbance. They adopted the deep feature extraction technique to pre-train a CNN model and transfer this knowledge to the KNN classifier. They experimented with four CNN models (AlexNet, VGGG16, VGG19, and Resnet50) to measure their performance in learning the EEG pattern. AlexNet, VGGG16, and Resnet50 had 99.8% accuracy results.

We also identified research on specific manifestations of epilepsy. Pisano et al. (2020) proposed a model to detect a specific type of epilepsy seizure, called nocturnal frontal lobe epilepsy (NFLE). They used a ResNet architecture with a fine-tuning transfer learning technique to improve performance due to the scarcity of NFLE data. The accuracy of the model was 94%. And Jiang, Chung e Wang (2019) aimed to build a method to recognize the multiclass epileptic EEG signal. They implemented a label space inductive

transfer learning model to improve the model learning about different seizure types. The solution performed effectively. However, the authors believe that some model structures can be further investigated to improve the classification of epileptic multiclass, such as optimizing hyperparameters of the model and reducing computational costs.

2.3.2.5 Motor and speech imagination - based on the mental stimulus to imagined speech recorded by EEG, García-Salinas et al. (2019) provided a new model to verify the possibility of symbolizing new words while maintaining training costs the same level. Inductive transfer learning was the approach taken by their model. At first, they developed a genetic algorithm to obtain the representative features of the data, called a codebook. Then they created a network to extract the features from the EEG signals and used the codebook information to help in the classification layer. The model did not score higher than the baseline model. The authors considered that the codebook did not represent the new words accurately. Therefore, the classification task had a lower performance. Tamm, Muhammad e Muhammad (2020) aimed to classify EEG signals associated with the imagination of pronouncing vowels. They developed a CNN model replicated from other research using the same dataset as the original models, but with a simpler architecture than the original models. They applied fine-tuning technique with three different approaches. The result did not perform desirable that was inferior to the replicated models. The main limitation noted was the complexity of the EGG and the effort required to process it.

Motor imagery is widely researched to enable communication between the brain and the computer. There are several approaches to improve the model accuracy and to cope with this type of EEG signal. The improvement of the classification rate is one of these studies and Parvan et al. (2019) investigated a combination of a four-layer CNN model with two fine-tuning strategies, applying preprocessing techniques, and data augmentation to find the best classification architecture for EEG motor imagery. In fine-tuning step, the weights used for knowledge transfer came from a pre-trained symmetric model. The preprocessing phase included removing the EOG noise with a regression algorithm, and the authors decided not to remove the other noises, such as heartbeats. Then they found the best model configuration with EEG without EOG, data augmentation, and the progressive fine-tuning application. Taheri e Ezoji (2020) prepared 3D EEG representations to realize two tasks: increasing the classification rate and identifying the right hand and right foot imaginary motor tasks. They performed resource extraction with a pre-trained AlexNet network and transferred their knowledge to a 5-layer CNN network. The accuracy of the model was 98.5%, but the training dataset had only five subjects that might suggest an overfitting scenario.

Lee et al. (2020) were looking for a solution to improve the task of classifying arm movement by imagining and executing the movement at the same time. They proposed a model based on a 3D convolution neural network (3DCNN) to extract the knowledge from the EEG datasets. Then, the relation network received the feature and calculated the similarities between the datasets. The developed model, called the BCI-Transfer

learning method based on Relation Network (BTRN), performed the classification step. The authors found that the result was consistent and relatively effective. Shovon et al. (2019) were also researching how to increase the motor imagery EEG classification with transfer learning and neural networks architecture. They transformed the EEG signal into 2D images and augmented them to generate more samples. After, they fed a multi-input CNN, a pre-trained ResNet-50, to extract the data features and transfer them to a deeper CNN, which learns about the complex structures of the features and classifies the imagery movement. Wu et al. (2019) presented a neural network architecture to classify accurately motor EEG images for small datasets. They developed two transfer learning techniques applied in two steps: first, extracting EEG features in the temporal and spatial domains and extracting band power-related features from the first extraction. Secondly, a CNN network classifies the signal based on the feature extraction data. In the best-case scenario, this model had an accuracy of 75.8%.

Li et al. (2023) introduced an Improved Label Space Alignment (ILA) method, combined with heterogeneous transfer learning, to enhance sample data utilization in scenarios where the label space is heterogeneous. The approach involves aligning the class centers of the source and target domains through clustering, class matching, and data alignment. The method was validated using three classification techniques in a binary classification heterogeneous scenario, which yielded accuracy rates of 20.88%, 10.69%, and 5.59%. Zhan et al. (2022) introduced a method utilizing the sequential coding experimental paradigm in brain-computer interfaces to reduce the burden of data acquisition. The proposed Multi-Band Data Stitching with Label Alignment and Tangent Space Mapping (MDSLATSM) algorithm, a novel heterogeneous transfer learning approach, bridges the source and target domains by stitching filtered multi-band data and aligning their covariance matrices. The method achieved an average classification accuracy of 64.01%.

Jiang, Fares e Zhong (2019) researched how the EEG signals and the images used to generate the brain signal are linked to the brain image classification task. They develeped a model that used two transfer learning techniques for extracting knowledge from the datasets. One technique is the Long-Term Memory Network (LSTM) to process the EEG signals and learn the features of the signals. Another is the CNN that process the most representative images to learn about the visual features of the EEG. This encoded knowledge was transferred to a third model to perform the classification task. The best result achieved was with a butterfly image and signal with 90% accuracy. Kant et al. (2020) investigated how different deep learning networks associated with continuous wavelet transform (CWT) can improve the EEG classification task. The transfer learning technique applied was to replace the fully connected layer and the output layer with the layers of the model pre-trained with EEG signals. The VGG16 model showed the best accuracy of 95%. For future work, they consider including a feature extraction step and the use of other classification methods.

After the training step, the challenge is to calibrate the model to an appropriate response, considering the nuances in the collected EEG signals for each individual. Dagois

et al. (2019) proposed to reduce the calibration requirements at the brain-computer interface. Then they developed a transfer learning algorithm to extract information about mental rotation from EEG and word generation. Next, they transferred the knowledge to three models: linear discriminant analysis (LDA), quadratic discriminant analysis (QDA), and support vector machine (SVM). The LDA model had the best result with an average accuracy of 0.8222. Azab et al. (2019) aimed to decrease the calibration time and maintain the classification rate of motor imagery-based brain-computer interface systems. They used a weighted logistic regression to learn about three data sets and then transferred the knowledge to a support vector machine and a logistic regression model based on multi-task learning to classify the signal. The classifier model showed good statistical results by the authors. Liang e Ma (2020) aimed to improve the results of calibrating the brain-computer interface system with some current user data. They developed a multi-source fusion transfer learning (MFTL) algorithm to classify the EEG motor images based on the Riemannian manifold framework. Feature extraction was the transfer learning technique applied in deep learning networks. The model performance was superior to previous models used as the baseline. Roy et al. (2020) showed a concept of Mega Blocks associated with a CNN to lead with inter-subject variations in the EEG of the motor imaging task to develop a calibration-free model. The implemented transfer learning technique used the Mega Blocks to update the parameters of the CNN. Then, they fed a CNN with the Mega Blocks so that the model could learn more about the micro features of the EEG. The optimization methods used were Adam and SGDM, and the model had an accuracy of 72.63% and 73.13%, respectively. The authors considered the reduction in calibration time a significant point in this research.

Many studies deal with different motor imaging problem scenarios. Xu et al. (2019) proposed a model to deal with the need for a large volume of labeled data, the high processing costs, and the time to train a model. They used a pre-trained VGG-16 model to extract features from EEG images. Transfer learning occurred in two steps: transferring the parameters from VGG-16 to a CNN model and feeding the CNN with extracted feature data. The average accuracy realized by the model was 74.2%. Zhang et al. (2020c) proposed a framework to handle fluctuation in the distribution of electroencephalogram (EEG) features for the motor imaging task. They used instance transfer learning to analyze the spectrogram of EEG signals and measure the similarity between subjects. They then transferred this knowledge to a CNN network to decode and classify the signal. The experiment showed an accuracy of 94.7%. Fauzi, Shapiai e Khairuddin (2020) presented a framework to handle a compact training dataset and realize higher accuracy of the brain-computer interface system. The idea was to use the common spatial pattern (CPS) as a transfer learning technique to compress the domain dataset and increase the performance of the training dataset in an extreme learning machine (ELM). As a result, the accuracy was 83%. Zhang et al. (2021) presented a model to handle personal differences in the EEG signal of various subjects. The model developed was a hybrid deep neural network with transfer learning (HDNN-TL) that combined a convolutional neural network (CNN) and a long short-term memory (LSTM). The implementation of transfer learning was by fine-tuning the fully connected layer that received the processed data from the CNN and

LSTM networks. The accuracy achieved by the model was 81%. Wang e Yang (2019) proposed a model found on transfer learning to demonstrate that participants performed the motor imagery task correctly. They trained a CNN model with an EEG signal with a subject group dataset, joined the dataset with another EGG dataset (with the same left and right-hand motor imaging task), and classified them with the pre-trained model. The model classification had an improvement in model accuracy. Özdenizci et al. (2019) aimed to provide a model to improve the communication between the individual with various neuromuscular disorders and the brain-computer interface. Therefore„ they used an EEG motor imagination dataset and applied a domain adaptation technique from a transducer transfer learning approach to achieve better accuracy. The model used the conditional variational autoencoder network to learn the data representations and transfer it is knowledge to the adversarial conditional variational autoencoder network. The average accuracy found was 63.8%.

2.3.2.6 Neuro muscular disorders - Tan et al. (2019) presented a brain-computer interface framework to help patients with robotic rehabilitation. An autoencoder framework consisting of a joint adversarial network (VGG16 and VGG19) and multiple regularized constraints make up this framework. The autoencoder layer implemented the transfer learning strategy. This network had to learn simultaneously to encode the source and target domain accurately. To mitigate the occurrence of negative transfer, the regularized manifold constraint attempted to prevent the geometric structure of the manifold in the target domain from being undone by the source domain. The model with VGG19 achieved a better result. Kundu e Ari (2019) proposed a model to improve the performance of the brain-computer interface speller method with sparse data for training. They developed the multiscale convolutional neural network (MsCNN) architecture composed of multi-resolution deep features, feature selection technique (Fisher ratio), and an ensemble of support vector machines (ESVMs) to classify the signal. In this model, homogeneous transfer learning followed the rule adaptation (RA) approach (all classification rules implement a single strategy). The proposed model had better result than the baseline models.

2.3.2.7 Sleep - Vilamala, Madsen e Hansen (2017) presented two models to create sleep pattern images that are easy to read from EEG signals to solve visual recognition tasks of scoring sleep stages. The VGG16 model was the basis for building the architecture of the proposed networks. The first model, called VGG16-FE, assumed a feature extraction function and was trained from scratch. In the second model, named VGG16-FT, they fine-tuned and updated all the weights in the network. The values of weights used to update VGG16-FT came from a pre-trained ILSVRC-2014 model. VGGG16-FT showed higher accuracy than VGGG16-FE. Chambon et al. (2018) designed a new CNN model for sleep stage classification. The approach sought to acquire knowledge from three types of signals (EEG, EOG, and EMG) end-to-end without considering the spectrograms or hand-crafted feature extraction. The transfer learning strategy developed used the first stage of CNN as a feature extraction of the signals. The model achieved higher accuracy than other state-of-the-art models and with low computational cost and runtime usage.

Phan et al. (2019) developed the SeqSleepNet consisting of three blocks: an attentional RNN network (ARNN), a sequence-level RNN, and a classification layer. The study applied three transfer learning strategies: parameter model by fine-tuning, example base of different EEG datasets, and different label spaces for EEG and EOG datasets. The fine-tuning model shows the best result with an accuracy of 85.5%. Phan et al. (2020) presented SeqSleepNet+ and DeepSleepNet+ responsible for gaining knowledge from a large dataset and transferring that learning to help automatic sleep preparation with a small dataset. Fine-tuning was the technique used to transfer the learning. The approach treated different transfer scenarios with groups of homogeneous and heterogeneous signal datasets (EEG, EOG, and EMG) and fine-tuning strategies. The result revealed that SeqSleepNet+ had the best results in most scenarios. Abdollahpour et al. (2020) introduced a new method for sleep stage classification by transferring EEG and EOG datasets knowledge. Two feature groups organized features extracted from the datasets, and each feature vector was converted into a horizontal visibility graph (HVG). The generated image fed a transfer learning convolutional neural network for data fusion (TLCNN-DF, proposed model) to classify the sleep stage. The authors found an accuracy of 93.58%. Jadhav et al. (2020) proposed a CNN and Squeezenet model for sleep stage classification based on a single EEG channel without manual feature extraction. They adopted pretrained weights from the CNN model to perform the fine-tuning process in Squeezenet and implemented a back-propagation model. The proposed model observed relevant generalization ability.

2.4 SUMMARY

This chapter provides a detailed overview of the literature related to transfer learning, particularly in the context of heterogeneity. It also presents the characteristics of electrical biosignals, with specific details on electrocardiogram (ECG), electroencephalogram (EEG), and electromyography (EMG), which are the types of electrical biosignals used in this work. Additionally, we review publications that have applied transfer learning concepts in relation to electrical biosignals.

We discuss fundamental concepts of transfer learning and focus on the issue of heterogeneous data to provide a theoretical foundation for the research. The principal methods for examining the characteristics of electrical signals are presented to expand the understanding of how this type of data can be analyzed. Finally, we review related works that demonstrate various approaches to applying transfer learning between heterogeneous data.

The main conclusions of this chapter are that there is a need to deepen the understanding of the possible applications of transfer learning between neural networks dealing with data from heterogeneous sources, yet within the same category.

The following chapter outlines our research process, explaining the methodology, base-

lines, and metrics employed.

Chapter 3

"For progress to be made, I think it's necessary to reach out to people who don't necessarily agree."
Chimamanda Ngozi Adichie

HETEROGENEOUS TRANSFER LEARNING: PROPOSAL AND OUTLINE

As mentioned in Chapter 1, this research investigated whether transfer learning using heterogeneous electrical biosignals in the frequency domain could enhance the predictive accuracy of the target model, see proposed architecture. Additionally, it contributes to mitigating the dependence on large datasets for training and calibrating models, presenting an alternative method to generalize electrical biosignal data in the frequency domain to be better mapped by LSTM neural networks.

3.1 METHODOLOGY

Our approach to investigate the possibility of transfer learning between non-identical electrical biosignals is illustrated in Figure 3.1. To evaluate the outcomes, we considered the balanced distribution of events in both the ECG and EMG datasets. We then employed the RMSE metric. In the following sections, we explain the electrical biosignal datasets, preprocessing, similarity analysis, and heterogeneous transfer learning steps.

3.1.1 Electrical biosignals datasets

This section describes the datasets used to investigate our proposed research question.

TUEG EEG Corpora[1] - the electroencephalogram (EEG) records obtained from the Temple University Hospital (TUH) between 2002 and 2019 (OBEID; PICONE, 2016). The dataset consists of 412,400 EEG recordings, acquired using groups of channels (24 to 36, 64 and 128 channels), sampled at 250 Hz with 16 bits per sample, and without noises.

[1] <https://isip.piconepress.com/projects/tuh_eeg/> - accessed on 17/06/2024

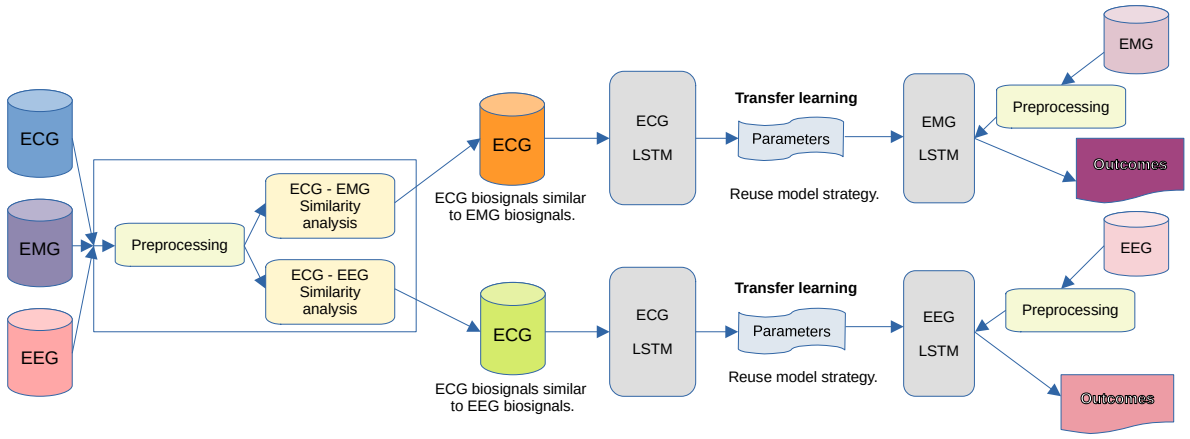

Figure 3.1: The architecture for transfer learning between heterogeneous electrical biosignals. After preprocessing, we conducted a similarity analysis, resulting in two ECG datasets: one with waves most similar to EMG and the other with waves most similar to EEG. We then trained two ECG models using the respective ECG datasets individually. Subsequently, we implemented a reuse model strategy, transferring the trained ECG LSTM parameters, along with their layers, weights, and biases, to EMG and EEG models to process EMG and EEG biosignals.

The recordings were annotated and registered in a European Data Format (EDF+), ensuring compatibility with existing EEG analysis software. This file's type has three parts: header, signals header and signal data (see details in table 3.1). The annotated document presents a succinct and comprehensive summary of the patient's medical history, diagnose (as in table 3.2, and prescribed medications, as prepared by a specialist physician.

ECG Heartbeat Categorization[2] - during the period between 1975 and 1979, the Massachusetts Institute of Technology (MIT) and the Beth Israel Hospital in Boston (now the Beth Israel Deaconess Medical Center) collaborated to create the MIT-BIH Arrhythmia Database (MOODY; MARK, 2001). This database comprises electrocardiogram (ECG) recordings from 47 different subjects, with approximately 60% of the recordings obtained from inpatients and the remaining 40% from outpatients at Boston's Beth Israel Hospital. The dataset consists of 123,998 ECG recordings, each of which was sampled at a frequency of 125Hz and characterized by 188 features. Two or more cardiologists independently annotated each recording, resulting in a classification into one of five possible categories (see table 3.3). The signal features were stored in a comma-separated values (CSV) format (KACHUEE; FAZELI; SARRAFZADEH, 2018).

[2] <https://www.kaggle.com/datasets/shayanfazeli/heartbeat> - accessed on 06/27/2023

Table 3.1: The TUEG EEG file structure follows the European Data Format (EDF+). The header contains patient and examination details. The signal header provides information about the electrical activity across different regions of the scalp, using the international standard known as the 10-20 system scalp map, illustrated in Figure 2.4 in Chapter 2. The signal data records the EEG values captured.

EDF Files Strutucture		
Header	**Signal Header**	**Signal Data**
Version Number	Label to Identify Type of Signal	Data Records
Patient ID	Reserved	
Gender	Number of Data Records	
Date of Birth	Duration of a Data Record in Seconds	
Patient Name	Number of Signals in a Data Record	
Patient's age at time of study	EEG Fp1, Fp2 (electrodes position)	
"Startdate" Label	EEG F3, F4 (electrodes position)	
Start Date	EEG C3, C4 (electrodes position)	
EEG Nº	EEG P3, P4 (electrodes position)	
Technician Name	EEG O1, O2 (electrodes position)	
EEG Machine Used	EEG F7, F8 (electrodes position)	
Additional Subfields	EEG T1, T2, T3, T4, T5, T6 (electrodes position)	
Start date (dd.mm.yy)	EEG Fz, Cz, Pz (electrodes position)	
Start time (hh.mm.ss)	EEG EKG1 (electrode position)	
	IBI, Bursts, Suppr	
	EDF Annotations	
	Signal Physical Dimension	
	Signal Physical Minimum	
	Signal Physical Maximum	
	Signal Digital Minimum	
	Signal Digital Maximum	
	Signal Prefiltering	

EMG Classify Gestures[3] - the acquisition of electromyography (EMG) signals was motivated by the goal of supporting an open-source prosthetic control project that sought to enhance the functionality of prosthetic devices by enabling them to operate with multiple degrees of freedom[4] (ZHAI et al., 2017). To this end, an armband equipped with eight sensors was used, which were placed on the surface of the skin to measure the electrical activity generated by the underlying muscles.

The EMG signals were recorded at a sampling rate of 200 Hz with a total of 11,678 recordings and yielded 64 features that were used to classify four possible gesture classes, as in table 3.4.

[3]<https://www.kaggle.com/datasets/kyr7plus/emg-4> - accessed on 06/27/2023
[4]<https://github.com/cyber-punk-me> - accessed on 06/27/2023

Table 3.2: The EEG biosignal classification describes elements of the label space that were annotated in the summary of the patient's medical history analyzed by a specialist physician.

EEG Biosignal - Classification	
Category	**Classification**
1	• Normal • No definitive electrographic seizures
2	• Abnormal
3	• Seizure • Spike and slow wave • Generalized periodic epileptiform discharge • Periodic lateralized epileptiform discharge • Eye movement • Artifact
10	• Not informed

3.1.2 Preprocessing

We preprocessed the datasets (EEG, ECG, and EMG) using the same method. First, we conducted feature exclusion to remove instances with missing values, which is necessary due to the neural network's restriction in handling this type of data. The EEG dataset did not contain missing values in specific rows, but it had columns comprising patients' session data and some signal channels without any values. We removed all these columns, thereby reducing the dataset from sixty-one to twenty features. The ECG and EMG datasets did not have any instances of missing values. In the next step, we separated the feature space from the label space and removed the noise from the biosignal by defining a frequency range between 10 and 15 Hz for the ECG and between 0.15 and 40 Hz for the EMG. This step allowed us to retain only the relevant signal information to feed the our model. The EEG dataset did not require this procedure because it was already cleaned from noise when the dataset was created, maintaining frequencies higher than 13 Hz. We also decided to trim the EEG waves to reduce its time series size and computational cost for processing this volume of data. The EEG time series originally had an average length of five minutes of recording. We applied the strategy to reduce the time series to 15 seconds for each sample, starting from the 181st second.

Then, we normalized the biosignal values between zero and one, and applied the Fourier transform method to convert them from the time domain to the frequency domain. In the last step, we segmented the datasets into folds with twenty features to maintain uniformity in the input vectors across the three biosignals. This segmentation was performed following the sequence of features in the dataset. This resulted in nine folds for ECG, three folds for EMG, and one fold for EEG.

Table 3.3: The ECG heartbeat classification details elements of the label space that were independently annotated by two or more cardiologists at the Massachusetts Institute of Technology (MIT) and Beth Israel Hospital in Boston.

ECG Heartbeat - Classification	
Category	**Classification**
N	• Normal • Left/Right bundle branch block • Atrial escape • Nodal escape
S	• Atrial premature • Aberrant atrial premature • Nodal premature • Supra-ventricular premature
V	• Premature ventricular contraction • Ventricular escape
F	• Fusion of ventricular and normal
Q	• Paced • Fusion of paced and normal • Unclassifiable

Table 3.4: The EMG gesture classification represents the elements of the label space obtained from an open-source prosthetic control project.

EMG Gesture - Classification	
Category	**Classification**
0	• Rock
1	• Scissors
2	• Paper
3	• OK

3.2 BASELINES

Given the absence of similar research developing methods to process non-identical electrical biosignals in the frequency domain using transfer learning techniques, we built the baseline models from scratch. We developed a lean architecture model due to limitations in the computational resources available.

After processing each baseline, we compared the test outcomes and identified the lowest RMSE among the EEG, ECG, and EMG models. We then selected the biosignal with the lowest RMSE as the source domain. Folds from this dataset were used to calculate the distance between it and the folds from the other two biosignals. The lowest distance results determined which baselines trained by the source domain folds would provide parameters for implementing transfer learning between the biosignals.

In the next sections, we detailed the architecture of each baseline along with its hy-

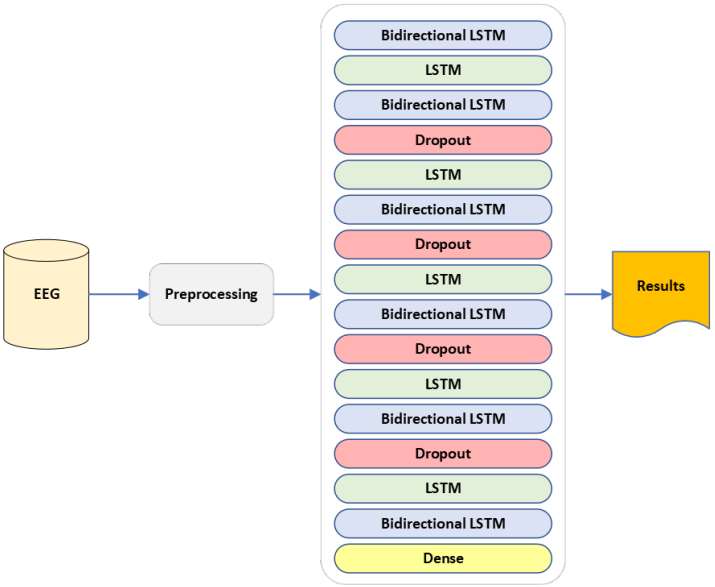

Figure 3.2: Architecture of the EEG model: 6 bidirectional LSTM layers, 5 LSTM layers, 4 dropout layers, and 1 dense layer.

perparameter configuration. All baselines were trained for seven epochs (20, 50, 100, 150, 200, 300, and 400).

3.2.1 EEG

The EEG baseline was defined with a input bidirectional LSTM layers, five LSTM hidden layers, five bidirectional hidden layers, four dropout layers, and a dense layers, see figure 3.2. The hyper parameters defined were: adam optimizer, dropout = 0.2, suffle = false (do not allow mix the time serie data), train batch size = 540000, and test batch size = 14000.

3.2.2 ECG

The ECG baseline was defined with a bidirectional LSTM input layers, five LSTM hidden layers, four dropout layers, and a dense layers, see figure 3.3. The hyper parameters defined were: adam optimizer, dropout = 0.2, suffle = false (do not allow mix the time serie data), train batch size = 11000, and test batch size = 2200.

3.2.3 EMG

The EMG baseline was defined with a input LSTM layers, four LSTM hidden layers, four bidirectional LSTM hidden layers, three dropout layers, and a dense layers, see figure

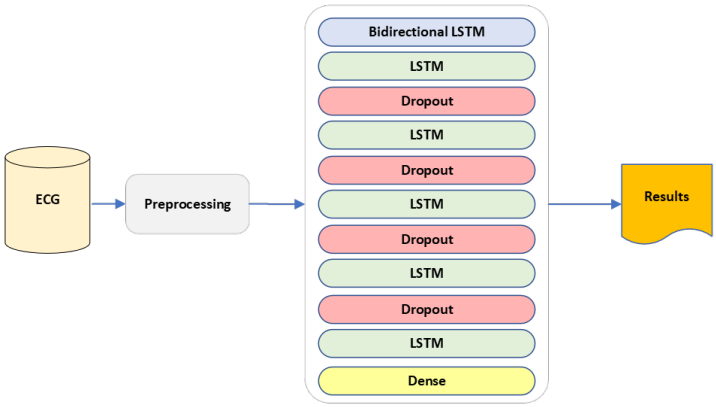

Figure 3.3: Architecture of the ECG model: 1 bidirectional LSTM layer, 5 LSTM layers, 4 dropout layers, and 1 dense layer.

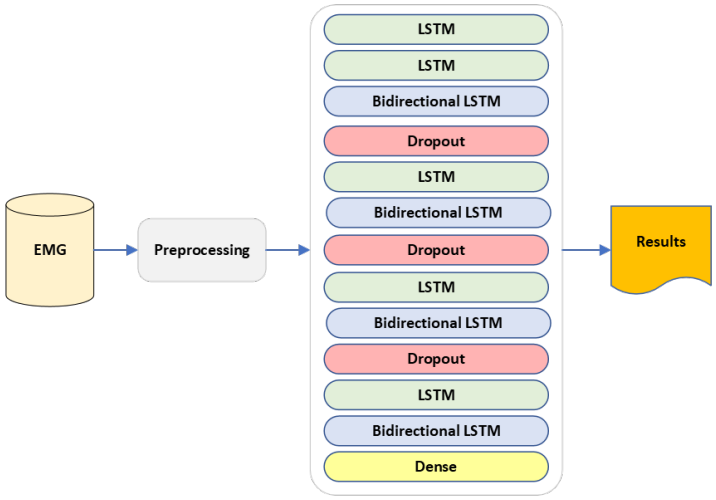

Figure 3.4: Architecture of the EMG model: 4 bidirectional LSTM layers, 5 LSTM layers, 3 dropout layers, and 1 dense layer.

3.4. The hyper parameters defined were: adam optimizer, dropout = 0.2, suffle = false (do not allow mix the time serie data), train batch size = 2800, and test batch size = 700.

3.2.4 Similarity analysis

As our experiment involves a heterogeneous dataset consisting of non-identical feature and label spaces, we integrated similarity analysis to mitigate the occurrence of negative transfer learning. This approach allowed us to observe how lower distances, indicating high similarity between biosignal waves, improved the LSTM model's understanding and generalization of biosignals, thereby mitigating negative transfer effects in our two transfer learning scenarios.

We selected the dynamic time warping (DTW) method for its superior distance measurement capabilities, which account for variations in wave time and amplitude. DTW addresses distortions and shifts in time series data by non-linearly aligning sequences, ensuring similar patterns are matched even if they occur at different times (GIORGINO, 2009). Based on this concept, we conducted an evaluation of the similarity between ECG and EMG biosignals, as well as between ECG and EEG biosignals, resulting in the creation of two ECG datasets with the most similar waves identified in the process.

3.2.5 Heterogeneous transfer learning

In the heterogeneous transfer learning process, the two ECG datasets with the most similar waves with EMG and EEG biosignals, identified in similarity analysis process, were selected as the source domains. They were submitted to their respective ECG model, with the same architecture than ECG baseline model. Then the ECG models parameters calculated were transferred, which were weights, biases, layers, and the overall structure of the network, to the EMG and EEG models, respectively.

This proposed transfer strategy, known as model reuse, facilitated the efficient configuration of neural network architectures for new tasks, thereby enhancing their ability to generalize new types of data and improve overall performance. Additionally, this approach aimed to reduce the need for extensive labeled data in the EMG and EEG target domains, as the knowledge obtained through these parameters encompasses a general understanding of electrical biosignals.

After the transfer of the ECG LSTM parameters, the EMG and EEG datasets were preprocessed following the steps described in Section 3.1.2 and then submitted to their respective models to train. As in the baseline process, the ECG and EMG models were trained at seven epochs (20, 50, 100, 150, 200, 300, and 400). Finally, the models calculated the value of each metric for each epoch.

3.3 MEASURES

Then we compared the results found with statistical methods to evaluate the results of the models. The method selected was root mean squared error (RMSE) to measure the results, as described below (WANG et al., 2023; ZHANG et al., 2020b; SILVA et al., 2020).

- Mean squared error - represents the mathematical measure of the average squared distance between the observed and predicted values, see 3.1.

$$MSE = \frac{\text{Sum of Squared Errors}}{\text{Number of Predictions}} \tag{3.1}$$

- Root mean squared error - serves as a metric for assessing the accuracy and quality of predictive outcomes, as in equation 3.2.

$$RMSE = \sqrt{MSE} \tag{3.2}$$

Finally, we reviewed and analyzed which approach presented the best results to prove our hypotheses.

3.4 SUMMARY

This chapter provides a detailed description of the methodology proposed in this work. We begin by presenting the characteristics of the datasets and the steps required to prepare the data for processing by neural networks. We then describe the architectures of the baseline models, the objectives, and the application of similarity analysis between electrical biosignals, as well as the implementation of transfer learning between heterogeneous data. Finally, we detail the metrics used to evaluate the obtained results.

In this way, we provide a thorough description of the steps required to investigate the feasibility of performing transfer learning with non-identical data, based on the analysis of the obtained results. Furthermore, upon execution of the outlined methodology, it will also be possible to address the secondary research questions.

The following chapter details the experiment phases, their outcomes, and the analysis of both the process and results.

Chapter 4

"I wanted you to know that I am ready to go", Childish Gambino

TRANSFER LEARNING WITH HETEROGENEOUS ELECTRICAL BIOSIGNALS: EXPERIMENTAL ANALYSIS

The primary objective of this chapter's experiments is to investigate how transfer learning can enhance the predictive accuracy of LSTM neural networks when processing diverse electrical biosignals. Our analysis is structured around the key research questions, which focus on scenarios where negative transfer might occur, whether processing data in the frequency domain can alleviate the effects of unbalanced data, and whether assessing the similarity between signals can significantly improve the accuracy of target LSTM models.

4.1 IMPLEMENTATION DETAILS

The experiment[1] utilizes the following tools: Jupyter Notebook version 6.4.12, Python version 3.9.13, along with the Keras and DTW libraries. The computer used was an Intel Core i5 with 2.60GHz x 8, 16GB memory, and Ubuntu 22.04.03 LTS.

4.1.1 Preprocessing

During the preprocessing stage, our primary focus was to prepare the diverse datasets to construct uniform and valid feature spaces for processing by an LSTM neural network. We transformed the biosignal datasets from time to frequency domain, aiming to reduce the mathematical complexity of the data (from mathematical sine functions to algebraic functions). Considering that, we investigated whether simplifying and generalizing the biosignal dataset could result in effective transfer learning outcomes in most of the proposed scenarios, including with unbalanced datasets. One benefit of this process was that even when using heterogeneous datasets with non-identical sources and labels, since they

[1]Code files - <https://github.com/DeinhaLeao/Master_Degree.git>

belong to the same category of data (electrical signals), we could analyze and apply similar preprocessing strategies to them. Our unique divergent treatment was to address the specific noise frequencies inherent in each biosignal. This standardization in preprocessing suggests that we could incorporate an even broader range of non-identical electrical biosignals without increasing the complexity or high cost associated with adapting the preprocessing techniques.

In terms of dataset composition, a significant portion of the EEG feature space had to be excluded due to the presence of numerous entries with missing values. This issue arose because the EEG dataset was collected over different periods using various equipment and channel configurations (64 and 128 EEG channels), including the most common configurations used in research, which range from 24 to 36 channels (OBEID; PICONE, 2016). Additionally, it lacked balanced treatment. Conversely, both the ECG and EMG datasets exhibited no missing values within their respective feature spaces. We chose to preserve these EEG characteristics — namely, the low number of features and imbalanced datasets — to observe the behavior of the LSTM model in the context of transfer learning. Our aim was to verify if improvements in outcomes could be obtained through the simplification of biosignal complexity in the frequency domain, even under these conditions, and to answer our secondary question about the LSTM's ability to mitigate the effect of unbalanced data.

4.2 BASELINE RESULTS

In regard to the baseline outcomes, we presumed that the mathematical simplification of the waves in the frequency domain would improve the LSTM model's ability to generalize the biosignals, resulting in lower root mean squared error. However, this hypothesis was not confirmed by the results with EEG and EMG dataset scenarios. The EEG baseline results demonstrated that, even in the frequency domain, the model struggled to accurately map the imbalanced data. Its RMSE rate underscored the low accuracy and quality of predictive outcomes, as is commonly understood in the state-of-the-art (WAN et al., 2021). We also considered another factor that might have influenced the accuracy: the preprocessing step involving the selection of the EEG segment for this experiment. Specifically, we chose a 15-second interval following the initial 3 minutes of the recording. It is possible that certain samples within this time frame may not accurately represent the occurrences of labeled brain disorders. This discrepancy could negatively impact the LSTM model's ability to comprehend and classify EEG biosignals efficiently.

In the EMG dataset scenario, the data was not unbalanced, but it had a limited number of samples for each event in the label space. The EMG baseline outcomes indicated that the smaller number of label samples adversely affects its training task, as is widely recognized in current research (ZHANG et al., 2021; TAN et al., 2018; XU et al., 2019). Contrary to our initial assumptions, the mathematical simplification of the EMG waves was insufficient for the model to mitigate the effects of the low sample size in the label

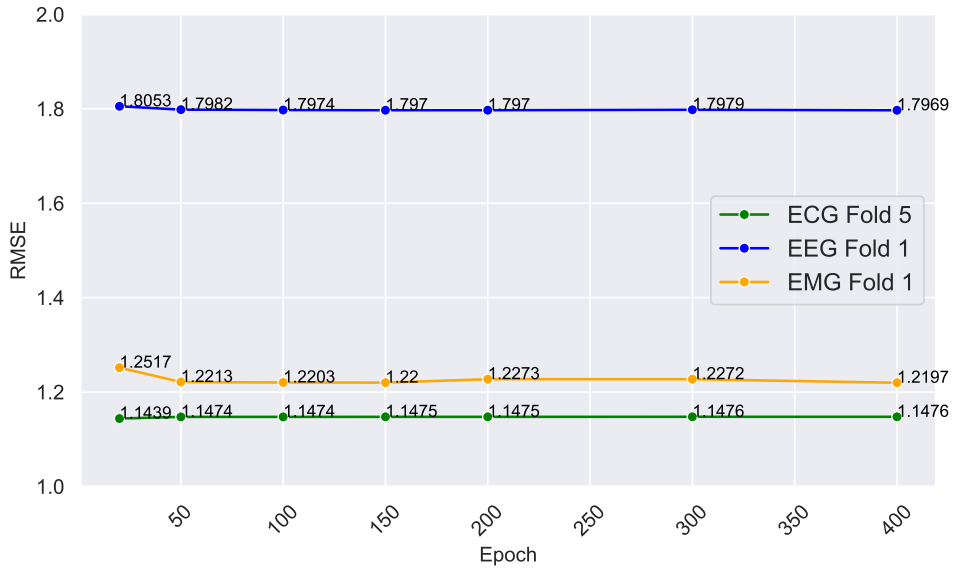

Figure 4.1: Comparison of the best RMSE baseline results, represented by ECG fold 5, EEG fold 1, and EMG fold 1.

space. Upon comparing the outcomes of both baselines, which process the EMG and EEG datasets, we found that, in our context, an unbalanced dataset presents a greater challenge for the neural network than a balanced dataset with a limited number of samples for each event in the label space.

The baseline obtained over the ECG dataset yielded the best outcomes in the context of our research. The ECG dataset exhibited characteristics such as balanced data and a substantial number of occurrences for each event in the label space. Among the nine ECG folds generated during the preprocessing stage, the baseline's outcome metrics for ECG fold 5 (see Figure 4.3d) demonstrated a slightly better understanding of ECG biosignals compared to the other processed ECG folds, as evidenced by the RMSE rate.

Upon examining the ECG and EMG baseline outcomes for each fold, we observed similar levels of accuracy, with minor variations in RMSE. Initially, we anticipated varying results for each fold, given that each was assigned a unique segment of the biosignal. We assumed that certain segments might more accurately represent heart and muscle activity than others. However, since these datasets were preprocessed and segmented beforehand by their creators to better represent heart and muscle states, we observed stable metric results across the processed ECG and EMG folds. After analyzing the baseline outcomes, we compared the testing RMSE results (see Fig. 4.1) and identified that the ECG model trained with ECG fold 5 presented the lowest RMSE. Based on this result, we selected the ECG dataset as the source domain and the EEG and EMG datasets as the target domains. We then calculated the distance between the ECG-EEG and ECG-EMG pairs. The shortest distance in each case determined which ECG baseline, trained on the different ECG folds, provided the best parameters for implementing transfer learning to the

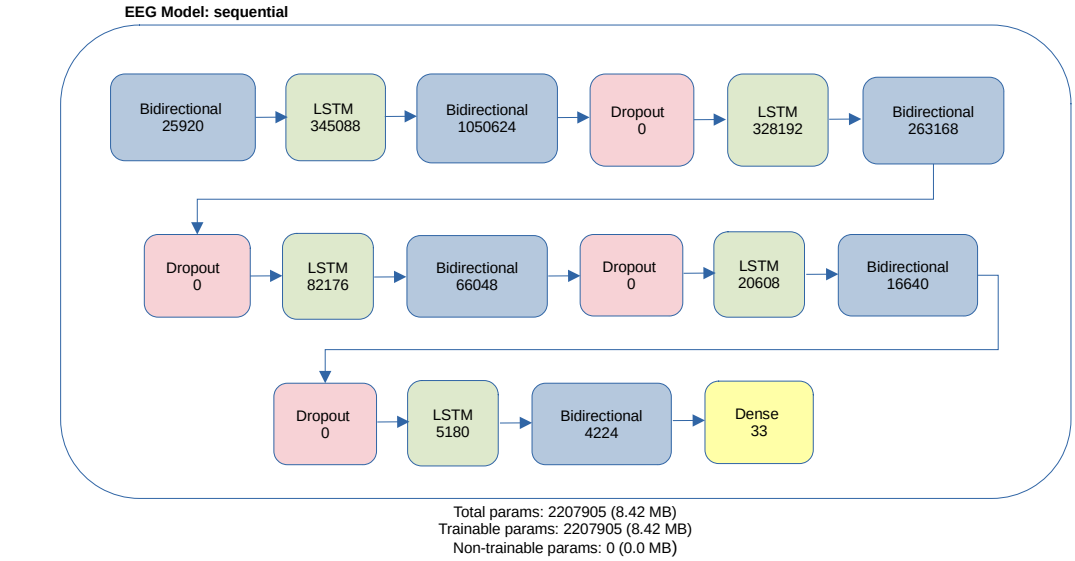

(a)

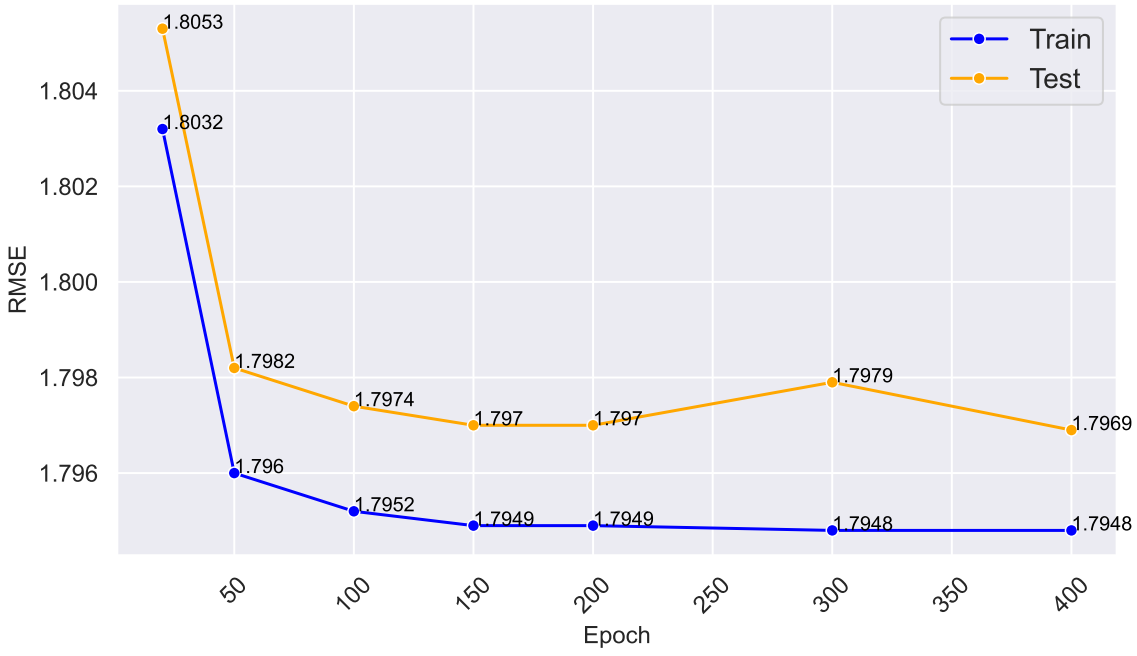

(b)

Figure 4.2: (a) Details of the EEG baseline model, including the parameters for each layer and a summary of the total number of trainable and non-trainable parameters in the entire model. (b) Comparison of the baseline outcomes of the LSTM model for EEG fold 1 during the training and testing process for each epoch.

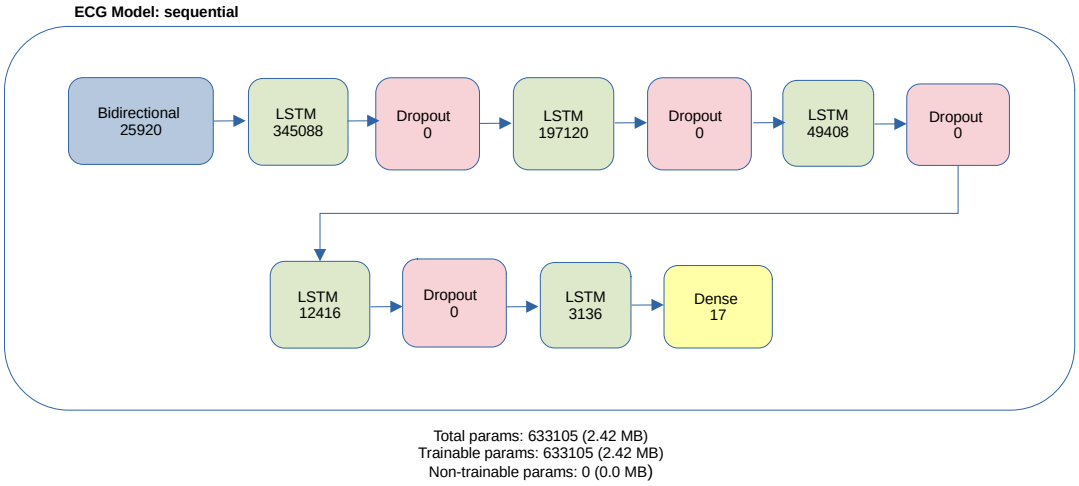

(a)

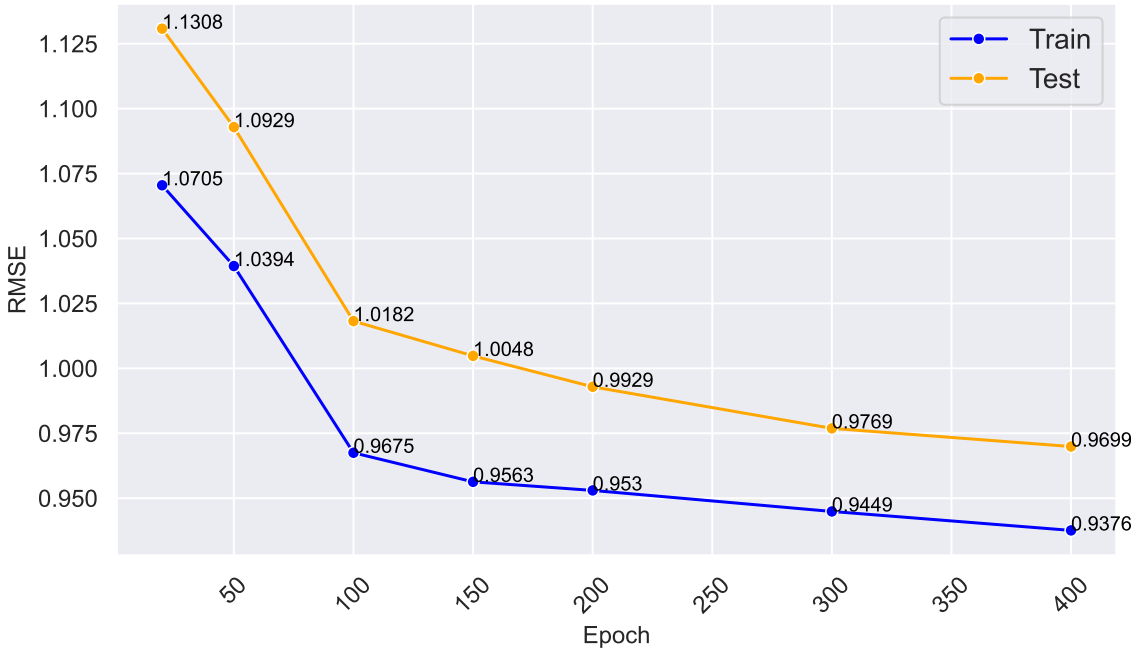

(b)

EMG and EEG models.

The baselines shared some hyperparameter configurations, which are beta_1 = 0.9, beta_2 = 0.999, epsilon = 1e-08, and decay = 0.0, with the activation function set to sigmoid. The specific details about each baseline architecture are described as follows.

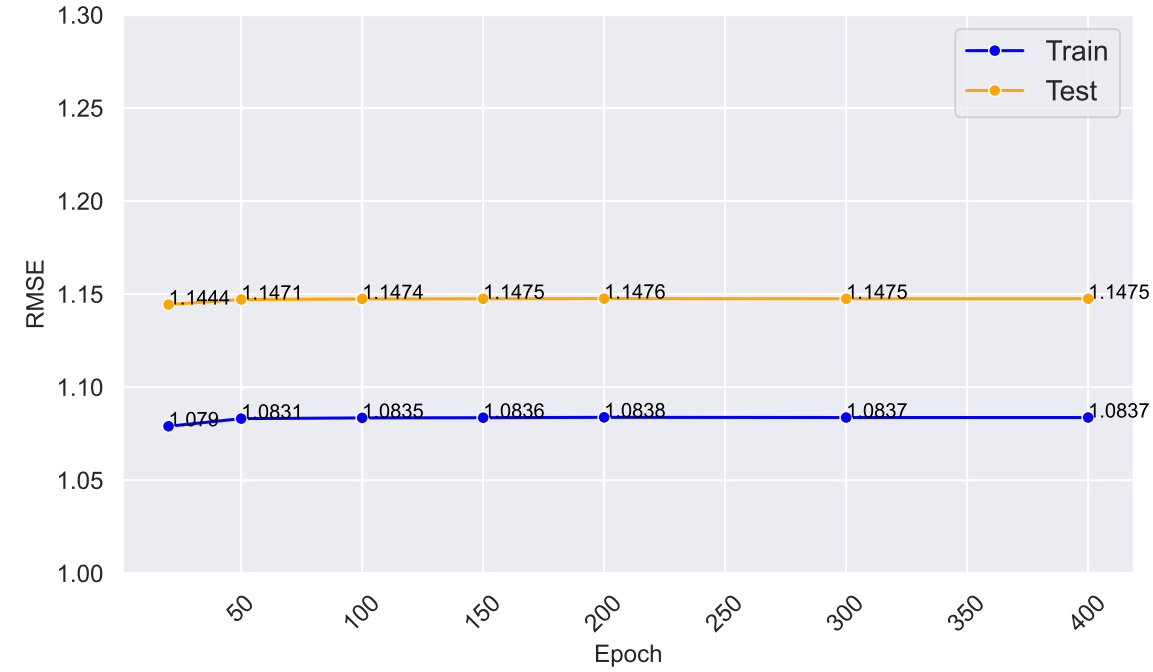
Train
Test
RMSE
Epoch
1.30
1.25
1.20
1.15
1.10
1.05
1.00
50
100
150
200
250
300
350
400
1.1444
1.1471
1.1474
1.1475
1.1476
1.1475
1.1475
1.079
1.0831
1.0835
1.0836
1.0838
1.0837
1.0837

(a)

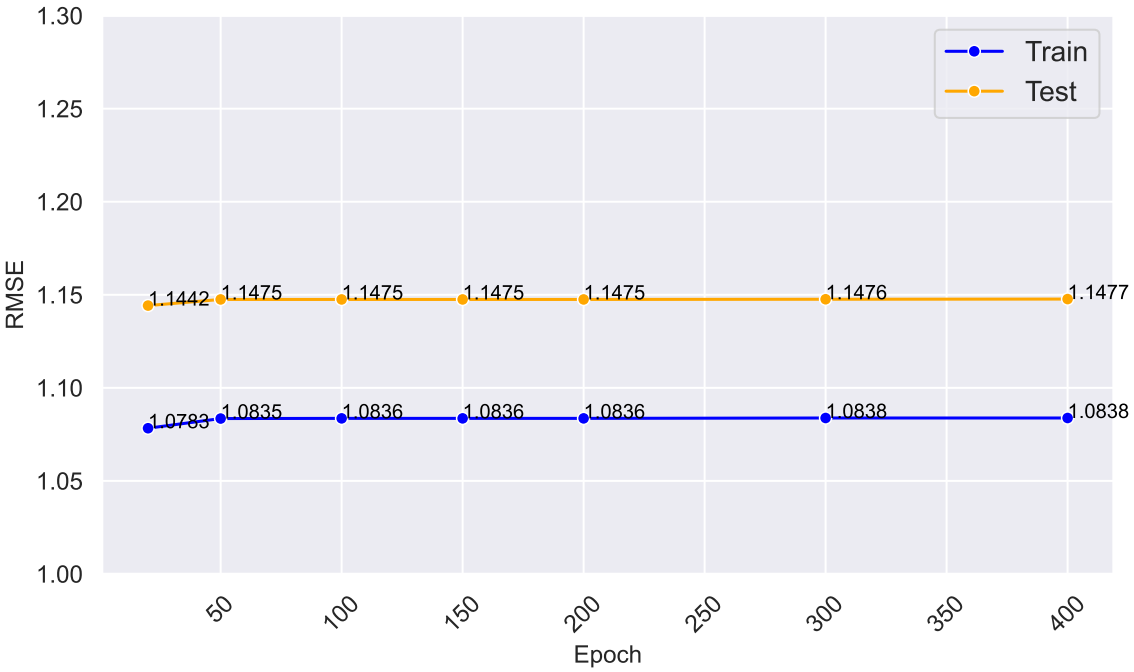
Train
Test
RMSE
Epoch
1.30
1.25
1.20
1.15
1.10
1.05
1.00
50
100
150
200
250
300
350
400
1.1442
1.1475
1.1475
1.1475
1.1475
1.1476
1.1477
1.0783
1.0835
1.0836
1.0836
1.0836
1.0838
1.0838

(b)

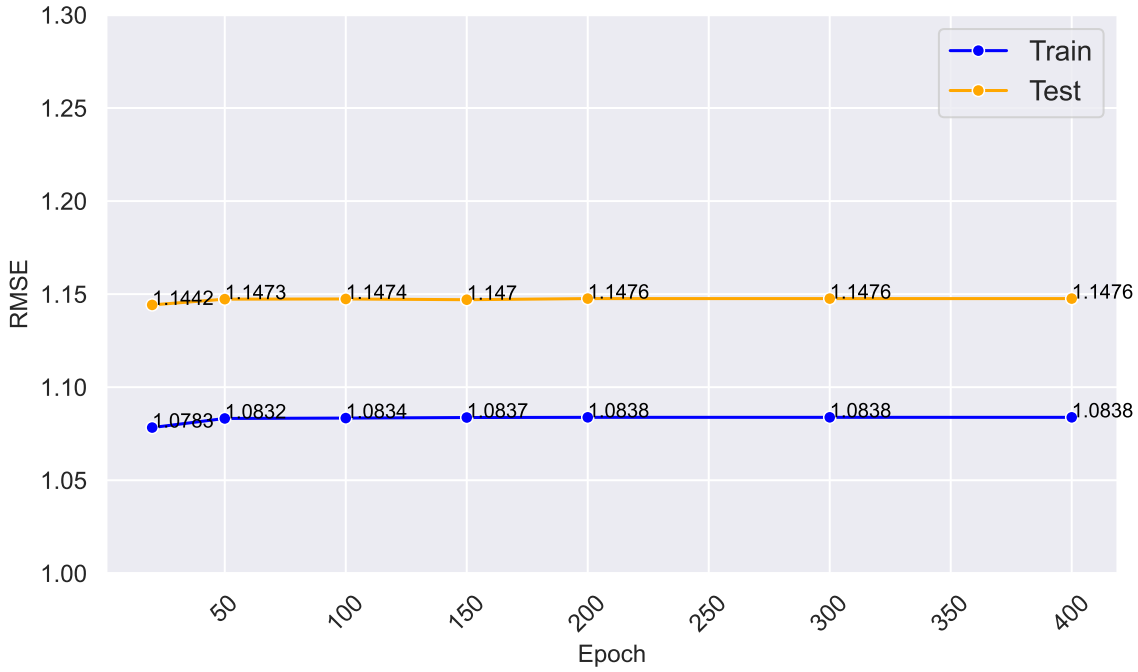
Train
Test
RMSE
Epoch
1.30
1.25
1.20
1.15
1.10
1.05
1.00
50
100
150
200
250
300
350
400
1.1442
1.1473
1.1474
1.147
1.1476
1.1476
1.1476
1.0783
1.0832
1.0834
1.0837
1.0838
1.0838
1.0838

(c)

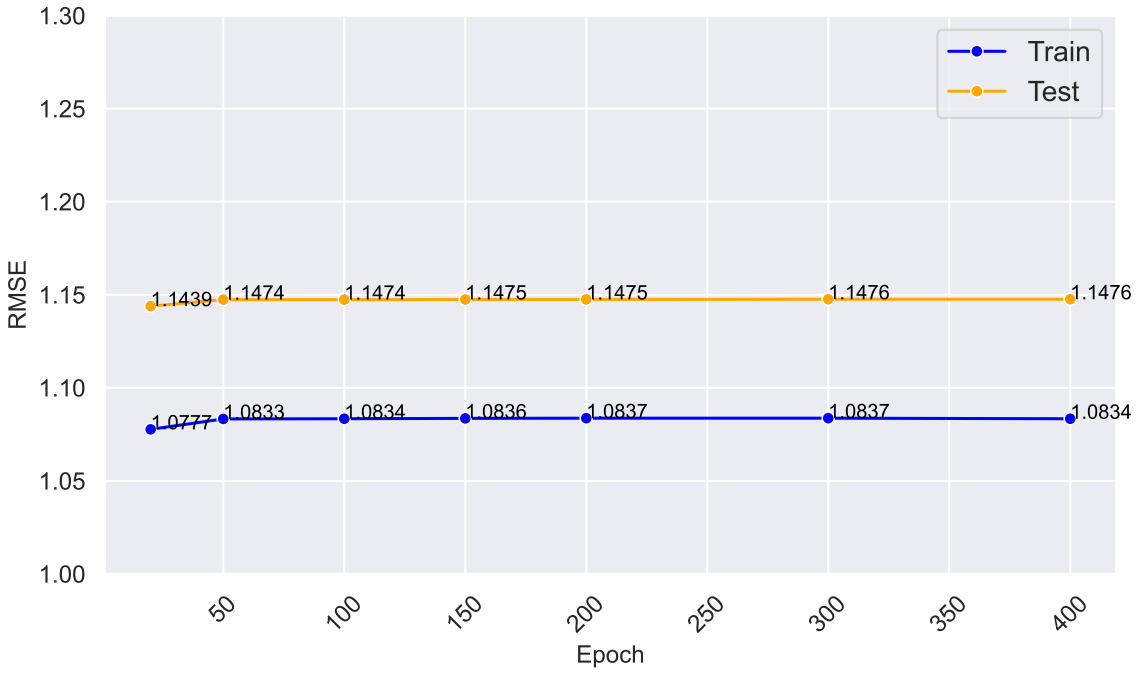
Train
Test
RMSE
Epoch
1.30
1.25
1.20
1.15
1.10
1.05
1.00
50
100
150
200
250
300
350
400
1.1439
1.1474
1.1474
1.1475
1.1475
1.1476
1.1476
1.0777
1.0833
1.0834
1.0836
1.0837
1.0837
1.0834

(d)

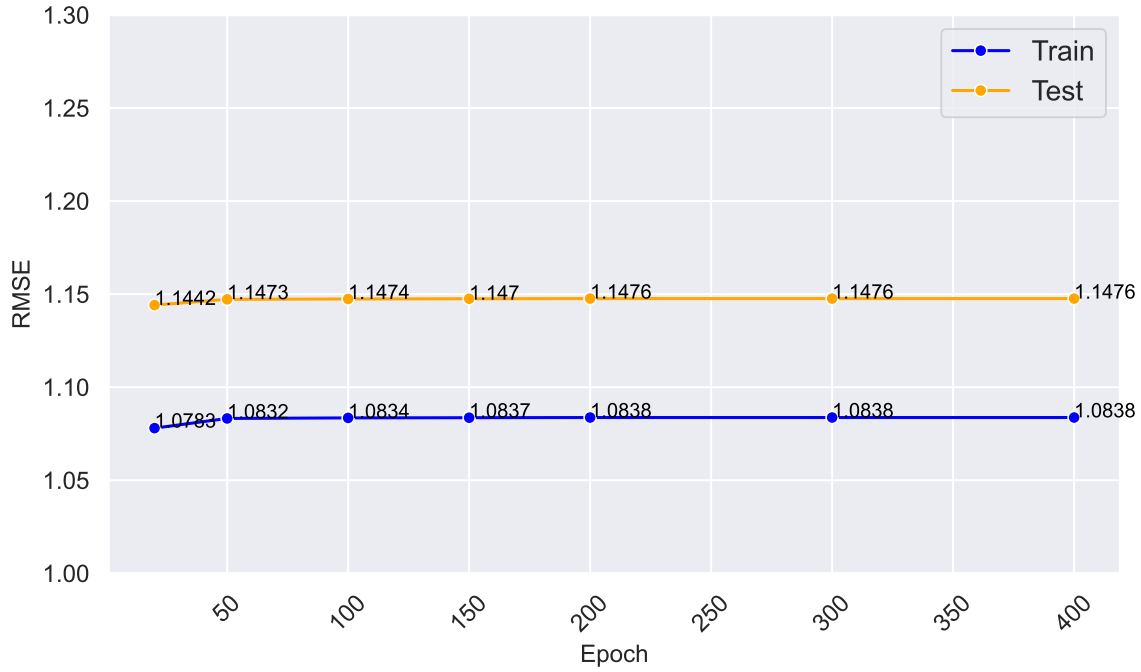
Train
Test
RMSE
Epoch
1.30
1.25
1.20
1.15
1.10
1.05
1.00
50
100
150
200
250
300
350
400
1.1442
1.1473
1.1474
1.147
1.1476
1.1476
1.1476
1.0783
1.0832
1.0834
1.0837
1.0838
1.0838
1.0838

(e)

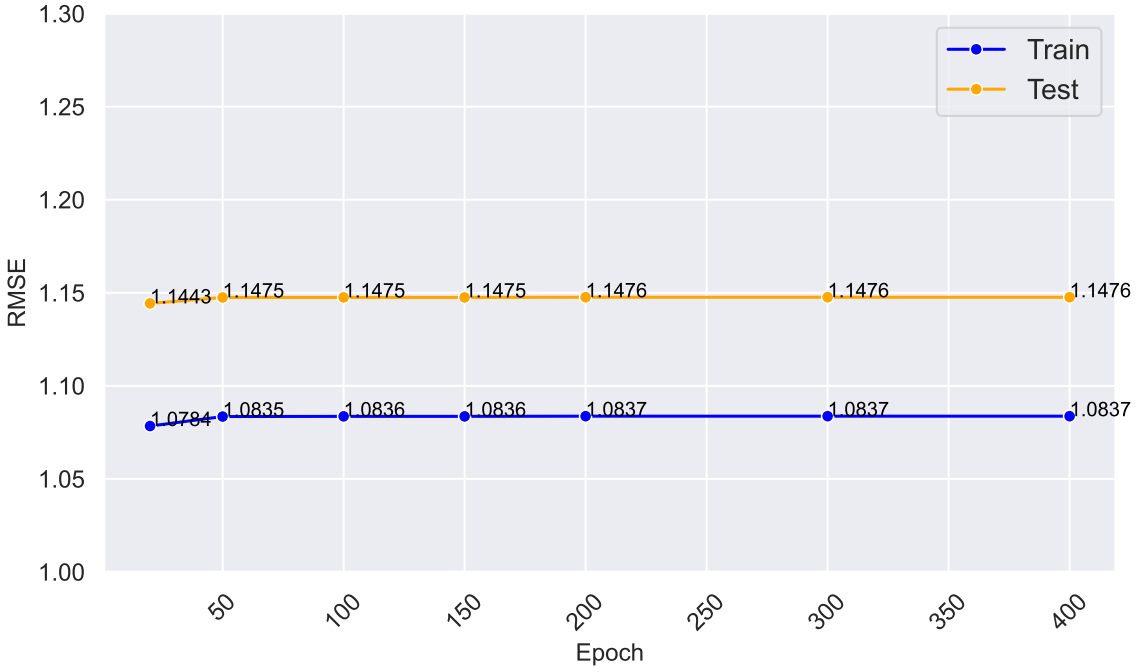
Train
Test
RMSE
Epoch
1.30
1.25
1.20
1.15
1.10
1.05
1.00
50
100
150
200
250
300
350
400
1.1443
1.1475
1.1475
1.1475
1.1476
1.1476
1.1476
1.0784
1.0835
1.0836
1.0836
1.0837
1.0837
1.0837

(f)

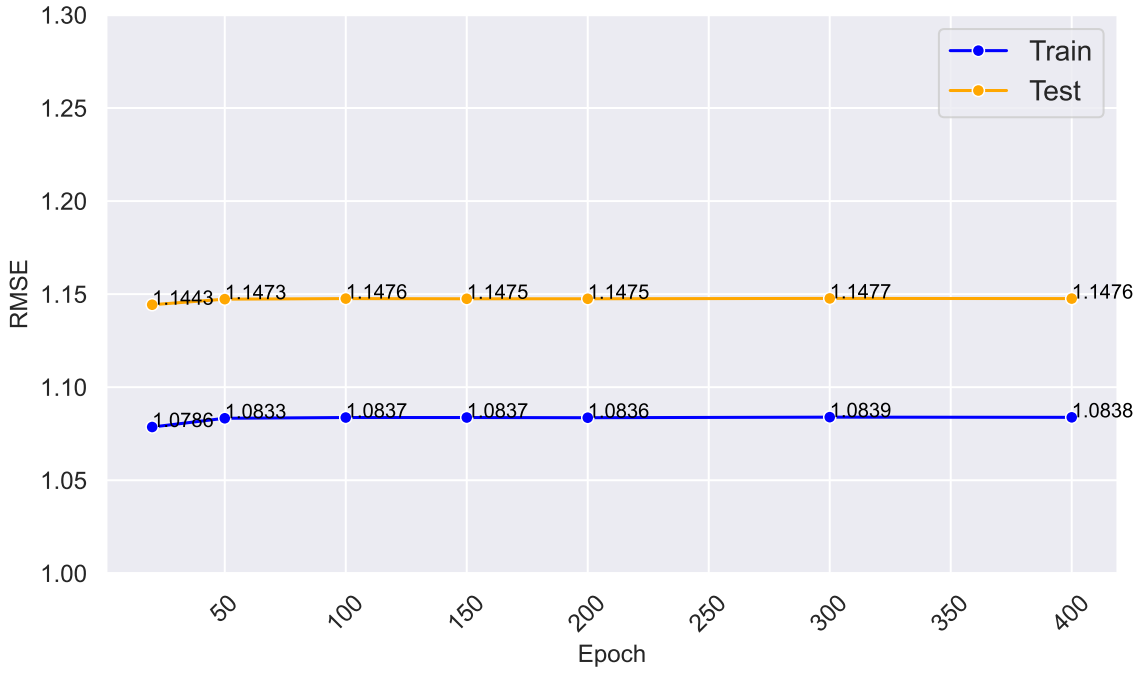

(g)

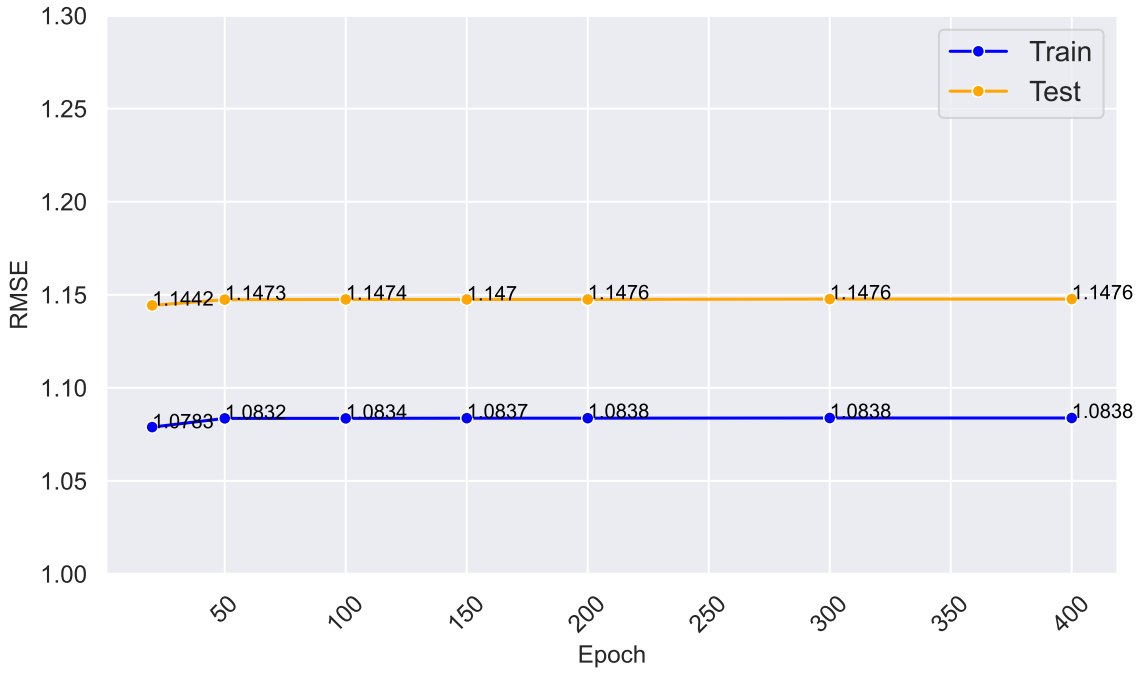

(h)

Figure 4.3: (a) Details of the ECG baseline model, showing the parameters for each layer and summarizing the total number of trainable and non-trainable parameters in the entire model. The figures from (b) to (j) represent the comparison of baseline outcomes of the LSTM model for the ECG folds during the training and testing process across each epoch, where the figures represent (b) ECG Fold 1. (c) ECG Fold 2. (d) ECG Fold 3. (e) ECG Fold 4. (f) ECG Fold 5. (g) ECG Fold 6. (h) ECG Fold 7. (i) ECG Fold 8. (J) ECG Fold 9.

4.2.1 EEG

We designed the EEG model, which comprises a total of 2,207,905 trainable parameters (refer to Figure 4.2a). The EEG TUEG dataset was collected and made available by Temple University Hospital (TUH) for various research purposes involving this type of biosignal. There is no recommended data split for training and testing in the projects. Therefore, we segmented the dataset, allocating 80% (329,920 registers) for training and 20% for testing (82,480 registers. The training batch size was set to 54,000, while the testing batch size was set to 14,000. The outcomes obtained for each epoch are detailed in Figure 4.2b.

4.2.2 ECG

We designed ECG model, which comprises 633,105 as a total trainable parameters (refer to Figure 4.3a). Following the dataset creators' guidelines, we executed the training and test phases with its specific dataset, which contains 102,106 and 21,892 registers, respectively. The training batch size was set to 11,000, and the testing batch size was set to 2,200. The results obtained for each epoch of the folds are detailed in Figures 4.3b through 4.3h.

4.2.3 EMG

We designed the EMG model, which consists of 557,569 trainable parameters (refer to Figure 4.4a). Similar to the EEG dataset, the creators of the EMG dataset did not suggest a specific percentage for splitting the dataset. Therefore, we followed the same strategy used with the EEG dataset and segmented the EMG dataset into 80% for training (9,342 records) and 20% for testing (2,336 records). The training batch size was set to 2,800, and the testing batch size was set to 700. The results obtained for each epoch of the folds are detailed in Figures 4.4b, 4.4a, and 4.4b.

4.3 EXPERIMENTAL RESULTS

We evaluated the performance of heterogeneous transfer learning using root mean squared error (RMSE), as detailed in Chapter 3. We chose the RMSE metric because it allowed us to analyze the impact on the distance between the outcomes of the baseline model and those of the heterogeneous transfer learning model, and to evaluate the possibility of transferring knowledge between heterogeneous electrical biosignals.

4.3.1 Similarity analysis

Our first step in trying to improve the quality of the source domain selected was to implement a similarity analysis based on the DTW method. However, due to the high computational cost of this operation, we decided to calculate the waves distances using only a sample of the datasets. We calculated the distances between the ECG and EEG signals, as well as between the ECG and EMG signals. Therefore, we selected 8% of the ECG and EEG datasets, as well as the entire EMG dataset. We calculated the distances

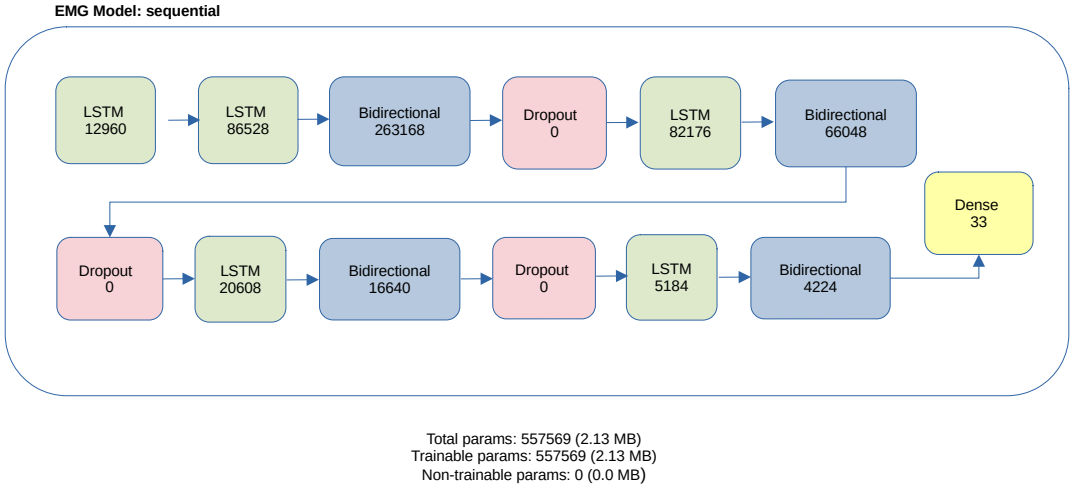

(a)

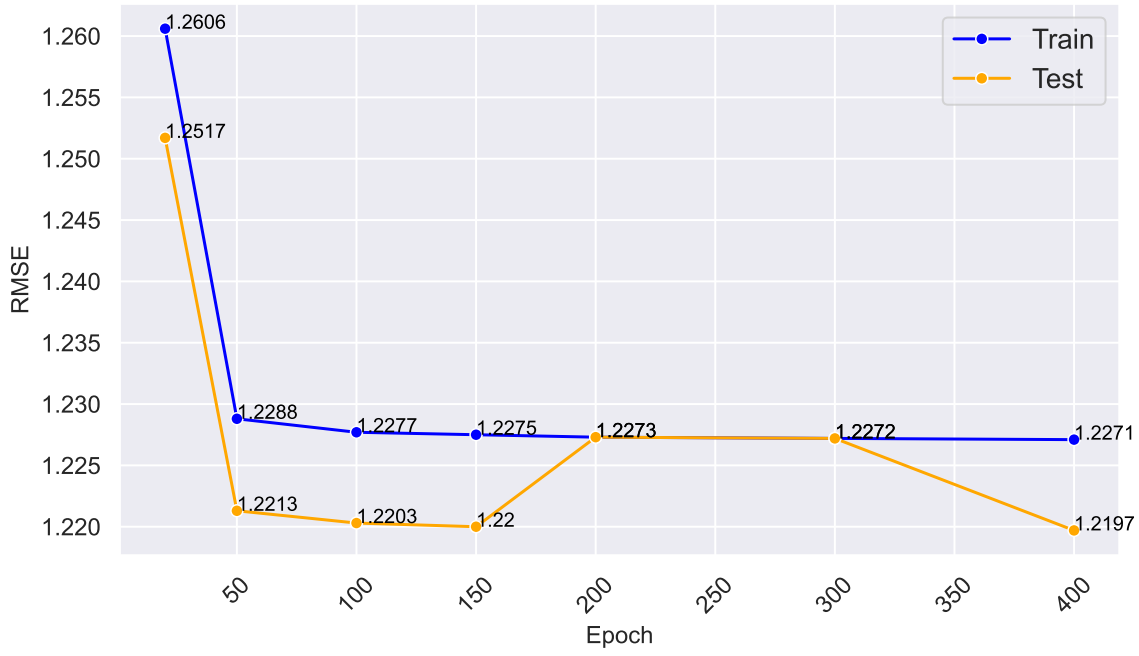

(b)

between the nine ECG folds and the EEG, as well as the three EMG folds, and then standardized them to a range between zero and one.

After calculating the distance among all the folds, we selected the ECG fold with the lower distances for ECG-EEG (as shown in Table 4.1) and ECG-EMG (as shown in Table 4.2), to be used a source domains to the EEG and EMG models.

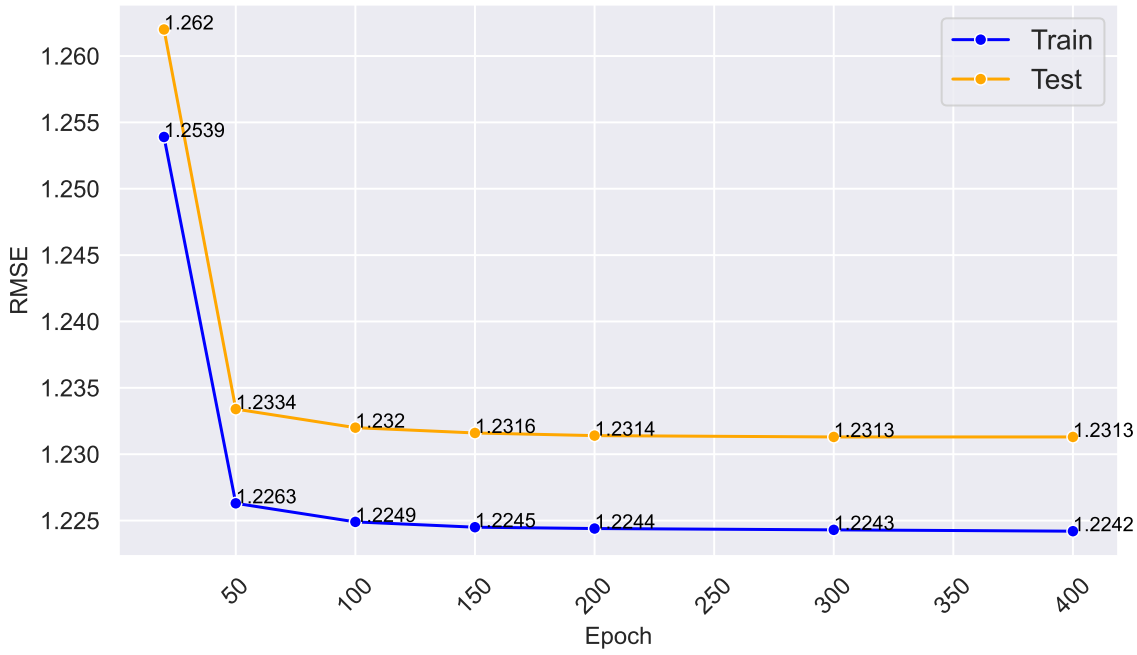

(a)

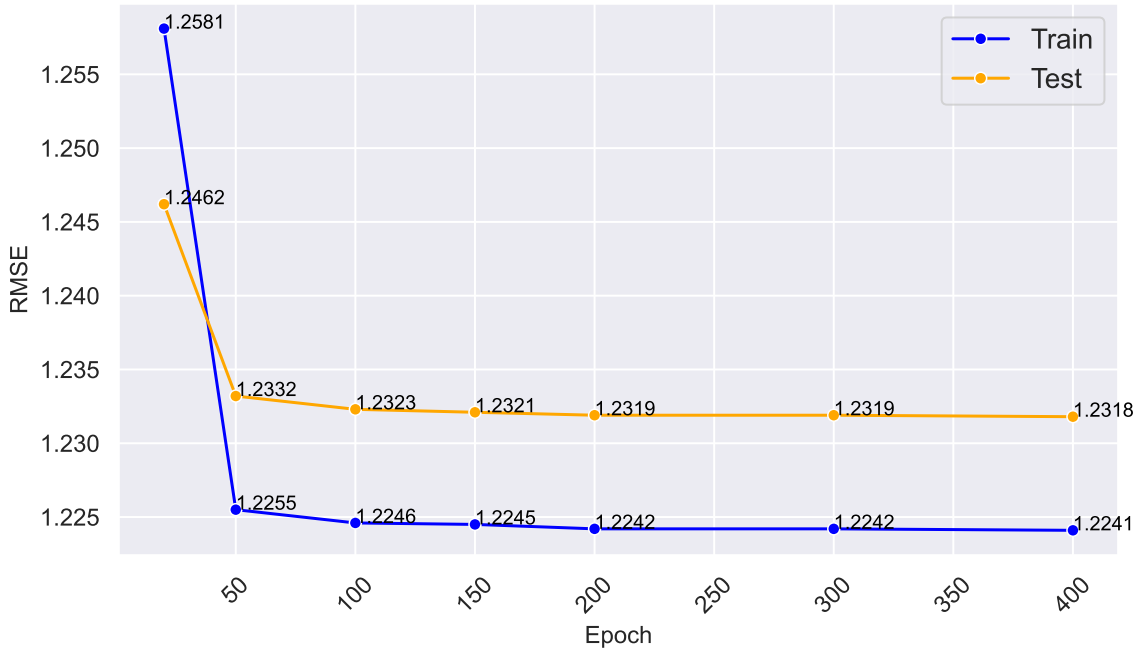

(b)

Figure 4.4: (a) Details of the EMG baseline, showing parameters for each layer and summarizing the total number of trainable and non-trainable parameters. The figures from (b) to (d) represent the comparison of baseline outcomes of the LSTM model for the EMG folds during the training and testing process across each epoch, where the figures represent (b) EMG Fold 1, (c) EMG Fold 2, and (d) EMG Fold 3.

Table 4.1: Results of the similarity analysis between ECG folds and EEG fold using the dynamic time warping (DTW) method.

[c]0.5

Similarities ECG-EEG	
ECG Folds	**ECG-EEG Fold 1**
1	0.69
2	0.10
3	0.16
4	0.59
5	1
6	0.58
7	0.47
8	0.19
9	**0**

Table 4.2: Results of the similarity analysis between ECG folds and EMG folds using the dynamic time warping (DTW) method.

[c]1

Similarities ECG-EMG			
ECG Folds	**ECG-EMG Fold 1**	**ECG-EMG Fold 2**	**ECG-EMG Fold 3**
1	**0**	0.97	0.97
2	0.57	**0**	0.43
3	0.59	0.44	**0**
4	0.86	0.80	0.80
5	1	1	1
6	0.80	0.78	0.79
7	0.72	0.67	0.68
8	0.58	0.47	0.49
9	0.49	0.33	0.36

4.3.2 Transfer learning

Based on our methodology, we observed the outcomes of the similarity analysis and selected the best ECG baseline models to determine the dataset folds that would serve as the source domains for the transfer learning process.

For the EEG model, we used the parameters from the ECG baseline trained on ECG fold 9 with 20 epochs, as presented in Figure 4.5a. For the EMG model trained on EMG fold 1, we utilized the ECG baseline parameters trained on ECG fold 1 with 20 epochs, with results shown in Figure 4.5b. For the EMG model trained on EMG fold 2, we employed the parameters from the ECG baseline trained on ECG fold 2 with 20 epochs, as shown in Figure 4.5a. Finally, for the EMG model trained on EMG fold 3, we used the ECG LSTM parameters trained on ECG fold 3 with 20 epochs; see Figure 4.5b for

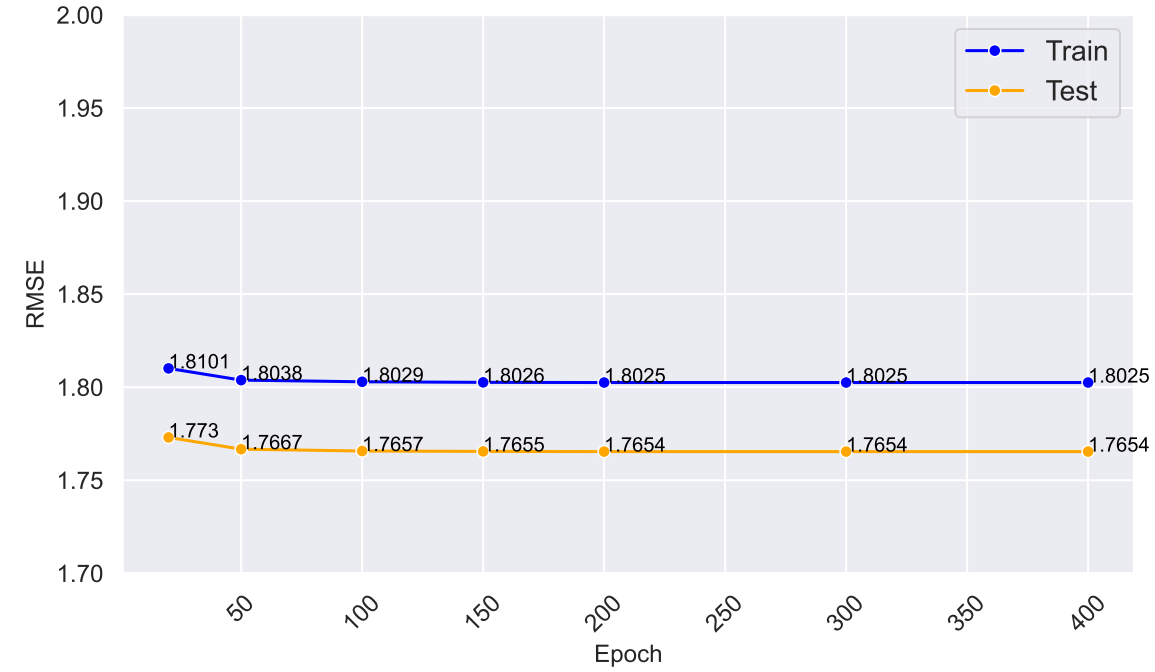

(a)

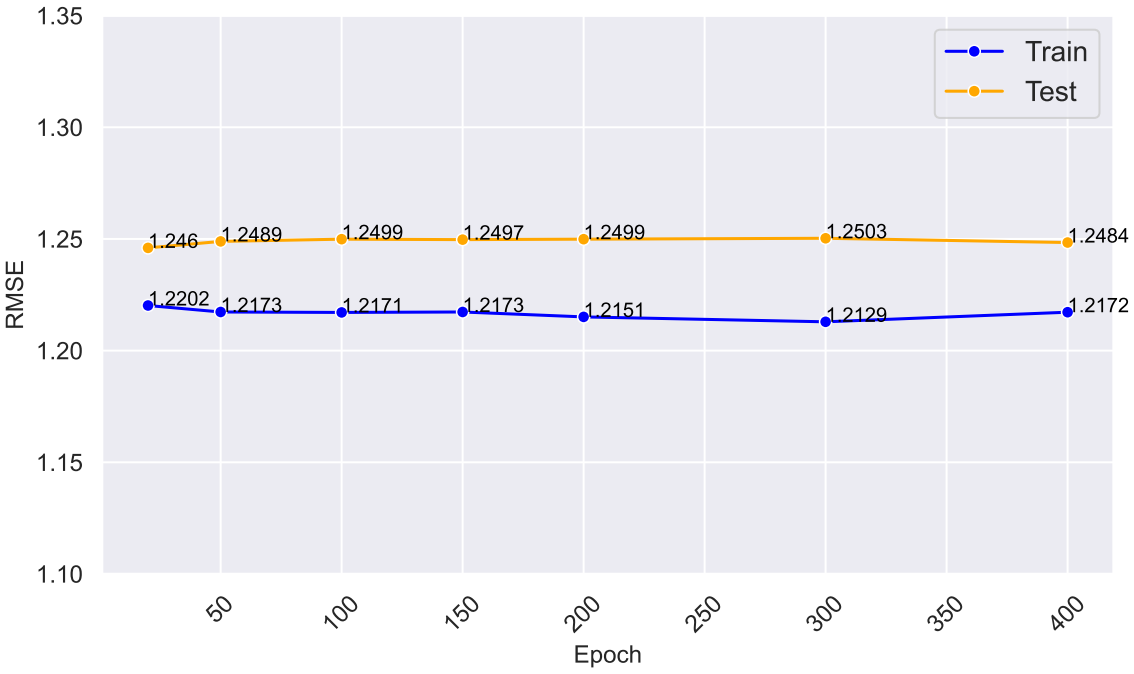

(b)

the results.

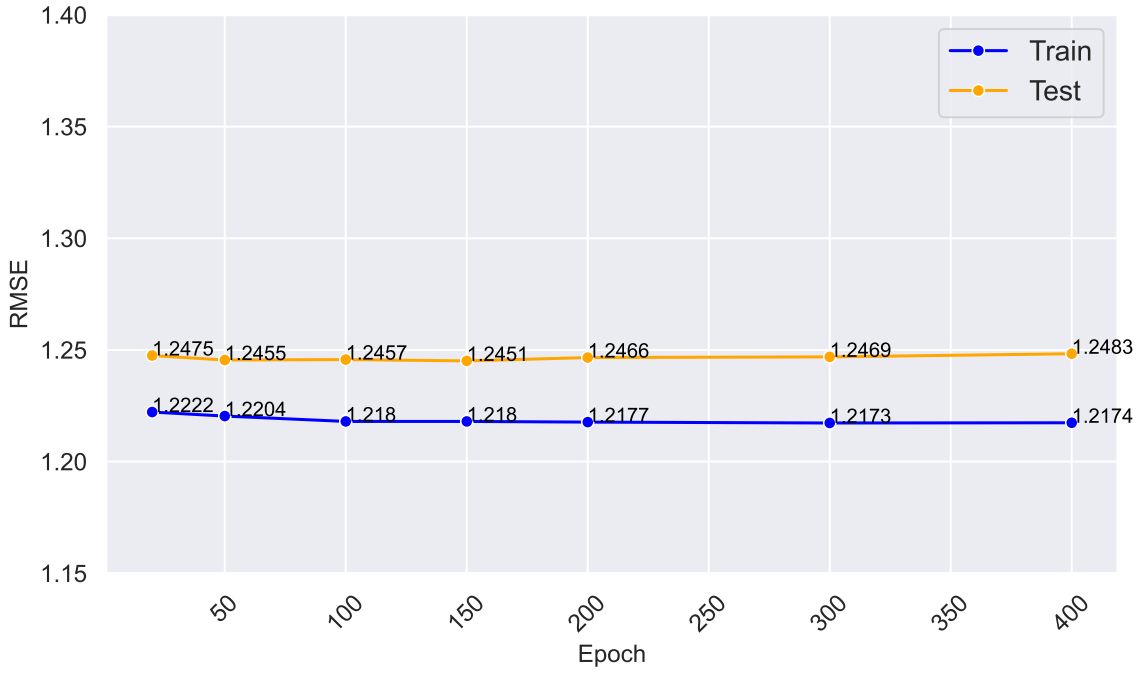

(a)

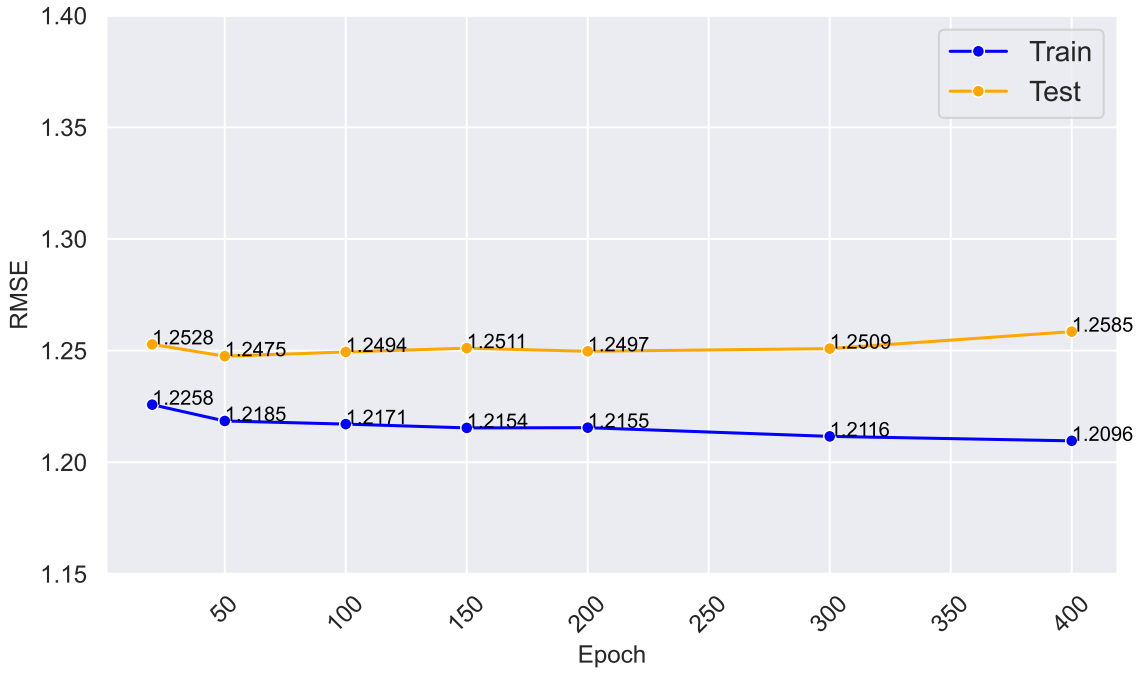

(b)

Figure 4.5: Outcomes of heterogeneous transfer learning from the ECG model trained on ECG fold 9 to the EEG model.

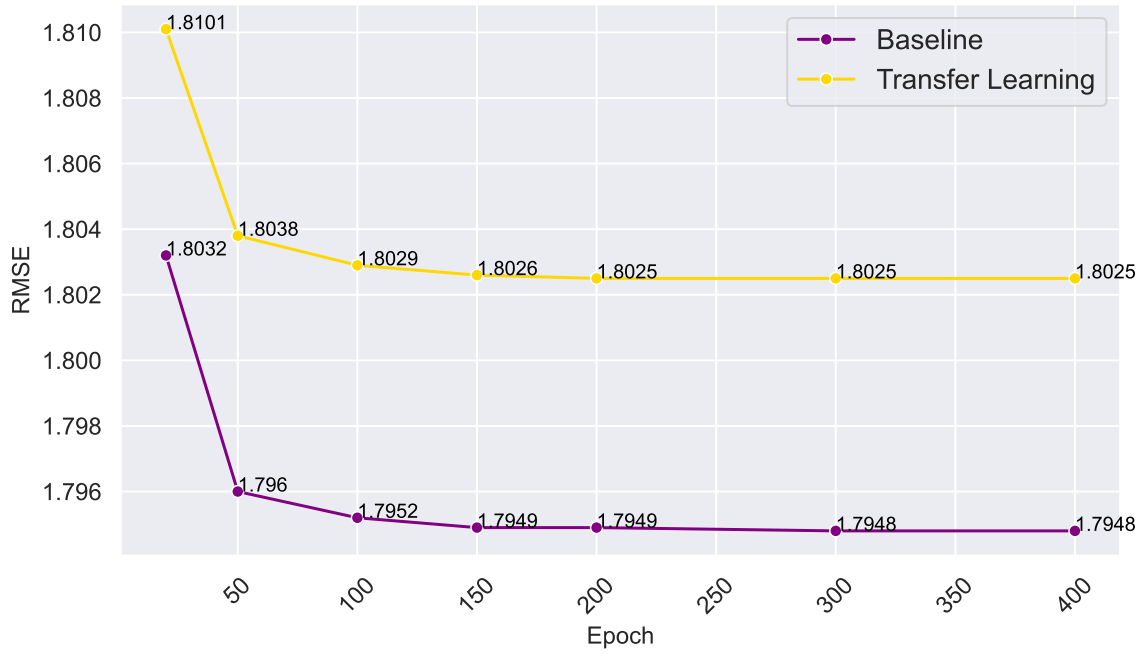
Baseline
Transfer Learning
RMSE
Epoch
1.810
1.808
1.806
1.804
1.802
1.800
1.798
1.796
50
100
150
200
250
300
350
400
1.8101
1.8038
1.8029
1.8026
1.8025
1.8025
1.8025
1.8032
1.796
1.7952
1.7949
1.7949
1.7948
1.7948

(a)

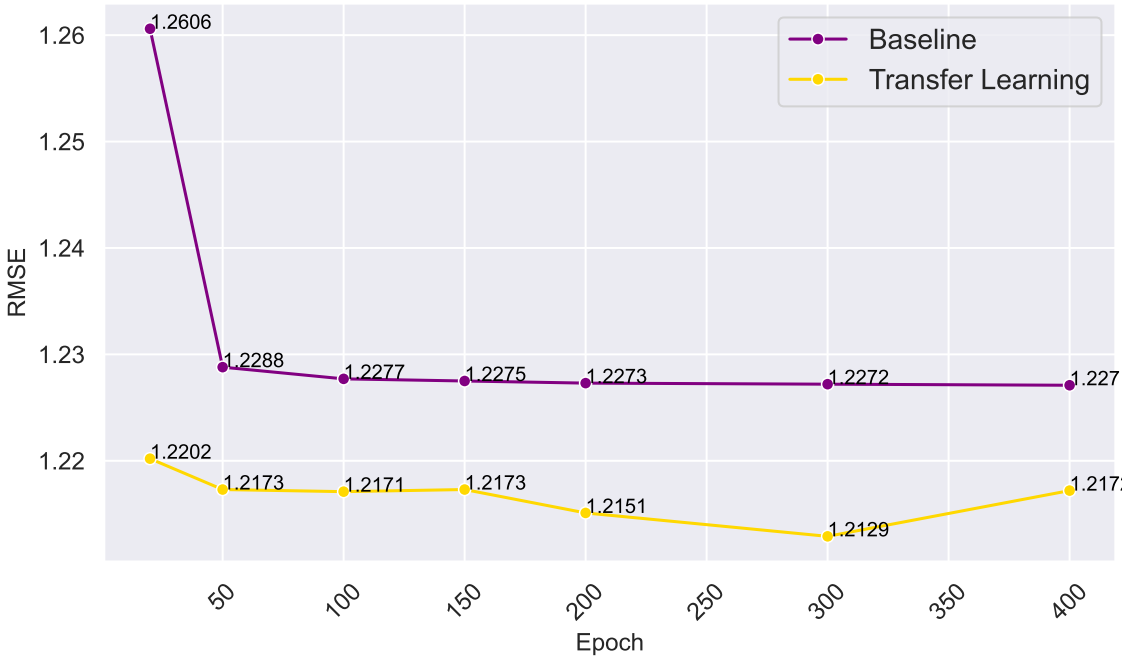
Baseline
Transfer Learning
RMSE
Epoch
1.26
1.25
1.24
1.23
1.22
50
100
150
200
250
300
350
400
1.2606
1.2288
1.2277
1.2275
1.2273
1.2272
1.2271
1.2202
1.2173
1.2171
1.2173
1.2151
1.2129
1.2172

(b)

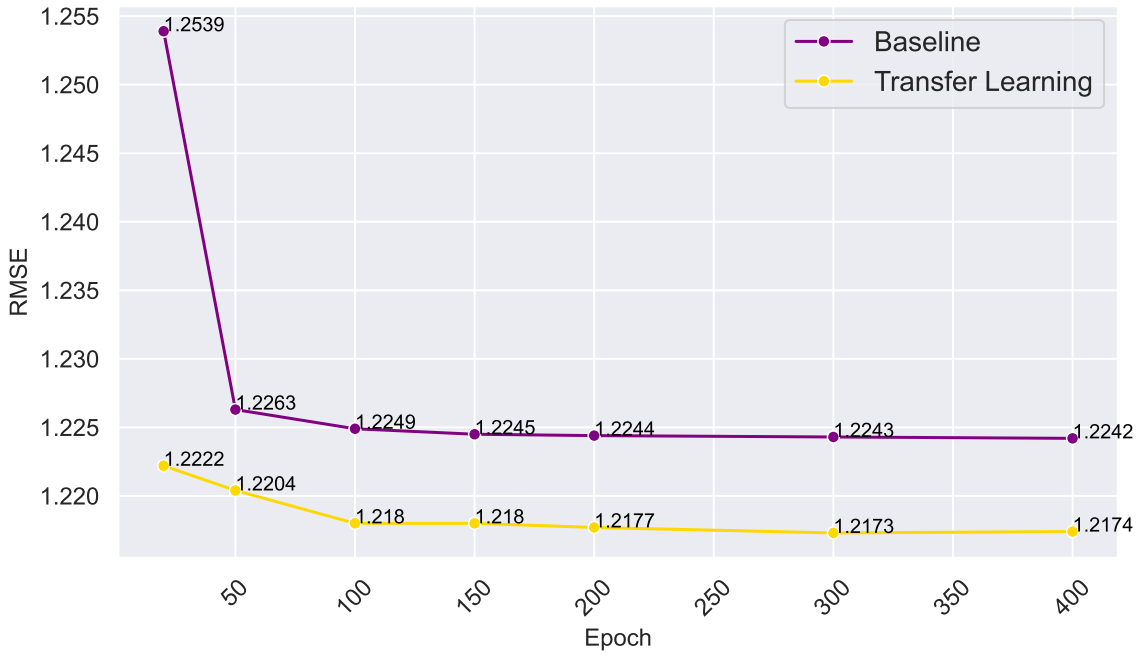

(a)

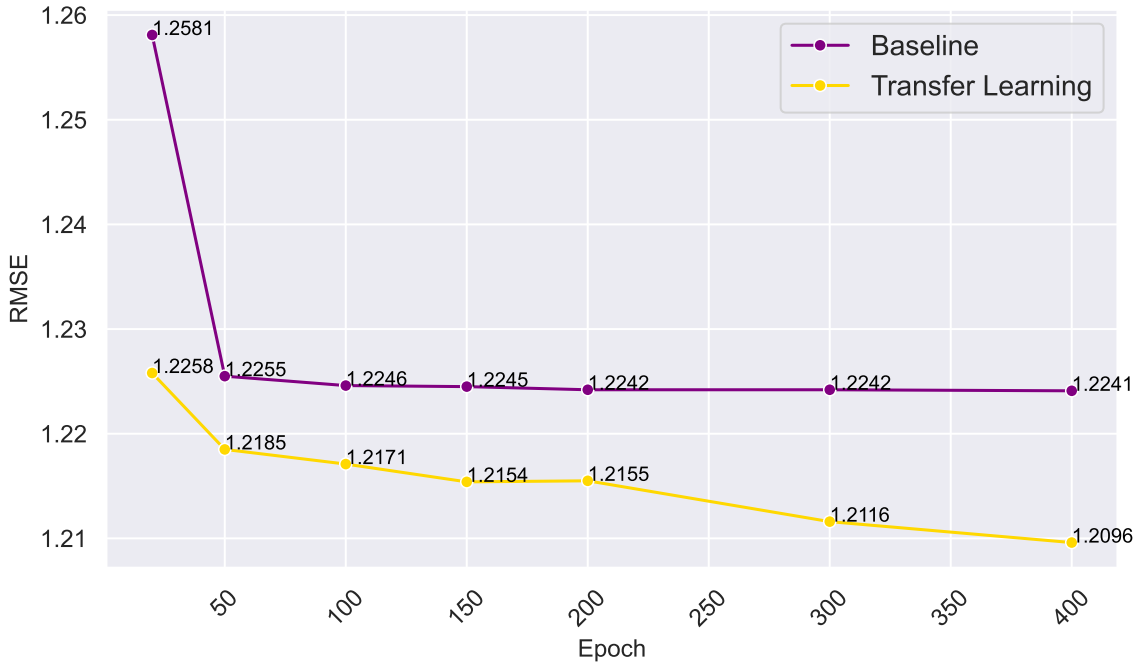

(b)

Figure 4.6: Comparative analysis of outcomes between the baseline model and the model with pre-trained parameters: (a) Comparison between the EEG baseline model and the EEG model with pre-trained ECG LSTM parameters from ECG fold 9; (b) Comparison between the EMG baseline model trained on EMG fold 1 and the EMG model with pre-trained ECG LSTM parameters from ECG fold 1; (c) Comparison between the EMG baseline model trained on EMG fold 2 and the EMG model with pre-trained ECG LSTM parameters from ECG fold 2; (d) Comparison between the EMG baseline model trained on EMG fold 3 and the EMG model with pre-trained ECG parameters from ECG fold 3.

To analyze the transfer learning outcomes, we conducted a comparison between the baseline for each biosignal and its respective transfer learning model that received the pre-trained parameters from the most similar biosignal fold, see Figures from 4.6a to 4.6b.

4.4 DISCUSSION

To address the research questions, we modeled transfer learning between LSTM neural networks using heterogeneous electrical biosignals, specifically ECG-EMG and ECG-EEG, with ECG as the source domain and EMG and EEG as the target domains. The proposed method is divided into similarity analysis and heterogeneous transfer learning processes.

About similarity analysis using DTW, we investigated whether utilizing features from the most similar signal segments, even in a heterogeneous dataset context, as a source domain could improve the target model outcomes. The computational cost of calculating the similarity analysis limited us to analyzing only 8% of all ECG and EEG database samples.Unlike the EMG dataset, which was small enough to be processed in its entirety. We suspect that this limitation distorted the similarity result and interfered with our database segment selection process. We calculated the similarity between all ECG folds (1 to 9) and the EEG fold, as well as the three EMG folds, using DTW. In the results, we observed a consistently high dissimilarity across all scenarios, which emphasized the heterogeneous characteristics between the EEG, ECG, and EMG electrical biosignals. We also noted that the ECG-EEG fold exhibited the highest distance compared to all ECG-EMG folds, as indicated in Tables 4.1 and 4.2.

Observing the similarities results, we visualized the difficulty of avoiding the effect of negative transfer when dealing with a heterogeneous dataset with non-identical features and label spaces in the transfer learning context, as pointed out by the state-of-the-art studies (CAO et al., 2019; LIN, 2019). Then, to mitigate this tendency, we implemented heterogeneous transfer learning using the reuse model strategy, considering that reusing all weights, biases, and parameters from all layers of the pre-trained ECG model could improve the performance of the target task. In parallel, when we transformed the datasets into the frequency domain, we aimed to reduce their mathematical complexity, making them easier to represent with algebraic functions. Additionally, we performed feature selection based on the results of the similarity analysis. These processes were intended to facilitate the generalization of the electrical biosignals by the predictive function. After training the target EMG and EEG models with the ECG LSTM parameters, we observed a positive transfer learning result in all ECG-EMG transfer learning scenarios, as shown in Figures 4.6b, 4.6a, and 4.6b.

In the ECG-EEG transfer learning context, we observed a slight decrease in the EEG model performance, as indicated in Figure 4.6a. We suspected that this decrease was influenced by our preprocessing segment strategy, the dataset's imbalance characteristics, and the high dissimilarity with the ECG biosignal (see Table 4.1), which resulted in

a negative transfer outcome. The difference between the results presented in the EEG baseline model and the ECG-EEG transfer learning model was small (-0.0077 in RMSE). Despite the high dissimilarity between the biosignals, we realized that the transfer of generalized knowledge from ECG did not result in a complete misunderstanding of the EEG biosignal by its model. We suppose that using another strategy for EEG preprocessing, specifically segmenting to obtain the most representative of the event into the biosignal wave, could improve its outcomes in the transfer learning context, even with the substantial dissimilarity between the ECG and EEG biosignals.

We also noted that the similarity analysis did not produce the expected effect on the model results. We anticipated the best transfer learning outcomes would occur from the ECG model trained on ECG fold 1 to the EMG model trained on EMG fold 1, from the ECG model trained on ECG fold 2 to the EMG model trained on EMG fold 2, and from the ECG model trained on ECG fold 3 to the EMG model trained on EMG fold 3, as indicated in Table 4.2. Instead, the best results were observed in the models: from the ECG model trained on ECG fold 3 to the EMG model trained on EMG fold 3, from the ECG model trained on ECG fold 1 to the EMG model trained on EMG fold 1, and from the ECG model trained on ECG fold 2 to the EMG model trained on EMG fold 2. We suspect that the computational cost limitation, which forced us to reduce the volume of data used to calculate the distance between the biosignals, distorted these results.

Finally, despite the previously mentioned limitations, we demonstrated that applying different strategies together effectively showed the feasibility of generalizing knowledge from one biosignal dataset and transferring it to enhance the predictive accuracy of another model, as in the ECG-EMG scenario. Furthermore, our findings suggest that processing data in the frequency domain can mitigate the effects of unbalanced data. However, it was not sufficiently effective to prevent slight negative transfer learning in the ECG-EEG scenario.

4.5 SUMMARY

In this chapter, following the execution of each step of the methodology described in the previous chapter, we conducted an analysis of the obtained outcomes. We first present the infrastructure used to process the data and then provide a detailed discussion of our observations regarding the preprocessing stages, baseline models, similarity analysis, and, finally, the heterogeneous transfer learning.

Through this analysis, we identified that it is possible to apply transfer learning between neural networks processing heterogeneous electrical biosignals in the frequency domain, resulting in increased accuracy of the target model. However, we also found that the scenario where ECG served as the source domain and EEG as the target domain led to negative transfer. This suggests that generalizing the data by transforming signals into the frequency domain was insufficient to mitigate the effects of unbalanced data.

Another key finding was that the evaluation of similarity for selecting ECG data as the source domain for training the model and transferring its parameters to the target model did not yield a significant positive impact.

In the following chapter, we provide concluding remarks, summarizing the key findings of this research and proposing directions for future work.

Chapter 5

"I'm gonna stand up and say out loud: yes honey I'm here, I'm black and I'm proud!" Nelle

CONCLUSION AND FUTURE WORK

In this study, we propose and validate a transfer learning approach between neural network models, each one designed to process heterogeneous electrical biosignal data; the common data representation was in the frequency domain. To validate our approach, we organized a methodology into four stages: preprocessing the ECG, EEG, and EMG biosignals datasets; building baselines from scratch; calculating the similarity with the DTW method between ECG-EMG dataset, as well as between ECG-EEG; and executing the heterogeneous transfer learning.

5.1 CONCLUSION

Throughout this dissertation, we have addressed the main research question: 'Does transfer learning between neural network models processing heterogeneous electrical biosignals in the frequency domain have the potential to increase the predictive accuracy of the target model?'. To this question, our findings suggest a viable approach to applying transfer learning between neural networks processing non-identical electrical biosignals, specifically ECG as a source domain and EMG as a target domain, thereby improving the accuracy of the target LSTM model. The strategy of simplifying the mathematical representation of waves in the frequency domain effectively addressed the limited number of samples per event in the EMG target dataset.

We also examined three secondary questions. The first is, 'In which scenarios did negative transfer occur?'. Our results indicate that while processing data in the frequency domain can mitigate the effect of unbalanced data, but it was insufficient to prevent slight negative transfer learning, particularly when using ECG as the source domain and EEG as the target domain. This suggests that proper preprocessing to address unbalanced data could enhance the LSTM model's performance.

The second question is, 'Can processing data in the frequency domain mitigate the effect of unbalanced data?'. The outcomes demonstrate that this simplification positively

impacted the generalization of biosignals in restrictive scenarios by the LSTM model. This finding is significant as it suggests the potential to reduce dependency on large datasets for training and calibration, thereby overcoming challenges in heterogeneous transfer learning.

The last question is, 'Can the evaluation of similarity between the signals lead to gains in the accuracy of the target model?' Our analysis revealed that the similarity evaluation did not yield significant gains in target model accuracy. The high computational cost necessitated a substantial reduction in data volume for this activity. This highlights the need to explore methods that balance computational cost and accuracy in similarity assessments, taking into account distortions and shifts in time series data during DTW calculations.

To address the research questions, we explored various scenarios to develop the proposed methodology. Initially, inspired by architectures in the reviewed papers, we implemented LSTM models for each biosignal with more than fifteen hidden layers. However, due to the large data volume, limited computational resources without GPU support, and the complexity of deep neural networks, we had to reduce the model architecture. We also devised a strategy to reduce the size of EEG and ECG biosignals to decrease their volume and enable feasible processing. During this process, we tested various parameter combinations and activation functions, ultimately selecting the sigmoid activation function.

The exploration process allowed us to investigate the feasibility of applying transfer learning between neural networks processing different types of electrical biosignals. We emphasized the importance of designing LSTM architectures with consideration of available computational resources and understanding the specific characteristics of each dataset to adjust neural network parameters effectively, thereby leveraging the model's learned knowledge. Despite certain limitations, such as limited computational resources, the high cost of calculating distances between biosignals, and others detailed in Chapter 4, our experiment demonstrates the potential to enhance the predictive accuracy of the LSTM model by reusing pre-trained parameters. As a result, this research opens avenues for exploring additional methods to achieve heterogeneous transfer learning.

All implemented algorithms have been published as an open-source package and are available online for free at <https://github.com/DeinhaLeao/Master_Degree.git> or <https://drive.google.com/drive/folders/1ciEtKhUUlkcFcNVOhXeM9E29qUGFjixT?usp=sharing>.

5.2 FUTURE WORK

The proposed experiment has raised some open questions and suggested potential research directions. The following points are listed for further exploration and development

of this study:

- Enhance the preprocessing step to use multiple techniques to extract relevant features and obtain the most representative biosignal segment.
- Explore alternative methods for calculating the distance between biosignals, aiming to reduce the computational cost of the process and facilitate the utilization of a substantial volume of data in this measure.
- Replicate the methodology using other kind of neural network, as Transformer.
- Perform a similar architecture appling datasets in the time domain and compare the outcomes in time and frequency scenarios.
- Investigate techniques to mitigate the imbalance dataset effect;

In a broader research timeline, it is possible to study in detail the effects of transfer learning on imbalanced electrical biosignal datasets. Other future works, for example, may focus on enhancing the robustness of model architectures and optimizing the hardware used to improve generalization results.

Another critical area for future research involves interdisciplinary cooperation. Collaborations across diverse fields such as medicine, physics, and among physicians can contribute to enhancing the selection of representative biosignal segments and the analysis conducted by both baseline and transfer learning models. If positive results are confirmed, future research could propose a methodology for implementing this solution in public health policies, with careful attention to ethical considerations in healthcare applications.

BIBLIOGRAPHY

ABDELHAMEED, A. M.; BAYOUMI, M. Semi-supervised deep learning system for epileptic seizures onset prediction. In: IEEE. *2018 17th IEEE International Conference on Machine Learning and Applications (ICMLA)*. [S.l.], 2018. p. 1186–1191.

ABDOLLAHPOUR, M. et al. Transfer learning convolutional neural network for sleep stage classification using two-stage data fusion framework. *IEEE Access*, IEEE, v. 8, p. 180618–180632, 2020.

AGRAWAL, A.; JANA, G. C.; GUPTA, P. A deep transfer learning approach for seizure detection using rgb features of epileptic electroencephalogram signals. In: IEEE. *2019 IEEE International Conference on Cloud Computing Technology and Science (CloudCom)*. [S.l.], 2019. p. 367–373.

ALHUSSEIN, M.; MUHAMMAD, G.; HOSSAIN, M. S. Eeg pathology detection based on deep learning. *IEEE Access*, IEEE, v. 7, p. 27781–27788, 2019.

ASSUNCAO, R. *Fundamentos Estatísticos de Ciência dos Dados*. 2021. Disponível em: <https://homepages.dcc.ufmg.br/~assuncao/EstatCC/FECD.pdf>.

AZAB, A. M. et al. Weighted transfer learning for improving motor imagery-based brain–computer interface. *IEEE Transactions on Neural Systems and Rehabilitation Engineering*, IEEE, v. 27, n. 7, p. 1352–1359, 2019.

BAJAJ, V. et al. Robust approach based on convolutional neural networks for identification of focal eeg signals. *IEEE sensors letters*, IEEE, v. 3, n. 5, p. 1–4, 2019.

BALAFAS, K.; RAJAGOPAL, R.; KIREMIDJIAN, A. S. The continuous wavelet transform as a stochastic process for damage detection. 2015.

BIRD, J. J. et al. Cross-domain mlp and cnn transfer learning for biological signal processing: eeg and emg. *IEEE Access*, IEEE, v. 8, p. 54789–54801, 2020.

BIZOPOULOS, P.; KOUTSOURIS, D. Deep learning in cardiology. *IEEE reviews in biomedical engineering*, v. 12, p. 168–193, 2019.

BROCKWELL, P. J.; DAVIS, R. A. *Introduction to time series and forecasting*. [S.l.]: Springer, 2002.

CAO, Z. et al. Learning to transfer examples for partial domain adaptation. In: *Proceedings of the IEEE/CVF Conference on Computer Vision and Pattern Recognition*. [S.l.: s.n.], 2019. p. 2985–2994.

CHAMBON, S. et al. A deep learning architecture for temporal sleep stage classification using multivariate and multimodal time series. *IEEE Transactions on Neural Systems and Rehabilitation Engineering*, IEEE, v. 26, n. 4, p. 758–769, 2018.

CHUANQI, T. et al. A survey on deep transfer learning. In: *The 27th international conference on artificial neural networks (ICANN 2018). Lecture Notes in Computer Science. Springer*. [S.l.: s.n.], 2018.

COHEN, A. Biomedical signals: Origin and dynamic characteristics; frequency-domain analysis. *The biomedical engineering handbook*, CRC Press Boca Raton, FL, v. 2, p. 951–74, 2006.

DAGOIS, E. et al. Bhattacharyya distance-based transfer learning for a hybrid eeg-ftcd brain-computer interface. In: IEEE. *ICASSP 2019-2019 IEEE International Conference on Acoustics, Speech and Signal Processing (ICASSP)*. [S.l.], 2019. p. 3082–3086.

DAOUD, H.; BAYOUMI, M. A. Efficient epileptic seizure prediction based on deep learning. *IEEE transactions on biomedical circuits and systems*, IEEE, v. 13, n. 5, p. 804–813, 2019.

ER, M. B.; ÇIĞ, H.; AYDILEK, İ. B. A new approach to recognition of human emotions using brain signals and music stimuli. *Applied Acoustics*, Elsevier, v. 175, p. 107840, 2021.

FAUZI, H.; SHAPIAI, M. I.; KHAIRUDDIN, U. Transfer learning of bci using cur algorithm. *Journal of Signal Processing Systems*, Springer, v. 92, n. 1, p. 109–121, 2020.

FENG, Y. et al. Compressive detection of stochastic sparse signals with unknown sparsity degree. *IEEE Signal Processing Letters*, IEEE, 2023.

GANDHI, V. *Brain-computer interfacing for assistive robotics: Electroencephalograms, recurrent quantum neural networks, and user-centric graphical interfaces*. [S.l.]: academic press, 2014.

GAO, Y. et al. Deep convolutional neural network-based epileptic electroencephalogram (eeg) signal classification. *Frontiers in neurology*, Frontiers Media SA, v. 11, 2020.

GARCÍA-SALINAS, J. S. et al. Transfer learning in imagined speech eeg-based bcis. *Biomedical Signal Processing and Control*, Elsevier, v. 50, p. 151–157, 2019.

GIORGINO, T. Computing and visualizing dynamic time warping alignments in r: The dtw package. *Journal of Statistical Software*, v. 31, n. 7, p. 1–24, 2009. Disponível em: <https://www.jstatsoft.org/index.php/jss/article/view/v031i07>.

HE, H.; WU, D. Different set domain adaptation for brain-computer interfaces: A label alignment approach. *IEEE Transactions on Neural Systems and Rehabilitation Engineering*, IEEE, v. 28, n. 5, p. 1091–1108, 2020.

ILAKIYASELVAN, N.; KHAN, A. N.; SHAHINA, A. Deep learning approach to detect seizure using reconstructed phase space images. *Journal of Biomedical Research*, Education Department of Jiangsu Province, v. 34, n. 3, p. 240, 2020.

JADHAV, P. et al. Automatic sleep stage classification using time–frequency images of cwt and transfer learning using convolution neural network. *Biocybernetics and Biomedical Engineering*, Elsevier, v. 40, n. 1, p. 494–504, 2020.

JIANG, J.; FARES, A.; ZHONG, S.-H. A context-supported deep learning framework for multimodal brain imaging classification. *IEEE Transactions on Human-Machine Systems*, IEEE, v. 49, n. 6, p. 611–622, 2019.

JIANG, Y. et al. Smart diagnosis: a multiple-source transfer tsk fuzzy system for eeg seizure identification. *ACM Transactions on Multimedia Computing, Communications, and Applications (TOMM)*, ACM New York, NY, USA, v. 16, n. 2s, p. 1–21, 2020.

JIANG, Z.; CHUNG, F.-L.; WANG, S. Recognition of multiclass epileptic eeg signals based on knowledge and label space inductive transfer. *IEEE Transactions on Neural Systems and Rehabilitation Engineering*, IEEE, v. 27, n. 4, p. 630–642, 2019.

KACHUEE, M.; FAZELI, S.; SARRAFZADEH, M. Ecg heartbeat classification: A deep transferable representation. In: IEEE. *2018 IEEE International Conference on Healthcare Informatics (ICHI)*. [S.l.], 2018. p. 443–444.

KANIUSAS, E. *Biomedical Signals and Sensors III: Linking electric biosignals and biomedical sensors*. [S.l.]: Springer, 2019.

KANT, P. et al. Cwt based transfer learning for motor imagery classification for brain computer interfaces. *Journal of Neuroscience Methods*, Elsevier, v. 345, p. 108886, 2020.

KARI, A.; SCHURIG, T.; GERSCH, M. The emergence of a new european data economy: A systematic research agenda for health data spaces. *SMR-Journal of Service Management Research*, Nomos Verlagsgesellschaft mbH & Co. KG, v. 7, n. 4, p. 176–198, 2024.

KATIRJI, M. B. *Electromyography in clinical practice*. [S.l.]: Oxford University Press, 2018.

KHAN, S. et al. Biometric systems utilising health data from wearable devices: applications and future challenges in computer security. *ACM Computing Surveys (CSUR)*, ACM New York, NY, USA, v. 53, n. 4, p. 1–29, 2020.

KUNDU, S.; ARI, S. Mscnn: a deep learning framework for p300-based brain–computer interface speller. *IEEE Transactions on Medical Robotics and Bionics*, IEEE, v. 2, n. 1, p. 86–93, 2019.

LEE, D.-Y. et al. Decoding movement imagination and execution from eeg signals using bci-transfer learning method based on relation network. In: IEEE. *ICASSP 2020-2020 IEEE International Conference on Acoustics, Speech and Signal Processing (ICASSP)*. [S.l.], 2020. p. 1354–1358.

LI, H. et al. Improved label space alignment for motor imagery classification. In: IEEE. *2023 IEEE 13th International Conference on CYBER Technology in Automation, Control, and Intelligent Systems (CYBER)*. [S.l.], 2023. p. 1197–1202.

LI, J. et al. Multisource transfer learning for cross-subject eeg emotion recognition. *IEEE transactions on cybernetics*, v. 50, n. 7, p. 3281–3293, 2020.

LIANG, H.; BRONZINO, J. D.; PETERSON, D. R. *Biosignal processing: principles and practices*. [S.l.]: CRC Press, 2012.

LIANG, Y.; MA, Y. Calibrating eeg features in motor imagery classification tasks with a small amount of current data using multisource fusion transfer learning. *Biomedical Signal Processing and Control*, Elsevier, v. 62, p. 102101, 2020.

LIN, Y.-P. Constructing a personalized cross-day eeg-based emotion-classification model using transfer learning. *IEEE journal of biomedical and health informatics*, v. 24, n. 5, p. 1255–1264, 2019.

LIU, Y. et al. Eeg-based cross-subject mental fatigue recognition. In: IEEE. *2019 International Conference on Cyberworlds (CW)*. [S.l.], 2019. p. 247–252.

MANSOOR, A. et al. Deep learning algorithm for brain-computer interface. *Scientific Programming*, Hindawi, v. 2020, 2020.

MOESLUND, T. B. et al. *Statistical machine learning for human behaviour analysis*. [S.l.]: Multidisciplinary Digital Publishing Institute, 2020.

MOODY, G. B.; MARK, R. G. The impact of the mit-bih arrhythmia database. *IEEE engineering in medicine and biology magazine*, IEEE, v. 20, n. 3, p. 45–50, 2001.

NAÏT-ALI, A. *Advanced biosignal processing*. [S.l.]: Springer Science & Business Media, 2009.

NARIN, A. Detection of focal and non-focal epileptic seizure using continuous wavelet transform-based scalogram images and pre-trained deep neural networks. *IRBM*, Elsevier, 2020.

NEJEDLY, P. et al. Intracerebral eeg artifact identification using convolutional neural networks. *Neuroinformatics*, Springer, v. 17, n. 2, p. 225–234, 2019.

OBEID, I.; PICONE, J. The temple university hospital eeg data corpus. *Frontiers in neuroscience*, Frontiers, v. 10, p. 196, 2016.

ÖZDENIZCI, O. et al. Transfer learning in brain-computer interfaces with adversarial variational autoencoders. In: IEEE. *2019 9th International IEEE/EMBS Conference on Neural Engineering (NER)*. [S.l.], 2019. p. 207–210.

PAN, S. J. Transfer learning. In: _____. *Data Classification: Algorithms and Applications*. [S.l.]: CRC Press, 2014. p. 537–558.

PAN, S. J.; YANG, Q. A survey on transfer learning. *IEEE Transactions on Knowledge and Data Engineering*, v. 22, n. 10, p. 1345–1359, 2010.

PARVAN, M. et al. Transfer learning based motor imagery classification using convolutional neural networks. In: IEEE. *2019 27th Iranian Conference on Electrical Engineering (ICEE)*. [S.l.], 2019. p. 1825–1828.

PHAN, H. et al. Deep transfer learning for single-channel automatic sleep staging with channel mismatch. In: IEEE. *2019 27th European Signal Processing Conference (EUSIPCO)*. [S.l.], 2019. p. 1–5.

PHAN, H. et al. Towards more accurate automatic sleep staging via deep transfer learning. *IEEE Transactions on Biomedical Engineering*, IEEE, v. 68, n. 6, p. 1787–1798, 2020.

PISANO, F. et al. Convolutional neural network for seizure detection of nocturnal frontal lobe epilepsy. *Complexity*, Hindawi, v. 2020, 2020.

PRESTON, D. C.; SHAPIRO, B. E. *Electromyography and neuromuscular disorders e-book: clinical-electrophysiologic correlations (Expert Consult-Online)*. [S.l.]: Elsevier Health Sciences, 2012.

QU, G.; YUAN, Q. Epileptogenic region detection based on deep cnn with transfer learning. In: IEEE. *2019 IEEE 11th International Conference on Advanced Infocomm Technology (ICAIT)*. [S.l.], 2019. p. 73–77.

RANGAYYAN, R. M. *Biomedical signal analysis*. [S.l.]: John Wiley & Sons, 2015.

ROMAY, M. M. G. et al. Improved activity recognition combining inertial motion sensors and electroencephalogram signals. World Scientific Publishing, 2020.

ROY, S. et al. Deep learning based inter-subject continuous decoding of motor imagery for practical brain-computer interfaces. *Frontiers in Neuroscience*, Frontiers Media SA, v. 14, 2020.

RUTH, P. S.; NEILS, C. M. *Biosignal Processing: Foundations for Biomedical Engineers*. [S.l.]: Independently published, 2020.

SEMMLOW, J. *Circuits, signals and systems for bioengineers: A MATLAB-based introduction*. [S.l.]: Academic Press, 2017.

SEMMLOW, J. L.; GRIFFEL, B. *Biosignal and medical image processing*. [S.l.]: CRC press, 2014.

SHALASH, W. M. Driver fatigue detection with single eeg channel using transfer learning. In: IEEE. *2019 IEEE International Conference on Imaging Systems and Techniques (IST)*. [S.l.], 2019. p. 1–6.

SHALBAF, A.; BAGHERZADEH, S.; MAGHSOUDI, A. Transfer learning with deep convolutional neural network for automated detection of schizophrenia from eeg signals. *Physical and Engineering Sciences in Medicine*, Springer, v. 43, n. 4, p. 1229–1239, 2020.

SHOVON, T. H. et al. Classification of motor imagery eeg signals with multi-input convolutional neural network by augmenting stft. In: IEEE. *2019 5th International Conference on Advances in Electrical Engineering (ICAEE)*. [S.l.], 2019. p. 398–403.

SILVA, F. H. et al. Classification of electroencephalogram signals for detecting predisposition to alcoholism using computer vision and transfer learning. In: IEEE. *2020 IEEE 33rd International Symposium on Computer-Based Medical Systems (CBMS)*. [S.l.], 2020. p. 126–131.

TAHERI, S.; EZOJI, M. Eeg-based motor imagery classification through transfer learning of the cnn. In: IEEE. *2020 International Conference on Machine Vision and Image Processing (MVIP)*. [S.l.], 2020. p. 1–6.

TAMM, M.-O.; MUHAMMAD, Y.; MUHAMMAD, N. Classification of vowels from imagined speech with convolutional neural networks. *Computers*, Multidisciplinary Digital Publishing Institute, v. 9, n. 2, p. 46, 2020.

TAN, C. et al. Autoencoder-based transfer learning in brain–computer interface for rehabilitation robot. *International Journal Of Advanced Robotic Systems*, SAGE Publications Sage UK: London, England, v. 16, n. 2, p. 1729881419840860, 2019.

TAN, C. et al. A survey on deep transfer learning. In: SPRINGER. *International conference on artificial neural networks*. [S.l.], 2018. p. 270–279.

VILAMALA, A.; MADSEN, K. H.; HANSEN, L. K. Deep convolutional neural networks for interpretable analysis of eeg sleep stage scoring. In: IEEE. *2017 IEEE 27th international workshop on machine learning for signal processing (MLSP)*. [S.l.], 2017. p. 1–6.

WAN, Z. et al. A review on transfer learning in eeg signal analysis. *Neurocomputing*, Elsevier, v. 421, p. 1–14, 2021.

WANG, D.; YANG, J. A method of expanding eeg data based on transfer learning theory. In: *Proceedings of the 2019 8th International Conference on Networks, Communication and Computing*. [S.l.: s.n.], 2019. p. 70–74.

WANG, F. et al. Emotion recognition with convolutional neural network and eeg-based efdms. *Neuropsychologia*, Elsevier, v. 146, p. 107506, 2020.

WANG, J. et al. Deep transfer learning-based multi-modal digital twins for enhancement and diagnostic analysis of brain mri image. *IEEE/ACM Transactions on Computational Biology and Bioinformatics*, v. 20, n. 4, p. 2407–2419, 2023.

WANG, K.-W. et al. A multivariate empirical mode decomposition–based data-driven approach for extracting task-dependent hemodynamic responses in olfactory-induced fmri. *IEEE Access*, IEEE, v. 7, p. 15375–15388, 2019.

WANG, Y. et al. Epileptic signal classification with deep transfer learning feature on mean amplitude spectrum. In: IEEE. *2019 41st Annual International Conference of the IEEE Engineering in Medicine and Biology Society (EMBC)*. [S.l.], 2019. p. 2392–2395.

WEISS, K.; KHOSHGOFTAAR, T. M.; WANG, D. A survey of transfer learning. *Journal of Big data*, SpringerOpen, v. 3, n. 1, p. 1–40, 2016.

WEISS, L. D.; WEISS, J. M.; SILVER, J. K. *Easy EMG e-book: A guide to performing nerve conduction studies and electromyography*. [S.l.]: Elsevier Health Sciences, 2015.

WHO, W. H. O. Comprehensive mental health action plan 2013–2030. World Health Organization, 2021.

WU, H. et al. A parallel multiscale filter bank convolutional neural networks for motor imagery eeg classification. *Frontiers in neuroscience*, Frontiers, v. 13, p. 1275, 2019.

XIE, L. et al. Generalized hidden-mapping transductive transfer learning for recognition of epileptic electroencephalogram signals. *IEEE transactions on cybernetics*, IEEE, v. 49, n. 6, p. 2200–2214, 2018.

XU, G. et al. A deep transfer convolutional neural network framework for eeg signal classification. *IEEE Access*, IEEE, v. 7, p. 112767–112776, 2019.

YANG, C. et al. Takagi–sugeno–kang transfer learning fuzzy logic system for the adaptive recognition of epileptic electroencephalogram signals. *IEEE Transactions on Fuzzy Systems*, IEEE, v. 24, n. 5, p. 1079–1094, 2015.

ZHAI, X. et al. Self-recalibrating surface emg pattern recognition for neuroprosthesis control based on convolutional neural network. *Frontiers in neuroscience*, Frontiers, v. 11, p. 266372, 2017.

ZHAN, Q. et al. A novel heterogeneous transfer learning method based on data stitching for the sequential coding brain computer interface. *Computers in Biology and Medicine*, Elsevier, v. 151, p. 106220, 2022.

ZHANG, B. et al. Cross-subject seizure detection in eegs using deep transfer learning. *Computational and Mathematical Methods in Medicine*, Hindawi, v. 2020, 2020.

ZHANG, H. et al. Bi-dimensional approach based on transfer learning for alcoholism predisposition classification via eeg signals. *Frontiers in Human Neuroscience*, Frontiers, v. 14, p. 365, 2020.

ZHANG, K. et al. Instance transfer subject-dependent strategy for motor imagery signal classification using deep convolutional neural networks. *Computational and Mathematical Methods in Medicine*, Hindawi, v. 2020, 2020.

ZHANG, R. et al. Hybrid deep neural network using transfer learning for eeg motor imagery decoding. *Biomedical Signal Processing and Control*, Elsevier, v. 63, p. 102144, 2021.

ZHANG, Z.; LI, X. Use transfer learning to promote identification adhd children with eeg recordings. In: IEEE. *2019 Chinese Automation Congress (CAC)*. [S.l.], 2019. p. 2809–2813.